Sc. D. Thesis

SEMICONDUCTOR CATALYSIS: SIMULTANEOUS MEASUREMENT OF KINETICS AND SURFACE ELECTRICAL PROPERTIES

by

Robert P. Merrill

Massachusetts Institute of Technology

April 1964

SEMICONDUCTOR CATALYSIS: SIMULTANEOUS MEASUREMENT OF KINETICS AND SURFACE ELECTRICAL PROPERTIES

by

Robert P. Merrill

Bachelor of Chemical Engineering, Cornell University, 1960

Submitted in Partial Fulfillment of the Requirements
for the Degree of Doctor of Science
at the
Massachusetts Institute of Technology

April 1964

Signature of Author: _____

Department of Chemical Engineering

Certified by: _____

Raymond F. Baddour, Thesis Supervisor

Accepted by: _____

Glenn C. Williams, Chairman
Department Committee on Graduate Theses

DEDICATION

To my father, Olonzo David Merrill, for his encouragement and help in my formative years, for the standard of excellence set in his own professional life, and with a feeling that the completion of this thesis represents a vicarious fulfillment of a goal, the realization of which the circumstances of his life would not permit; I dedicate this Thesis.

R.P.M.

SEMICONDUCTOR CATALYSIS: SIMULTANEOUS MEASUREMENT OF KINETICS AND SURFACE ELECTRICAL PROPERTIES

by
Robert P. Merrill

ABSTRACT

As a contribution to the developing science of catalysis, this research focused on exploring theoretically and experimentally the relationship between the surface electrical properties of a semiconductor catalyst and its catalytic activity.

A method was developed for introducing the specific properties of the surface bond between the adsorbed species and the catalytic surface into the physical description of the semiconductor surface. This was done using statistical mechanics to formulate the chemical potential of bonding electrons. With a parabolic approximation to the interaction energy of the surface bond, the vibrational terms were found to dominate. The fraction of the adsorbed species which are ionized by exchange of charge with the surface is simply related to the force constant of the surface bond. This leads to compensation in the Arrhenius equation for systems having un-ionized n-type species in the rate limiting step and to drastic poisoning and/or promoting effects for systems involving ionized n-type species in the rate limiting step. The reverse is true for p-type species.

A program is proposed for the measurement of surface conductivity and recombination velocity on germanium simultaneously with the measurement of reaction kinetics of the decomposition of ethanol.

The equipment to carry out these measurements has been designed and constructed. Included is a system to operate a unique radio-frequency mass spectrometer, which was used to analyze the decomposition products. Key experiments to demonstrate the facility of the design, including measurements of ethanol decomposition on vacuum cleaved germanium and surface electrical properties of etched germanium wafers, were made.

In the kinetic experiments it was found that the catalysts produced by vacuum cleavage are much more active than catalysts produced by crushing in air and subsequent reduction in hydrogen, though the activation energies are similar. Treating the vacuum crushed catalyst with hydrogen lowers both the activation energy and the rate. Evidence is presented for the possible formation of a germanium hydride on the clean surfaces and the formation of an oxy-hydrogen complex on air-crushed catalysts.

Thesis Supervisor

Raymond F. Baddour
Professor of Chemical Engineering

Department of Chemical Engineering
Massachusetts Institute of Technology
Cambridge 39, Massachusetts

April 30, 1964

Professor Philip Franklin
Secretary of the Faculty
Massachusetts Institute of Technology
Cambridge 39, Massachusetts

Dear Sir:

The thesis entitled "Semiconductor Catalysis: Simultaneous Measurement of Kinetics and Surface Electrical Properties" is herewith submitted in partial fulfillment of the requirements of the degree of Doctor of Science.

Respectfully submitted,

Robert P. Merrill

Robert P. Merrill

ACKNOWLEDGEMENTS

The help and encouragement of Professor R. F. Baddour, the author's thesis supervisor are acknowledged. In particular the author is grateful for the maximum amount of freedom which was extended to him during the comception of the research program and the completion of the experiments and theoretical work. While this freedom did not always result in the most rapid solution of the problems encountered, it served to make the completion of the thesis an educational experience of the highest sort.

Thanks are due the many individuals who assisted in various ways with the experimental work: Allan Thieme, Charles Selvidge, Harry C. Greenlaw, Jr., Lucio Pontecorvo, Stanley R. Mitchell, Donald Sandstrom and Victor Myette of the Raytheon Manufacturing Company, and Ed Warefort of Lincoln Laboratory.

Spectroscopic argon was furnished by the Linde Company, and germanium samples were supplied by Lincoln Laboratory and the Bell Telephone Laboratory.

The program was funded by the Chemistry Section of the Office of Naval Research, and some of the initial experimental work was supported by funds contributed by Union Carbide Corporation.

The author acknowledges personal support in the form of fellowships and assistantships from the Esso Foundation, Union Carbide, and the Office of Naval Research.

Much encouragement and stimulation was received from discussion of the work with other graduate students in the department, notably Michael Modell and Max Deibert.

Finally, appreciation is expressed to the author's wife and three daughters for their patience and understanding, particularly during the periods of prolonged absence from home required by the nature of the experimental work.

TABLE OF CONTENTS

LIST OF TABLES

LIST OF FIGURES

I. SUMMARY

A. Introduction

Heterogeneous catalytic systems have in recent years been widely used in the chemical process industries. However, much of the research in the field, especially the early work, has been highly empirical. With recent advances in physics and chemistry (particularly solid state theory and high vacuum technology) and the development of a number of new experimental devices, the art of contact catalysis has begun to emerge as a science.

In this research the need for measuring meaningful surface properties in catalytic systems during the course of a catalytic reaction was considered to be essential for further development of the new science. Specifically, the surface conductivity and surface recombination velocity of a semiconductor catalyst have been shown to be theoretically related to their activity and selectivity. Accordingly, an experimental program has been undertaken which will permit the simultaneous measurement of these surface electrical properties and the catalytic activity of germanium during the decomposition of ethanol on initially clean surfaces.

B. Theoretical and Experimental Background

As early as 1938 Wagner and Hauffe (18) interpreted nitrous oxide decomposition and carbon monoxide oxidation on nickel and cuprous oxides by considering the electronic state of the catalyst. Later attempts (especially on metals) were questioned as several investigators, notably Balandin (2, 3, 4, 5) and Beek (20) suggested

that geometric "fit" between the catalyst and the reactive adsorbed species was important. Dowden and Reynolds (22), however, in studying ethylene hydrogenation on nickel-copper alloys found that the activity of the catalyst declined in parallel with the filling of d-band vacancies by the valence electrons of copper. At the same time, from the geometric point of view, the lattice was expanding in the direction of greater activity.

The charge transfer theory of catalysis as formulated by Hauffe (6, 7, 8, 9), Dowden (10), Volkenshtein (11, 12, 13, 14, 15), and others attributed an especial importance to the electronic properties of semiconductor catalysts. Many investigators (see for example Schwab and Block (24)) have found correlations of one sort or another between measured and/or assumed values of the electrical properties of catalysts and their activity. Much of this work, though, has not agreed with the theoretical predictions (e.g. Frolov and Krylov (32)), and in some cases work performed by two different investigators (compare (24) with (25)) gave opposite results. These studies all contain one or more of the following deficiencies:

1. The electrical properties were not measured -- only inferred.

2. The changes in the catalyst compositions used were large enough (1% or more) that activity of the impurity atom itself, rather than its effect on the electrical properties, may have been responsible for the observed differences in activity.

3. No measurements of surface properties were made.

4. The surfaces tested were not prepared in such a way that theoretical treatment of the electrical properties was possible.

5. Electrical properties were not measured at the temperature and in the same environment as the kinetic studies.

Progress in the theoretical approach has been somewhat more satisfactory, and some of the recent approaches have been quantitative enough (see for example Volkenshtein (15) and Garrett (18)) to permit careful design of experiments which could test in a meaningful way their fundamental postulates.

All of these theories, however, are directed only toward the properties of the solid. The adsorbed species are treated as surface impurities, and no information is introduced quantitatively into the theory which reflects properties specific to the adsorbed species. Further theoretical progress could obviously be made if the chemical properties of the surface bond between the catalyst and the adsorbed species could be introduced into the formulation of the electronic state of the surface.

C. Theoretical Results

Volkenshtein has pointed out that strong interaction can occur between a gas and a semiconductor surface without charge transfer which influences the electronic transport properties of the surface. Simultaneously with the establishment of such a bond, a surface impurity state is formed on the catalyst surface. This impurity may

act as a donor or acceptor, and when it does charge transfer is said to occur, a surface charge being either localized or released, and the transport properties of the surface being changed accordingly. Volkenshtein did not note in his theory that the very act of charge transfer perturbs this surface bond. The perturbation will be a function of the adsorbed specie as well as the physical characteristics of the catalyst surface. It is here than (i.e. in this perturbation) that the characteristics of the specific surface bond can be incorporated into the theory.

The thermodynamic driving force for charge transfer is the difference between the chemical potential of electrons in the surface bond and the chemical potential of those in the solid. The charge transfer would continue with its attendant perturbation of the surface bond until the chemical potential of the bonding electrons is equal to the work function of the catalyst surface. The chemical potential of bonding electrons can be calculated statistically and is shown to be equal to:

$$\mu_e = U + \frac{\partial U}{\partial \theta} + kT\frac{\partial \ln q_z}{\partial \theta} \qquad (15)$$

where:

μ_e = chemical potential of bonding electrons
U = ionization potential of bonding electrons
θ = fraction of adsorbed species ionized
k = Boltzman's constant
T = absolute temperature
q_z = vibrational partition function of surface bond

The fraction ionized is given by Fermi statistics:

$$(1 - \theta) = \frac{1}{\exp(E/kT) + 1} \tag{8}$$

where:

$$\frac{\Delta E}{kT} = \frac{\theta}{kT}\frac{\partial U}{\partial \theta} + \frac{\partial \ln q_z}{\partial \theta}$$

To a first approximation equation (16) can be developed to:

$$\frac{\Delta E}{kT} = \theta K \frac{(\Delta R)}{kT}\frac{\partial(\Delta R)}{\partial \theta} + \left\{\frac{\theta}{2}\frac{(\Delta R)^2}{kT} + \frac{1}{8\pi^2 m\nu^2}\left[1 - \frac{h\nu}{kT} + \frac{1}{12}\left(\frac{h\nu}{kT}\right)^2 + \frac{1}{720}\left(\frac{h\nu}{kT}\right)^4\right]\right\}\frac{dK}{d\theta} \tag{24}$$

where:

K = Force constant for surface bond
R = bond length (separation parameter)
m = vibrational reduced mass
ν = fundamental vibrational frequency

For systems of interest in catalysis equation (24) simplifies to:

$$\frac{\Delta E}{kT} = \frac{1}{2K}\frac{dK}{d\theta} \tag{25}$$

which when combined with (8) for ΔE of a few kT or more and integrated gives:

$$\ln \frac{K}{K^o} = -2\left[(1 - \theta)\ln(1 - \theta) + \theta\right] \tag{20}$$

Equation (28) shows that K/K^o is a monotonically increasing function of θ. This result can be shown to predict that if an ionized n-type specie is involved in the rate limiting step, then compensation between the pre-exponential and the activation energy in the Arrhenius equation would be expected. If an un-ionized species

is involved, then no compensation occurs, and small changes in the activation energy about an experimentally determined value would make it impossible as a practical matter to measure the resulting new rate of reaction. Systems of this type would be expected to exhibit the drastic poisoning and/or promotion effects so common to many catalytic systems. The reverse is true for p-type adsorbents.

Using the available data on hydrogenation reactions on germanium surfaces, it is possible from these considerations to conclude that the rate limiting step involves un-ionized species. It is also possible to predict qualitatively the electrical response of clean germanium surfaces during the dehydrogenation of ethanol.

Many systems may not be adequately described by the first order approximation of (24) and combining (8) and (16) may be more difficult. Nevertheless, it is clear from this work just how one might introduce the characteristics of the surface bond into the physical description of the surface. Furthermore, these effects do not appear to be negligible, but rather seem to be the controlling factors.

D. Experimental Design

The experimental program initiated with this thesis was designed to eliminate the objections which were previously raised in connection with the earlier work relating the electrical properties of semiconducting catalysts to their catalytic behavior. Facilities have been assembled and tested for measuring surface electrical

properties in situ at reacting temperatures in the presence of reaction gases. By using an elemental semiconductor for a catalyst, a wide variety of electrical properties may be obtained with only minute doping. The surfaces studied may be prepared atomically clean prior to contacting them with reactant, and the whole study may be conducted in a high vacuum system to minimize extraneous contamination of the surfaces.

The system chosen to meet these rather stringent requirements was the decomposition of ethanol on germanium. Catalysts were prepared by crushing germanium in ultrahigh vacuum. The surface electrical properties will be measured on thin wafers cut from the same crystal as the crushed material. The necessary electrical contacts to the wafers have been made. The wafers may be cleaned in situ by argon ion bombardment prior to contacting them with the reaction gases. The electrical measurements are made using low-duty-cycle square-wave pulses. Both surface conductivity and recombination velocity can be measured.

The reaction kinetics are measured with an on-line mass spectrometer which is bakeable with the rest of the high vacuum system. This instrument was specially designed and constructed for this work.

E. Experimental Results

1. Kinetics of Ethanol Decomposition on N-type Germanium

The decomposition of ethanol on germanium surfaces produced by vacuum cleavage was measured between 200°C and 270°C. Only dehydro-

genation was observed, in agreement with Volkenshtein's theory (15). The apparent activation energy derived from first order kinetics was 27 Kcal/mole, in good agreement with that of Frolov and Krylov (32) who prepared their catalysts by grinding germanium in air and subsequently reducing with hydrogen. The rates on the vacuum crushed catalyst, however, were 10^4 times their values for n-type germanium.

In a second series of studies the vacuum crushed catalyst was aged in hydrogen for several hours at 500°C. As a result its activation energy dropped to 11.4 Kcal/mole and the pre-exponential dropped by a factor of 10^6. These values are quite different from any of the values obtained by Frolov and Krylov on n-type germanium and are closer to the values they obtained on p-type material.

It is possible that the kinetics on the hydrogen treated surface is really characteristic of a germanium hydride of some sort. Based on the work of Maxwell and Green (66) it is suggested that Frolov and Krylov measured kinetics on a germanium oxy-hydride surface which is unlike either the vacuum crushed or hydrogen treated catalyst used in this work.

2. Electrical Measurements

To test the feasibility of making the electrical measurements in situ, the procedures to be used were tried on a sample of one ohm-centimeter n-type germanium mounted on an open bench. The welded platinum leads, used because of their stability at high temperatures, were found to be non-ohmic. The use of a differential amplifier for the voltage measurements, however, permits subtracting of the voltage

across the current carrying contacts and thus measurement of the proper boltage. Because of the high resistance of the contacts, however, the range of investigation is limited to a rather small range of negative currents. The use of a high-impedance pre-amplifier would increase this range considerably.

Field effect measurements were found to be quite difficult because of the problem of accurately positioning the required electrode. Illumination with infrared radiation gave positive results, and it is recommended that the surface recombination velocities be measured photometrically with the aid of a gallium-arsenide recombination-radiation diode.

F. Conclusions

Results obtained on the kinetics of ethanol decomposition by germanium catalysts crushed under high vacuum show that these catalysts are different from ones crushed in air and subsequently reduced with hydrogen. It appears that in the latter case, oxy-hydride sites may be formed on the surface.

Equipment for measuring surface electrical properties of germanium catalysts in situ has been assembled and tested and appears capable of measuring surface electrical properties and kinetics simultaneously.

II. INTRODUCTION

The large and increasing research activity in the area of heterogeneous catalysis, both in this country and abroad, is an indication of the importance of this subject to modern science and technology. Heterogeneous catalysis has been used to some extent for many years, but recently the use of solid catalysts has spread to almost every facet of the process industries. Nearly all the early work in this field and much of the current work is highly empirical. However, with the recent progress in the physics and chemistry of the solid state and in the understanding of chemical bonding, the art of contact catalysis has begun to emerge as a science.

This new science must ultimately combine the solutions of basic problems of mass and heat transfer, of primary interest to chemical engineers, with the results of the developing theories of surface physics and contact catalysis which are largely based on recent advances in the chemistry and physics of solid state, and on some recent advances in techniques specifically suited for the study of surface species (e.g. surface infrared spectroscopy). The science of catalysis is unique in that it cuts across many of the long-established academic disciplines.

It is somewhat disappointing, however, to note that the science of catalysis has had little effect as yet on the development of successful industrial catalysts. As Heinemann recently pointed out (1) ".... in reality, applied catalysis is still an art which profits only little by the science of catalysis which has slowly

been emerging."

He further stressed ".... the need for a large volume of well-directed work in catalysis to study the chemistry off and on the surfaces during reaction."

This thesis is just such a study in which the surface electrical properties of a semiconductor catalyst are shown to be related to the catalyst reactivity and selectivity. A unique feature of the experimental program proposed is the measurement for the first time of meaningful electrical properties of a catalytically active surface during the course of the chemical reaction which it catalyzes. The design and construction of the experimental equipment is detailed and the preliminary data which has been obtained is discussed within the framework of the theoretical development presented. In order to characterize the chemical state of the surface and to insure reproducibility of the results, studies were conducted on surfaces which were atomically "clean" at the start of the catalytic reaction.

III. THEORETICAL BACKGROUND

A. Geometric and Electronic Factors in Catalysis

Modern catalysis theories directed toward the solid state revolve around two basic considerations - (1) the effect of the inter-atomic distance and lattice geometry of the solid catalyst, and (2) the effects of the electronic configuration of the catalyst on its reactivity and selectivity. The former, notably developed by Balandin (2, 3, 4, 5) approaches the problem from the consideration of the interaction of the chemisorbed species with particular sites on the surface of the catalyst. Thus, it is important to match the geometry of the lattice with that of the chemisorbed molecule. Further, small changes in the atomic spacing about a favorable orientation will result in induced strain of the bonds or a lessening of such strain. Thus Balandin (4) finds a measurable change in the activation energy with small changes in the interatomic distances of the catalyst.

The electronic theory of catalysis suggested by Hauffe (6, 7, 8, 9), Dowden (10), Volkenshtein (11, 12, 13, 14, 15), and others, seeks to explain the catalytic activity of a particular solid on the basis of possible charge transfer between the solid and the gas where the adsorbate may act either as an electron donor or an electron acceptor, forming primary bonds with the surface which may be ionic or homopolar in nature. In general, of course, the bond will be a hybrid with some ionic nature and some homopolar nature.

Obviously, a thorough understanding of catalysis will eventually weld these two approaches into a single consistent theory. Notwithstanding the recent attempt by Balandin (16) to establish such a unified approach, at present it seems that the best experimental approach is to concentrate on one of these effects.

B. The Charge Transfer Theory of Catalysis

The early developments of the theory assumed that chemisorption occurred entirely as a result of charge transfer. Calculations based on this assumption predicted that surfaces become saturated with chemisorbed species at coverages of the order of 1%. A point, in fact, is that chemisorption normally produces at least a monolayer of adsorbed species and often more. The point must be that chemisorption can occur with and without charge transfer. Volkenshtein (15) has incorporated this into his more recent development of the theory in which he recognizes two kinds of chemisorption; that without charge transfer with the surface, which he terms "weak chemisorption" and that which does involve charge transfer which he calls "strong donor" or "strong acceptor" type depending on whether an electron is donated or accepted by the adsorbed species. It is reasonable to consider that weak chemisorption involves only minor overlapping between the orbitals of the adsorbate and those of the solid. Simultaneously, a donor or acceptor level, as the case may be, is established within the forbidden gap of the semiconductor. Strong chemisorption occurs when the impurity level so formed becomes ionized.

Since the ionization probability for impurities is a function of the difference between the energy level of the impurity and the Fermi energy, one might expect that changes in the Fermi energy induced by even minute changes in the catalyst composition would control the amount and type of strongly adsorbed species on the surface. Thus, the Fermi level, as controlled by bulk doping, may be thought of as a regulator of catalytic behavior. To illustrate this formulation of the theory, Volkenshtein's mechanism (15) for the decomposition of ethanol on semiconductor surfaces is shown below.

On P-Type Surfaces

1. Adsorption of CH_3CH_2OH accompanied by cleavage of the C - O bond to produce strongly adsorbed n-type CH_3CH_2 fragments and weakly adsorbed OH radicals.

$$L + CH_3CH_2OH + pL \longrightarrow CH_3CH_2pL + \dot{O}HL \qquad (1)$$

Here "L" represents a latice site; "p", a positive hole in the valence band; and the superscript "." a free radical of the depicted species.

2. The free radical, OH, combines with one hydrogen on the CH_3CH_2 fragment to give desorbed H_2O and strongly adsorbed ethylene radical.

$$CH_3CH_2pL + \dot{O}HL \longrightarrow CH_2\dot{C}H_2pL + H_2O \qquad (2)$$

3. The ethylene free radical desorbs to give ethylene and regenerate the hole in the valence band.

$$CH_2\dot{C}H_2pL \longrightarrow CH_2CH_2 + pL \qquad (3)$$

On N-Type Surfaces

1. Adsorption of CH_3CH_2OH accompanied by cleavage of the O - H bond to form CH_3CH_2O, which is held by a "strong donor" bond, and weakly adsorbed H radical.

$$CH_3CH_2OH + L + nL \longrightarrow CH_3CH_2OnL + \dot{H}L \qquad (4)$$

2. Reaction of the H radical with one hydrogen on the CH_3CH_2O fragment to give strongly absorbed CH_3CHO radical and desorbed H_2.

$$CH_3CH_2OnL + HL \longrightarrow CH_3\dot{C}HOnL + H_2 \qquad (5)$$

3. Desorption of the aldehyde radical to give acetaldehyde and regenerate the electron in the conduction band.

$$CH_3\dot{C}HOnL \longrightarrow CH_3CHO + nL \qquad (6)$$

Given such a mechanism, one would expect that p-type surfaces would catalyze dehydration of ethanol while n-type surfaces catalyze dehydrogenation of ethanol. Thus, if one were to conduct a series of experiments where the surface is varied from n-type to p-type, a significant change in the decomposition product distribution should be evident for the ethanol system.

Two assumptions are implied in this development: (1) charge transfer equilibrium is achieved at the surface of the semiconductor, (2) the energy of the impurity when charge transfer equilibrium is achieved is not a function of the position of the Fermi energy at the surface. The first assumption is problematical and the second

seriously questioned as a result of a simplified statistical mechanical approach to chemisorption on semiconductors which will be presented later.

C. Quantitative Theory

Garrett (18) has developed the theory quantitatively along the lines outlined by Hauffe (6) for the case when charge transfer equilibrium is not necessarily attained. His calculations which are given for an assumed bimolecular reaction predict (1) only certain ranges of the reaction variables result in rates of reaction which are controlled by solid state properties, (2) where solid state properties do control, changes in the kinetic behavior of the system with changes in solid state parameters can be different for one set of reaction variables than for another, and (3) correlations with fundamental significance can only be expected between the reaction rate and precisely defined and carefully measured properties of the solid -- in most ranges of reaction variables, these quantities are characteristic of the surface rather than of the bulk of the catalyst.

Garrett's work, though specific to the reaction he assumed, is the only really successful attempt to formulate the theory quantitatively, and it is likely that his approach can be extended to cover more realistic systems. Certainly the treatment of the reactions which are controlled by the solid state as non-equilibrium processes is much preferred over Volkenshtein's equilibrium explanations which can be questioned.

In summary, it may be said that a completely satisfactory theory of charge transfer catalysis has not yet been formulated, but its development very recently has become quantitative enough to allow careful design of experiments which will test in a meaningful way its fundamental postulates.

IV. EXPERIMENTAL BACKGROUND

A. Historical Development

As early as 1938, Wagner and Hauffe (18) attempted an electronic interpretation of their studies of nitrous oxide, N_2O, decomposition and carbon monoxide oxidation on nickel oxide and cuprous oxide, which are semiconductors. They reasoned that the transfer of electrons to the solid catalyst could occur more easily in the neighborhood of impurity atoms than in the pure material. Furthermore, the rate limiting step they postulated involved electron transfer to the solid. It should be recognized that such reasoning is merely an extension of Taylor's noted "active center" theory of catalysis.

Beek (20) was able to correlate the data available in 1945 for the hydrogenation of ethylene with the lattice spacing of the metal catalysts. He found a maximum activity for nickel, rhodium, paladium and platinum whose lattice spacings cluster around 3.8 A°. A later study by Beek (21) suggests that this correlation between the lattice parameters of several different metals occurs primarily because of differences in the electronic character of the metals which are incidentally reflected in the lattice spacing. Differences in activity from one crystal plane to another of the same catalyst, Beek argues, do reflect the effects of geometric changes in the catalyst. It should be noted, however, that the electrical properties of a single crystal are markedly anisotropic, and a similar electronic argument could be presented for the different activity of different crystal planes.

That this "geometric factor" can be much less important than the electronic nature of the catalyst is graphically demonstrated by the work of Dowden and Reynolds (22). They investigated the hydrogenation of ethylene on nickel-copper alloys and found that the catalytic activity of the alloys declined in parallel with the filling of 3d-band vacancies by the valence electrons of copper at the same time the crystal was expanding in the direction of greater catalytic activity from the simple geometric view. Lo (23), much more recently was able to correlate his studies of the reactions between carbon monoxide and hydrogen on supported ruthenium-silver alloys with Dowden's d-band theory while the simple geometrical approach was inadequate. Thus, it seems that when charge transfer with the catalyst is important in the reaction mechanism, the electronic properties are more important than geometric considerations.

B. Semiconductor Catalysis

More recently, experiments on semiconductors have been interpreted in terms of the charge transfer theory, which has been described in detail earlier, and treats the catalytic surface as a homogeneous unit. A classic reaction which illustrates the success of such approaches as well as many of their major difficulties is the oxidation of carbon monoxide on nickel oxide catalysts. Schwab and Block (24) studied this system and found that the activation energy on nickel oxide doped with 1 percent chromic oxide, Cr_2O_3, or more was 19 kcal/mole, while the activation energy on nickel oxide doped to greater than 1 percent Lithium oxide Li_2O was 12 kcal/mole.

They assumed that the rate limiting step involved transfer of electrons to the solid. Nickel oxide is a p-type semiconductor and addition of lithium oxide increases the number of positive holes, while addition of chromic oxide decreases the number of holes. Thus, lithium doped nickel oxide would tend to favor the oxidation reaction. Parravano (25), on the other hand, performed similar experiments and found just the opposite results. A number of writers (see for example (26) and (27)) have attempted to explain the differences on the basis of Parravano's lower temperatures and the possibility of different operative mechanisms. While internally consistent, each of these explanations requires its own set of assumptions whose validity has not been demonstrated. It should be noted, of course, that Garrett's development mentioned in Section III, Theoretical Background, predicts just this kind of ambiguity (i.e., the changes in solid state parameters can affect the kinetics in different ways, depending on the reaction variables of the experiment).

It is impossible to examine these results critically on the basis of Garrett's predictions or even Volkenshtein's for several reasons:

1. The electrical properties were never measured, but only inferred from the composition changes.

2. The composition changes were of the order of 1 percent or more, and it is impossible at this level of doping to separate the effect of the impurity atoms themselves on the kinetics of the chemical reaction from their effect via changes in the electrical properties of the solid.

3. There is no guarantee that bulk compositions extend to the surface without measurement of some surface property which is sensitive to composition. In particular, surface excesses and deficiencies are likely to be a strong function of preparation techniques, and it is well-known that catalysts are also very sensitive to preparation techniques.

On the other hand, work by Schwab (28), Penskofer (29), and others, has demonstrated similar effects with elemental semiconductors where electrical properties have been measured and dopant levels are kept below 0.01 percent to 0.1 percent. Electrical measurements were not made at reaction temperatures nor were they made in the presence of reacting species, and nearly always they were made on bulk material rather than in the surface layers. Furthermore, the correlations have often been made with electrical conductivity without a knowledge of how the mobilities of the charge carriers might change.

Some measurements of surface conductivity in the presence of reacting species have been made by Bielanski and coworkers (20, 31). They measured the dehydrogenation of various primary alcohols on both n-type and p-type semiconducting oxides and found that the conductivity of n-type catalysts increased with the addition of alcohol to the system, while the conductivity of p-type catalysts decreased. Their catalysts were sintered powders, and it is likely that their measurements do represent surface conductivities. It is impossible, however, with presently-known techniques to measure the

mobilities on powdered or polycrystalline samples, and Bielanski, et al, were not able to explain their results on the basis of any of the charge transfer theories. Rather, they chose to express the correlations empirically and use these results in a set of chemisorption studies of the individual reactants and products to deduce a possible mechanism for the dehydrogenation of isopropyl alcohol. In particular, they suggested that acetone is the primary surface species during the dehydrogenation.

Working with the ethanol-germanium system, Frolov and Krylov (32) were not able to explain their results on the basis of Volkenshtein's development of the charge transfer theory of catalysis. In fact, they report that both p-type and n-type germanium catalyze dehydrogenation and present convincing, though not conclusive, evidence that oxygen-lean germanium surfaces extract oxygen irreversibly from ethanol. They were able to show that the activation energy for the dehydrogenation was greater on n-type than on p-type germanium.

Even if Volkenshtein's equilibrium-type theory were correct, it is not surprising that Frolov and Krylov did not find agreement with the theory. They made no surface electrical measurements and did not use reproducibly "clean" surfaces. The electrical measurements that were made were not at reaction temperatures, nor were they made in the presence of ethanol. Furthermore, at the reaction temperatures (200 to 270°C), the equilibrium intrinsic conductivity swamps the impurity conductivity up to dopant levels of the order of 10^{18} atoms/cc, while they found marked differences in the activation

energies at dopant levels much lower than that. Thus, it seems reasonable that the equilibrium theory may not apply to this system, and a knowledge of the cross-sections for electron and hole capture, as well as the non-equilibrium distribution of electrons, might be required. It is just this situation which Garrett treated for his hypothetical reaction and a similar treatment should be applied to this real system.

In order to interpret the results of a catalytic study of this nature in terms of the charge-transfer theories, it is necessary to carry out the reaction on a surface which is electrically describable. Much has been said in recent years about the possibility of atomically "clean" surfaces. Dillon (40) has pointed out that surfaces which may be "clean" for one set of experiments are not necessarily "clean" for another. Boddy (40) described surfaces which he called electrically "clean" in some electrochemical studies, and Alpert (40) suggested that the proper term to use would be "describable" surfaces rather than "clean" surfaces. Such describable surfaces have been produced for the elemental semiconductors by at least three methods on single crystals. Farnsworth (33) using argon ion bombardment has produced surfaces of germanium and silicon which are atomically clean as evidenced by slow electron diffraction studies. Palmer and Dauerbaugh (34) have produced describable surfaces by cleavage of single crystals in high vacuum. Harvey and Gatos (35) found that germanium surfaces in carefully purified and scrupulously deoxygenated water gave charging curves and photo-response characteristic of oxygen free surfaces. They further observed that germanium

oxides are soluble in the carefully prepared water, but elemental germanium is not, and concluded that germanium samples immersed in their ultra-pure water were oxide free and to this extent "clean".

The method of Harvey and Gatos has been investigated further by Selvidge (50). He was able to show that such surfaces have less than 1/2 monolayer of reducible oxygen. This, however, is not adequate proof of a clean surface. For these purposes one-half monolayer of oxygen would control the surface electrical properties. Thus, this method would not be acceptable without further work to establish more precisely the level of cleanliness.

Shooter and Farnsworth (36) have made an attempt to study the hydrogen-deuterium exchange reaction on single crystals of germanium which were cleaned by the ion bombardment technique. They were not able to measure the rate of reaction, presumably because the small area of the germanium wafer did not present enough active surface to detect this relatively slow reaction. An attempt to make similar measurements on sputtered germanium films also met with negative results. Sandler and Gazith (37) in an earlier study had reported moderately active surfaces of sputtered germanium for the exchange reaction. Shooter and Farnsworth emphasize the necessity of using describable surfaces in theoretical catalytic studies by concluding that the activity measured by Sandler and Gazith is not an intrinsic property of germanium and suggest rather that the activity was due possibly to metallic impurities or surface defects.

Moore et al (53) studied hydrogen-deuterium exchange on germanium crushed in the atmosphere and subsequently activated in hydrogen at 700°C. They found a marked increase in activation energy in going from p-type to n-type germanium. They also investigated the decomposition of formic acid on the same catalysts and found p-type catalysts to be much more active than n-type and to favor dehydrogenation.

Their work is particularly interesting because they used three different dopant materials for both p-type and n-type catalysts yet their activities for each set of catalysts is comparable. This would seem to rule out any specific effect of the dopant as opposed to its effect on the electronic properties of the catalyst.

Loebl (38) is presently attempting to study the ortho-para hydrogen conversion on germanium crushed in high vacuum. While dealing with much larger surface areas than Shooter and Farnsworth, he still has had trouble achieving observable results (39).

A number of investigators have been able to relate surface electrical properties of germanium to the adsorption of gases (see for example (54)). These have included studies with oxygen, carbon monoxide, hydrogen, ethanol and isopropyl alcohol.

Thus, although the charge transfer theories of catalysis have led to numerous examples of correlations between the electrical properties of catalysts and their catalytic activity and/or adsorptivity, not one of these can be explained quantitatively by

any of the existing theories. Some of the results are even qualitatively conflicting. Though some work has been done on reproducible surfaces, very little of it has been successful, and no concurrent measurements of electrical properties have been tried.

It is not surprising, in the light of Garrett's theoretical work, that hastily conceived experiments without careful measurement of meaningful surface properties and judicious selection of the reaction variables have, in some cases, failed to show the results of the theory in its simple and qualitative form.

No experiment has yet been performed prior to this work which can be used to make a definitive test of the charge-transfer theory of catalysis. Clearly, a suitable test of the theory requires concurrent measurements of surface electrical properties and reaction kinetics on reproducibly "clean" surfaces. Furthermore, the studies should be made on materials whose electrical properties can be varied over wide ranges without substantially affecting its chemical composition.

V. THEORETICAL RESULTS

A. The Energetics of Chemisorption

A gas may be adsorbed on semiconductors in a number of different modes. For illustrative purposes, an hypothetical diagram of a system which can undergo activated chemisorption is seen in Figure 1. Low-temperature physical adsorption occurs when the molecule is trapped in the minimum of the Leonard-Jones potential. At higher temperatures appreciable numbers of the gaseous molecules have energies higher than the activation energy for chemisorption $(\Delta E^*)_A$ and chemisorption occurs. The heat of chemisorption is ΔE and the activation energy for desorption is $(\Delta E^*)_D$. It should be noted that at high enough temperatures desorption to a dissociated molecule can occur. In this case, the solid has catalyzed molecular dissociation.

As Volkenshtein (15) has pointed out, charge transfer, when it occurs, on semiconductors involves transfer between surface states of the solid and states in the chemisorption bond. In Figure 1 a possible Born-Oppenheimer potential for chemisorption with charge transfer (Volkenshtein's "strong chemisorption") is shown. In the case presented, the removal of an electron from the sorption bond is illustrated. At infinite separation this potential corresponds to an ionized free molecule. The only thing one can say a priori about the shape of this potential curve is that it will be different from the curve for chemisorption without charge transfer. For illustrative purposes, a case is shown where the bottom of the charge-transfer potential well is below that for the molecule without charge transfer. Of course it could be above or there may be no

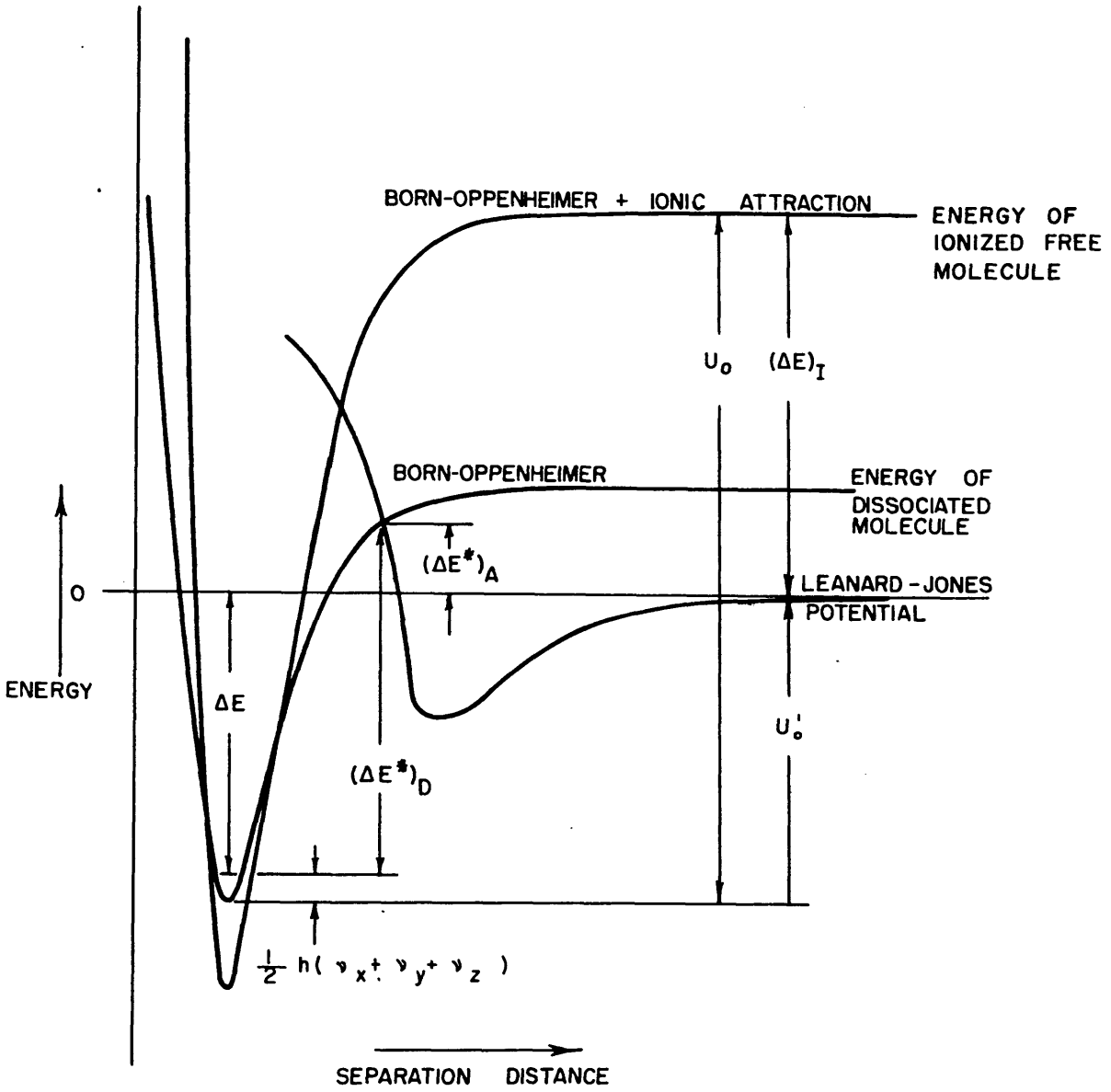

THE ENERGETICS OF CHEMISORPTION

Figure 1.

potential well in the curve at all.

At any given level of charge transfer the true potential diagram for the chemisorbed system would be intermediate between the two shown. A crude approximation of the quantum mechanical wave function might be expected to be,

$$\psi = \frac{1}{N} [(1 - \theta) \psi_o + \theta \psi_+] \qquad (7)$$

where:

θ = fraction of molecules ionized
ψ_o = wave function for un-ionized state
ψ_+ = wave function for ionized state
N = normalizing factor.

Naturally, the variational theorum may be applied to ψ_o and ψ_+ with screening constant variation or hybridization via LCAO or other standard methods in order to obtain a minimum energy for each value of θ considered. By using a simple system as a prototype, one could gain some insight as to how such charge transfer might change the potential of the chemisorption bond.

B. Charge Transfer

Charge transfer will occur in the direction of the thermodynamic driving force. Thus, if the chemical potential of electrons is higher than the Fermi energy (chemical potential of electrons in the solid), electrons will be transferred to the solid. If it is lower, electrons will be transferred to the sorption bond. This transfer will continue until the chemical potential of electrons in

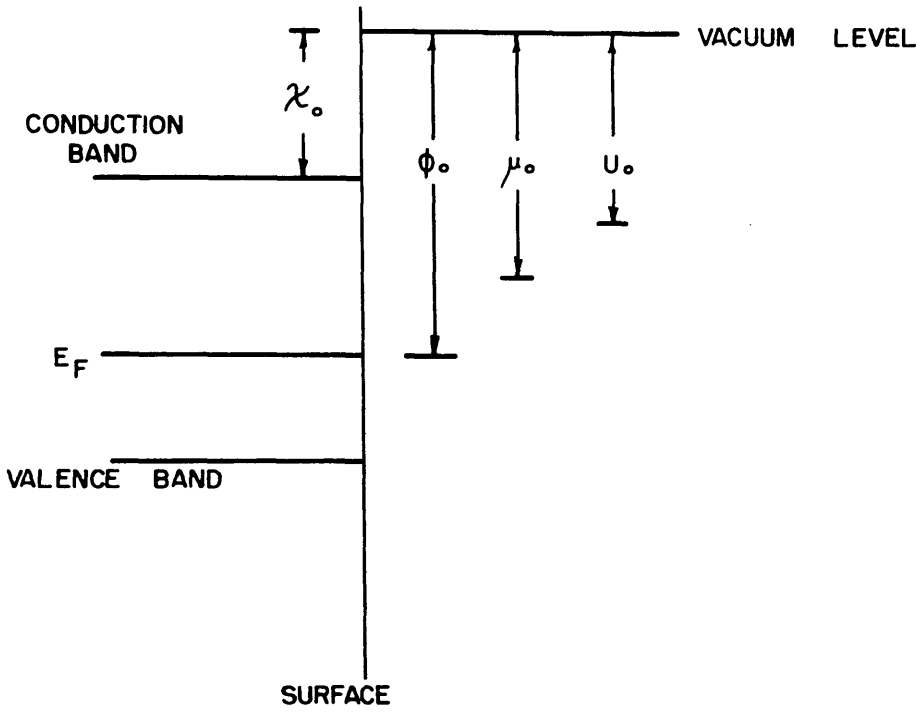

ENERGY DISTRIBUTION BEFORE CHARGE TRANSFER

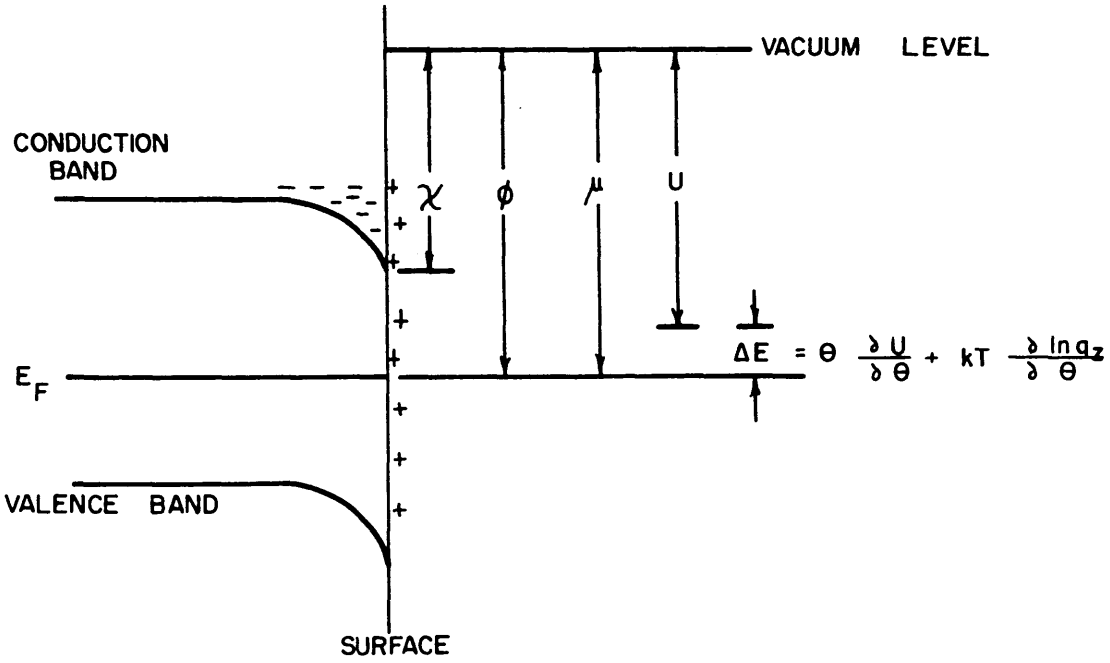

ENERGY DISTRIBUTION AFTER CHARGE TRANSFER

ENERGETICS OF CHARGE TRANSFER

Figure 2.

the chemisorption bond is equal to the Fermi energy of the solid.

The case analogous to that discussed in connection with Figure 2 is illustrated in Figure 2. Before charge transfer, the chemical potential of the electron in the sorption bond, μ_o, is less than the work function ϕ_o. This is the case for electron transfer from the sorption bond to the solid surface. As this occurs, the potential curve takes on more and more of the character of the ionization potential curve, U_o increases to U and μ_o increases to μ. When $\mu = \phi$ then the transfer stops. At this point θ and ΔE are related by Fermi statistics,

$$(1 - \theta) = \frac{1}{\exp(\Delta E/kT) + 1} \qquad (8)$$

Thus if ΔE were known, it would be possible to calculate θ. From θ one can obtain a complete description of the electronic configuration of the boundary layer by integrating Poisson's equation into the surface as proposed originally by Garrett and Brattain (44), or more conveniently by the methods developed by Lee and Mason (17).

A more pertinent problem to the catalytic behavior of semiconductors is to describe the variation in ΔE and hence θ as a function of the Fermi energy. In the Volkenshtein (15) development ΔE is assumed to be,

$$\Delta E = \phi_o - U_o \qquad (9)$$

Such an assumption not only places very unusual restrictions upon μ, but it also ignores any perturbation of the sorption bond with

increasing θ. Volkenshtein assumes that as the Fermi energy E_F is varied by doping or other means, the electron affinity, χ, remains constant. Thus, an increase in E_F means a corresponding decrease in ϕ and an increase in ΔE. Thus, changes in ΔE result in changes in θ as per equation (8), and hence the catalytic activity can be related, Volkenshtein argues, directly to the Fermi energy. A point in fact is that the work function, ϕ, is relatively independent of the Fermi energy (see for example Gobeli and Allen (49)). Thus, if Volkenshtein's assumption expressed in equation (3) were correct, one might find that θ is completely independent of E.

C. Statistical Description of the Chemical Potential

The problem resolves itself, then, into one of describing U and μ as a function of E_F. Given this information θ could be described as a function of the impurity doping within the semiconductor. Such an approach would be most desirable since E_F is a unique function of the impurity doping in the bulk and can be easily calculated from bulk resistivity data. Furthermore, it is constant throughout the space charge region near the surface.

The energy of the sorption bond, U, can in principle be calculated quantum mechanically and could be crudely done for some simple systems at least by the methods outlined above. The chemical potential, μ, can best be handled by statistical thermodynamics.

For simplicity it is assumed that the chemisorption is of the Langmuir type with no surface diffusion. There is a doubly degenerate

vibrational degree of freedom in the plane of the surface and one perpendicular to the surface. The one-particle partition function is given by,

$$q_1 = q_{xy} q_z q_e q_i$$

where:

q_{xy} = vibrational partition function parallel to adsorbing surface
q_z = vibrational partition function perpendicular to adsorbing surface
q_e = electronic partition function
q_i = internal partition function to account for the part of the molecule not involved in the sorption bond.

Including the degeneracy induced by vacant sites and assuming no interaction between adsorbed species the N-particle partition function is given by

$$Q_N = \frac{M!}{N!\ (M - N)!}\ q^N \qquad (10)$$

M = number of adsorption sites
N = number of adsorbed molecules

A well known result of statistical mechanics is that the Helmholtz free energy, A, is:

$$A = -k \ln Q_N \qquad (11)$$

Using Stirling's approximations for ln n!

$$A = kT\ [M\ln M - N\ln N - (M - N)\ln(M - N) + N\ln q] \qquad (12)$$

To obtain the chemical potential the quantity $(\partial A/\partial N_e)_{T,V}$ must be calculated.

Remembering that we seek the chemical potential for electrons and thus $(\frac{\partial N}{\partial N_e}) = 0$ since the transfer of electrons does not change the number of adsorbed molecules, μ is,

$$\mu_e = \left(\frac{\partial A}{\partial N_e}\right)_{T,V} = kT\ (\ln q_e + N_e \frac{\partial}{\partial N_e} \ln q_e + N\frac{\partial}{\partial N_e} \ln q_{xy} q_z q_i) \qquad (13)$$

The first term in equation (13) is the work required to remove one electron from a chemisorption bond. The second term is the work required to change the electronic energy of all the remaining electrons in sorption bonds by an amount corresponding to the slight change in the potential curve due to the removal of one electron. While the partial derivative is small compared to the first term in the equation, N_e can be very large so the term is appreciable. The third term is the work required to change all the adsorbed molecules (exclusive of the electrons in sorption bonds) to conform with the increased perturbation of the potential. Again, though the partial derivative is small, N is very large and the term is significant. For further simplicity, it is assumed that q_{xy} and q_i are not affected nearly as much as q_z. Now the electronic partition function is,

$$q_e = \exp(U/kT) \qquad (14)$$

and recalling that $\theta = \frac{N_e}{N}$ (13) becomes

$$\mu = U + \theta\frac{\partial U}{\partial \theta} + kT\frac{\partial \ln q_z}{\partial \theta} \qquad (15)$$

Thus the quantity required, ΔE, is

$$\frac{\Delta E}{kT} = \frac{\theta}{kT}\frac{\partial U}{\partial \theta} + \frac{\partial \ln q_z}{\partial \theta} \qquad (16)$$

It should be noted that q_z is a function of the shape of the Born-Oppenheimer curve so that if this curve can be calculated as a function of θ, the whole problem is solved. Of course this calculation is much too complicated for any real system. Some insight could be gained by doing the calculation for a σ bond between two 1S orbitals or perhaps even a 1S orbital and a SP^3 hybrid. A first beginning might be to add an electrostatic term to the hydrogen molecular ion and use it as a prototype for the charge transfer bond and then use the hydrogen molecule as a prototype for chemisorption without charge transfer. But these calculations are beyond the scope of this thesis. What is clear is that the fraction of the adsorbed molecules which are ionized are functionally related to the position of the Fermi level and hence the bulk impurity doping. It is important to note that the relationship is not nearly so straightforward as Volkenshtein has supposed.

Of course, if charge transfer equilibrium is not attained in a kinetic situation, then θ will be somewhat less than the equilibrium value and surface properties must be measured to characterize the system.

D. Model for Application of the Theory

It is interesting to examine the results of the theoretical development of chemisorption for a model which is simple enough to

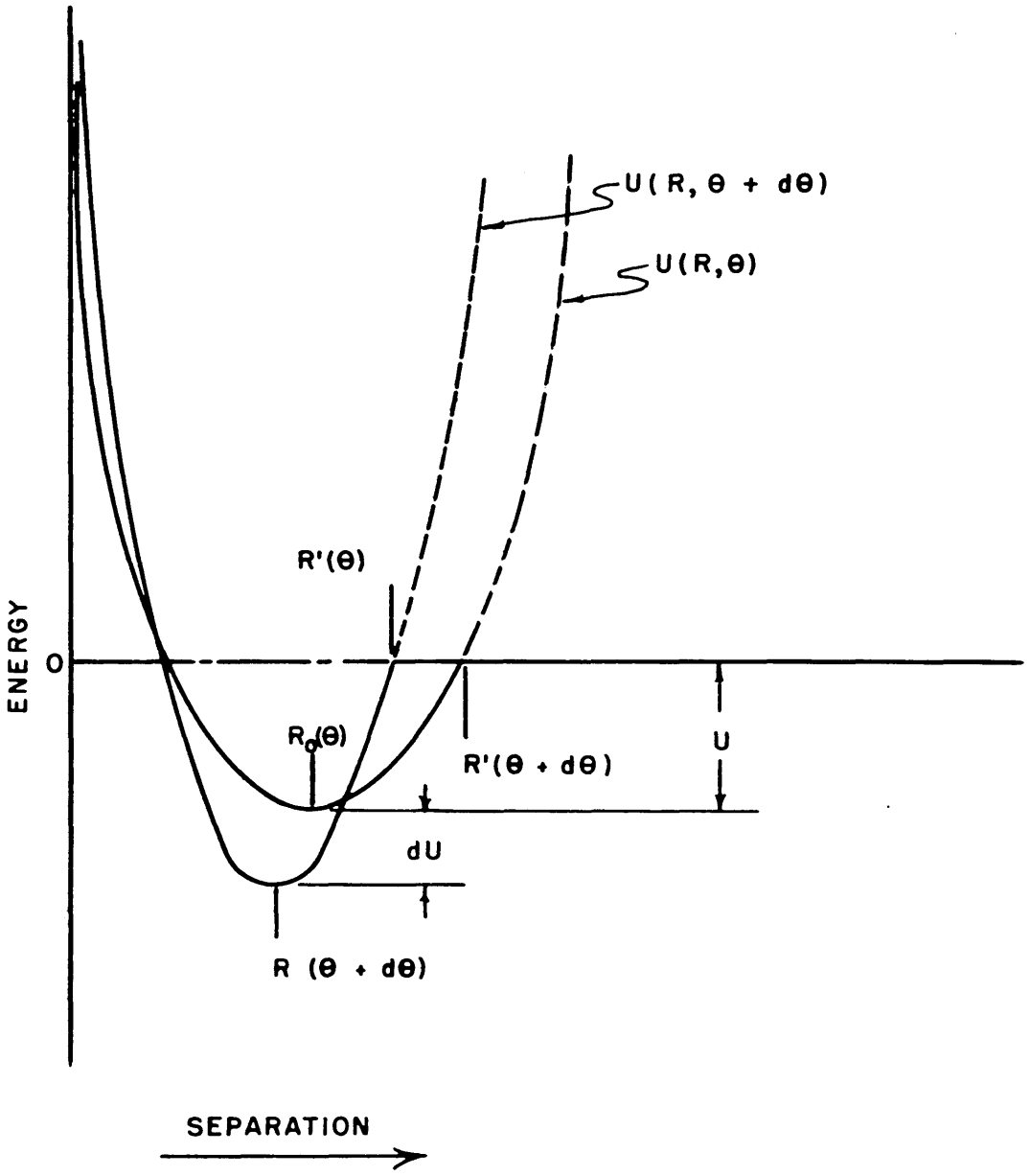

PARABOLIC MODEL FOR CALCULATING U - Ø

Figure 3.

represent analytically without recourse to any quantum mechanical calculations. One possibility is illustrated in Figure 3. Here the Born-Oppenheimer potential is approximated by a parabola about the minimum in the true potential curve, which occurs at a separation, Ro. Where the parabola intersects zero energy, the model changes abruptly to give an horizontal line for all separations greater than R'. Thus the energy can be expressed as:

$$u(R) = \frac{1}{2} K [-(R' - R_o)^2 + (R - R_o)^2] \qquad (17)$$

where:

$u(R)$ = energy as a function of R
R = separation coordinate
K = force constant
R' = value of R where $u(R) = 0$
R_o = value of R where $u(R)$ is a minimum

The dissociation energy, U, can be written as:

$$U = \frac{1}{2} K(\Delta R)^2 \qquad (18)$$

where:

$$\Delta R = (R' - R_o).$$

E. Calculation of U-ϕ

If we write (18) for the case of an ionized and dissociated species then the dissociation energy describes the electronic energy of the chemisorption bond, taking the vacuum level of the solid as an

energy datum (see Figures 1 and 2). Equation (18) can now be differentiated to give the first term in equation (16).

$$\theta\frac{\partial(U/kT)}{\partial\theta} = \frac{\theta K}{kT}(\Delta R)\frac{\partial(\Delta R)}{\partial\theta} + \frac{\theta}{2kT}(\Delta R)^2\frac{dK}{d\theta} \tag{19}$$

A parabolic energy describes the familiar harmonic oscillation with energies,

$$U(\nu) = -U + (n + \tfrac{1}{2})h\nu \tag{20}$$

where:

h = Planck's constant
ν = fundamental vibration frequency
n = vibrational quantum number

For values of $\frac{h\nu}{kT} < 1$ it can be shown (62) that

$$\ln q = kT\left[\ln\frac{h\nu}{kT} - \frac{1}{2}\frac{h\nu}{kT} + \frac{1}{24}\left(\frac{h\nu}{kt}\right)^2 - \frac{1}{2880}\left(\frac{h\nu}{kt}\right)^4 \ldots,\right] \tag{21}$$

Remembering that the frequency is given by

$$= \frac{1}{2\pi}\sqrt{\frac{k}{m}} \tag{22}$$

where m is the vibrational mass, and differentiating (21) one obtains for the second term in equation (16):

$$\frac{\partial \ln q_z}{\partial\theta} = \frac{1}{8\pi^2 m\nu^2}\left[1 - \frac{h\nu}{kT} + \frac{1}{12}\left(\frac{h\nu}{kT}\right)^2 - \frac{1}{720}\left(\frac{h\nu}{kT}\right)^4 \ldots\right]\frac{dk}{d\theta} \tag{23}$$

Thus, the quantity, E, in figure (2) which is really $(U - \phi)$ can be written:

$$\frac{\Delta E}{kT} = \theta K\frac{(\Delta R)}{kT}\frac{\partial(\Delta R)}{\partial\theta} + \left\{\frac{\theta}{2}\frac{(\Delta R)^2}{kT} + \frac{1}{8\pi^2 m\nu^2}\left[1 - \frac{h\nu}{kT} + \frac{1}{12}\left(\frac{h\nu}{kT}\right)^2 + \frac{1}{720}\left(\frac{h\nu}{kT}\right)^4\right]\right\}\frac{dK}{d\theta} \tag{24}$$

The fundamental restriction on equation (24) (i.e., that $h\nu/kT \ll 1$) will always be met for catalytic systems whose activation energies are several times greater than $h\nu$. If $h\nu/kT$ is near unity, then the series in $h\nu/kT$ of equation (24) is approximately $\frac{1}{12}$. If $h\nu/kT \ll 1$ then the series reduces to unity. Thus, at low temperatures and/or large $h\nu$ (i.e., high energy system bonds) the series will reduce the weighting of the third term in (24) by as much as 0.1 of its value at higher temperatures and smaller values of $h\nu$. In other words, the steeper the parabola in units of kT the less will be the difference between the vibrational energies with and without charge transfer.

The quantity, (ΔR), in equation (24) can be thought of as an interaction distance and will be equal to few angstroms. The vibrational mass, m, may take on values as low as 1 amu for hydrogen or as high as 16 for oxygen bonds. Using such values and fundamental vibration of 10^{13} cycles per second one obtains:

$$\frac{(\Delta R)^2}{kT} = \frac{(10^{-8})^2}{(1.38 \times 10^{-16})\ (600)} = 1.18 \times 10^{-3} \text{ sec}^2/\text{g}$$

$$\frac{1}{8\pi^2 m^2} = \frac{1}{8\pi^2 (91 \times 10^{-28})\ (10^{13})^2} = 1.4 \times 10^{-2} \text{ sec}^2/\text{g}$$

The value of 10^{13} cycles per second corresponds to about 2 kT at 600°K so that the series will reduce the vibrational term by another factor of ten. At lower frequencies the vibrational term assumes more importance, and it is at these conditions that one would expect a catalytically active system since the activation energy will usually be several $h\nu$. For example, if ν is as low as 10^{12}

cycles per second, then the vibrational contribution will be 100 to 1000 times as great as the electronic portion. Thus, if the derivative $dK/d\theta$ is appreciable (i.e., if charge transfer changes the force constant appreciably), then its effect on the vibrational energies is a more important factor in determining the value of ΔE and hence θ than its effect on the electronic energy.

It is now useful to consider the first term in equation (24). Reference to Figure 10 shows that there are two ways U can be changed by charge transfer. An increase in K results in a narrower parabola, and in order to maintain the same R' the curve moves down, causing U to increase. It is also possible that R' will change, in which case U will change with $\partial(\Delta R)/\partial\theta$. From the previous calculation on equation (24), however, one can readily see that the fractional change in (ΔR) must be 100 times as great as the fractional change in K in order for the first term to be significant. This does not mean that changes in (ΔR) are not important in catalysis. If the correct Born-Oppenheimer potential intersects the Leonard-Jones potential in the steep repulsive portion (see Figure 1), then small changes in R' either by a change in R_o or (ΔR) can have a large effect on the activation energy of desorption. They will have, however, little effect on θ and hence the pre-exponential terms of the rate constant will be relatively independent of (ΔR).

E. Effect of Impurity Doping

When the Fermi energy of a solid system is changed by doping the bulk with impurities, the work function might be expected to change. Dillon and Farnsworth (63), however, found only small changes (less than 0.1ev) for different n-type samples of germanium cleaned by ion bombardment. Gobeli and Allen (49) made a more systematic study on vacuum cleaned surfaces of both p-type and n-type silicon. They found only slight changes in the work function until the materials approach degeneracy at very high dopant levels where the change is very great for even small changes in the Fermi energy.

A decrease in the work function, ϕ, for donor surfaces will result in less perturbation of the sorption bond before charge transfer equilibrium is achieved. This would increase U and R_o and thus tend to cause a decrease in the activation energy of desorption. An increase in ϕ has the same effect on acceptor surfaces.

Since, as shown earlier, the vibrational term is the dominant term for systems of interest as catalysts in equation (24), it can be simplified to give:

$$\frac{U - \phi}{kT} = \frac{1}{2K} \frac{dK}{d\theta} \tag{25}$$

If $U - \phi$ is a few kT (valid for small θ), then the Fermi distribution (equation (8)) may be adequately approximated by the Boltzman distribution, and using (25) it can be written

$$\ln(1 - \theta) = \frac{-1}{2K} \frac{dK}{d\theta} \tag{26}$$

which can be integrated to give

$$\ln \frac{K}{K^o} = -2\left[(1 - \theta)\ln(1 - \theta) + \theta\right] \qquad (28)$$

Equation (28) is a monotonically increasing function and is valid for small θ. By reference to equation (8) the reader can see that when $dK/d\theta = 0$ then $\theta = \frac{1}{2}$ and in the region of $\theta = \frac{1}{2}$, $\frac{K}{K^o}$ is larger than the value calculated from (28), but it still increases monotonically in θ. Thus, as the system is more perturbed as a result of a change in the work function, the fraction of the adsorbed species ionized increases. Since perturbation of the system raises the activation energy for n-type adsorbents, it is concluded that the variation in the fraction of adsorbed ionized species is parallel with the variation in the activation energy. Thus, if an ionized specie is kinetically important, one would expect to find compensation in the Arrhenius equation. If an un-ionized specie is important, then no compensation or even negative compensation (i.e., the pre-exponential increases when the activation energy decreases) would be expected. In the latter case one would expect to find the severe effects of poisoning and/or promotion which are present in many catalytic systems. For p-type adsorbents the reverse is true, i.e., un-ionized species result in compensation.

Measurements of catalysis on hydrogen reduced germanium surfaces have been made for hydrogen deuterium exchange (37 and 53), ortho-parahydrogen conversion (37), formic acid decomposition (53), and ethanol decomposition (32). In all of these cases the activation energy is related linearly to the logarithm of the pre-exponential,

although the slope of E_a versus ln C^o is always such that complete compensation never occurs. For the hydrogenation-dehydrogenation reactions the rates are highest on p-type samples. In the case of dehydration of formic acid there is no perceptible correlation between the rate of reaction and the conductivity type.

Assuming charge-transfer achieves thermodynamic equilibrium, these data seem to indicate that for hydrogen treated germanium surfaces, hydrogenation reactions involve in the rate limiting step an ionized surface specie for n-type reactants and an un-ionized specie for p-type reactants.

Conductivity measurements (64) indicate that adsorption of hydrogen increases the p-type nature of the surface conductivity of germanium, and it is expected in the light of the above reasoning that this enhancement in p-type conductivity will be less the more p-type the original surface. Thus it may be expected that the hydrogenation of ethanol, for instance, on clean germanium surfaces will increase the p-type nature of the surfaces and result in increased p-type conductivity. This increase in p-type conductivity should diminish with increasing rates of dehydrogenation.

VI. DESIGN OF EXPERIMENT

A. Selection of a System

Since a knowledge of the electrical properties of the surface is essential for developing and testing any electronic theory of contact catalysis, the ultrapure semiconductor metals whose bulk properties have been so well characterized seem to be best suited for the catalyst. Describably "clean" surfaces of germanium can be reproducibly achieved by either ion bombardment in high vacuum or cleavage in vacuum. Techniques for making surface measurements on germanium are well developed (41). Thus, germanium is selected as a promising material for initial study.

The mechanism discussed in Section III, Theoretical Background, for ethanol decomposition on elemental semiconductors suggests that p-type germanium would favor dehydrogenation while n-type would favor dehydration. Such a change in selectivity would be a particularly stringent test of the theory. Frolov and Krylov (32) have demonstrated the activity of germanium for ethanol decomposition, though, as noted earlier, no concurrent electrical measurements were made and no attempt was made to achieve an electrically describable surface. Earlier work here at M.I.T. (48) confirmed that crushed germanium will catalyze the decomposition of ethanol, but the details of Frolov and Krylov's work were not reproduced, and the tests were not extensive enough to test the predicted change in selectivity. Moore et al, as noted before, showed that a shift in selectivity with electrical properties occurred in the decomposition

of formic acid over germanium. Thus the ethanol-germanium system seemed to be well suited for making the definitive studies which are required to provide a critical test of the charge transfer theory, particularly with respect to catalyst selectivity.

One possible difficulty in using the germanium system is that for the range of temperatures for which it exhibits activity for ethanol decomposition the intrinsic charge carrier concentration is of the order of 10^{18} per cc. The work of Frolov and Krylov (32), however, showed marked effects of doping at concentrations as low as 10^{15} per cc. It is possible that there is a migration of dopant materials to the surface, or a wider band gap at the surface due to oxygen extraction from ethanol. It is also possible that the surface does not attain charge transfer equilibrium and hence it would be the steady state concentration of charge carriers rather than the thermodynamic value which would affect the kinetics.

B. Experimental Program

The experimental program which is proposed includes (1) Measurements of the kinetics of ethanol decomposition over several samples of crushed germanium with similar electrical properties, but with different dopants, (2) Concurrent measurement of the surface conductivity, the surface recombination velocity of current carriers, and reaction kinetics of ethanol decomposition on samples of n- and p-type germanium.

In order to interpret the results of the electrical measurements it is necessary to conduct them on a well-defined geometric shape. The usual procedure is to use a wafer thin enough so that the electrical properties of the surface make a measurable contribution to the electrical properties of the sample. Measurement of the kinetics, however, requires a large surface area (i.e., several hundred square centimeters). The difficulty of producing such a large surface area on a sample thin enough to make electrical measurements and with a well-defined geometric shape is formidable. Thus, it was decided to measure the catalytic activity on surfaces produced by cleavage in a vacuum crushing apparatus (see Appendix A. Experimental Apparatus for details) and monitor the surface electrical properties on a thin wafer cleaned in situ by argon ion bombardment.

In this thesis the design and construction of the equipment necessary to carry out the above experimental program were completed and key experiments to illustrate the facility of the design were conducted. The kinetics of ethanol decomposition on n-type germanium cleaved in vacuum were measured, and similar studies were made on the cleaved surfaces after treatment with hydrogen. The latter work seemed pertinent because of the number of studies which have recently been reported on hydrogen treated germanium surfaces produced in air. Some surface electrical measurements on etched germanium were also conducted in the atmosphere to test out the experimental procedure for making the electrical measurements in situ.

C. Experimental Apparatus and Procedure

1. Preparation of Catalyst Samples

The large surface area necessary for the kinetic measurements is produced by crushing massive chips of germanium under vacuum by impact with a magnetically operated hammer. This produces largely (111) surface since this is a plane of easy cleavage (67) for germanium. The details of the crushing procedure are presented in Appendix B. Experimental Procedure. The details of the crushing apparatus are recorded in Appendix A. Experimental Apparatus.

The crushed catalyst is then added to the reactor through a double break seal. This method permits the addition of approximately 0.2-1.0 square meters of virgin (111) surface to the reactor at a pressure of 10^{-8} to 10^{-9} torr. At this pressure there is not enough gas in the whole system to contaminate an appreciable portion of the surface.

2. Electrical Measurements

The wafer for the electrical measurements is cut from the (111) plane of the same crystal used to supply the crushed material. The wafer is cut into Hall effect bridges and optically ground to 0.005 inches thick. The slice is etched and platinum leads are welded to the sample. It is mounted in the system on a quartz optical flat and the necessary electrical connections made. It is possible to position an electrode 0.001 inch away from the surface during a run by laying it on a set of 0.006 inch thick quartz

shims (see Figure 4). Movement of the electrode is accomplished in situ by means of a bellows assembly. The electrical measurements are made with square wave pulses and an oscilloscope. The details of the measurement technique are discussed in Appendix D. Measurement and Interpretation of Electrical Properties, and the vacuum cell in which the measurements are made is described in Appendix A. Experimental Apparatus. Appendix B. Experimental Procedure gives the full details of the preparation of the electrical samples.

3. Kinetic Experiments

A block diagram of the vacuum reactor is seen in Figure 5, a photograph of the equipment is shown in Figure 6, and a complete description of the system is found in Appendix A. Experimental Apparatus. Purified anhydrous ethanol was held at 0°C in an ice bath and metered into the system through a trap containing crushed germanium and then passed through freshly-flashed aluminum getter. It then passes through the reactor which is maintained at the desired temperature by a specially fitted heating mantle.

A sample of the reaction mixture passes continuously through an on-line mass spectrometer which was designed and constructed (see Appendix A. Experimental Apparatus) especially for these studies, and the remaining gas bathes the wafer on which the electrical measurements are made. An internal heater underneath the sample support permits control of the sample temperature. All temperatures are measured with chromel-alumel thermocouples. At the close of the

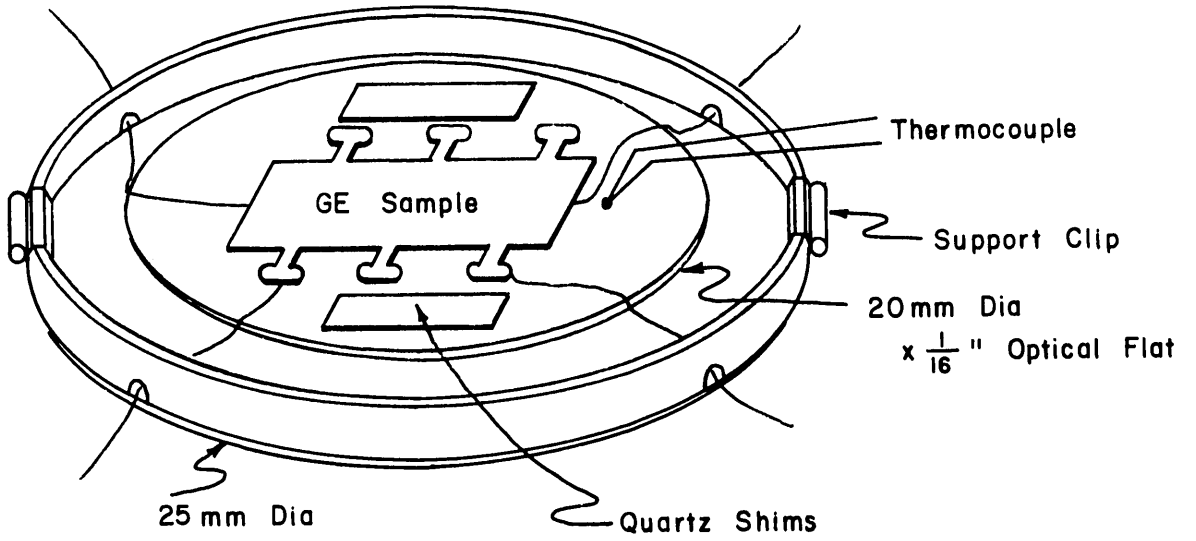

SAMPLE HOLDER DETAIL

Figure 4.

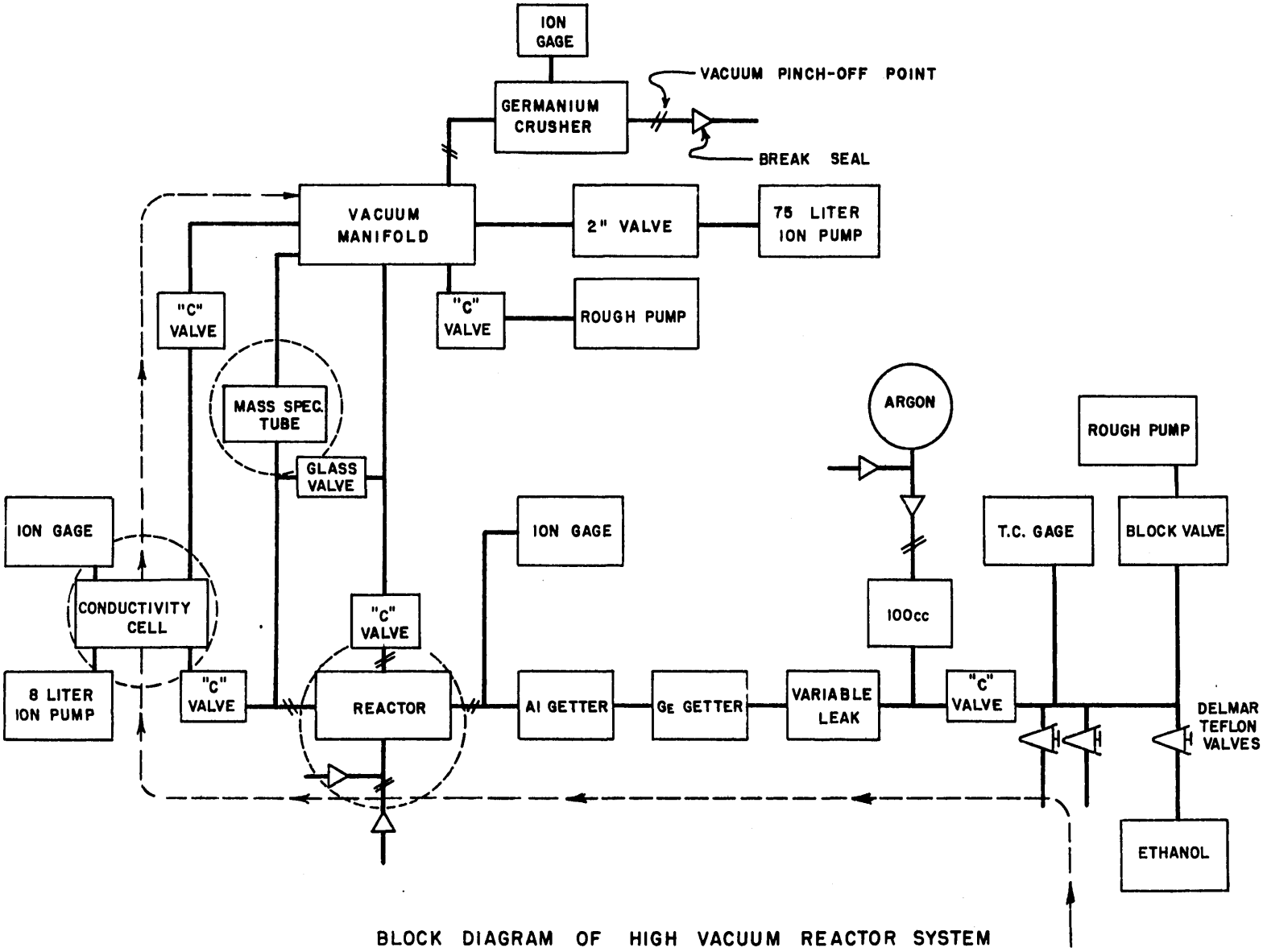

BLOCK DIAGRAM OF HIGH VACUUM REACTOR SYSTEM
Figure 5.

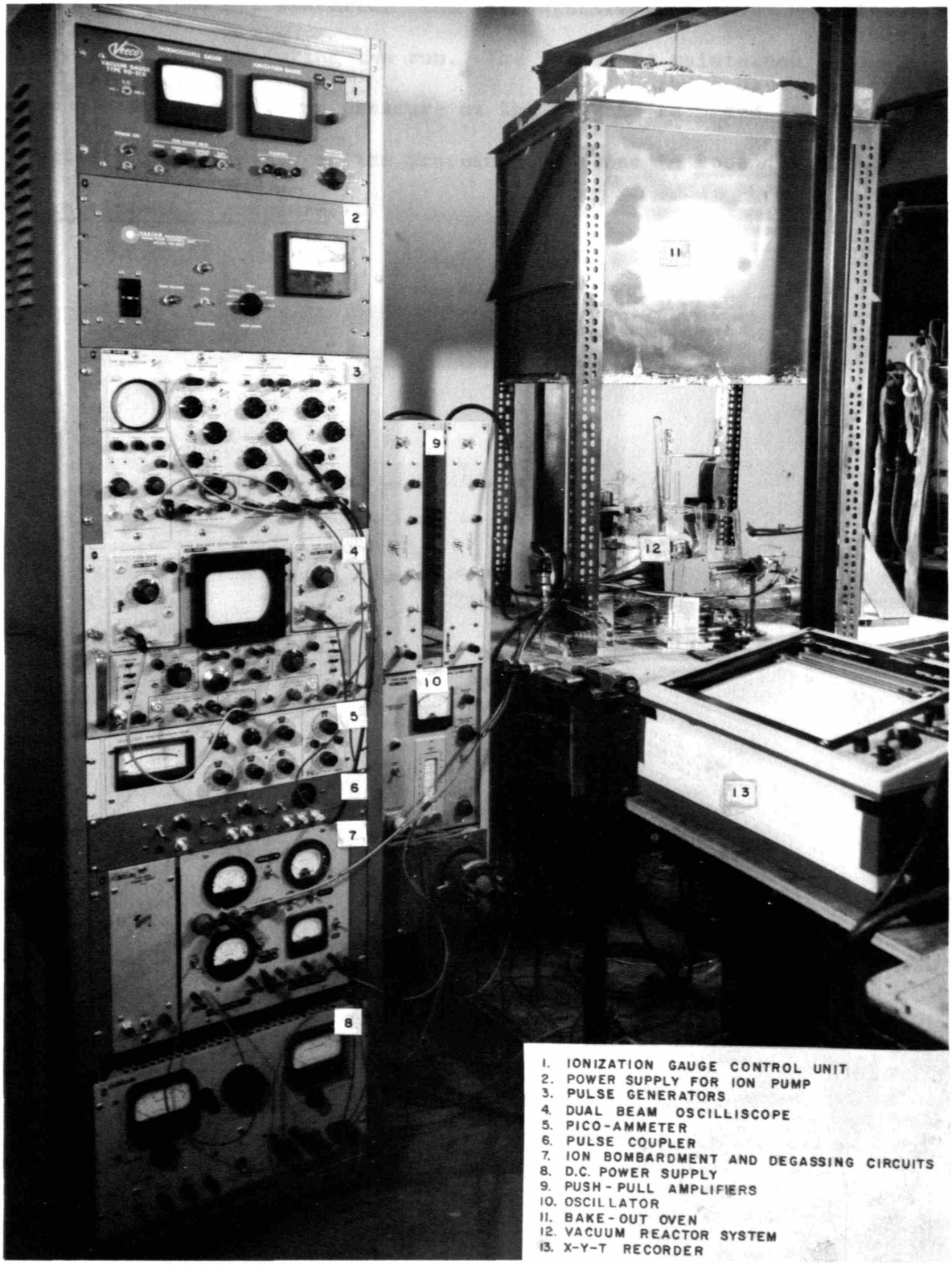

OVERALL VIEW OF APPARATUS

Figure 6.

run the leak rate and pressure drops through the various sections of the apparatus are measured. The mass spectrometer gives a continuous pressure reading during the run. The vacuum is maintained by a 75 liter ion pump, and pressure at the pump is recorded. A more detailed description of the procedure is found in Appendix B. Experimental Procedure.

VIII. EXPERIMENTAL RESULTS

A. Ethanol Decomposition on N-Type Germanium

1. Studies on Clean Surfaces

The decomposition of ethanol was investigated on clean surfaces of n-type germanium produced by cleavage in vacuum. The germanium used had been doped to a level of $10^{20}/cm^3$ with antimony. The kinetics of the decomposition reaction were studied between 200°C and 270°C at a pressure of 10^{-3} mm Hg. The flow rate was 6.29×10^{-10} moles per second and the surface area was 800 $(cm)^2$. Under these conditions conversions of ethanol to acetaldehyde and hydrogen up to 50 percent were measured. No evidence of ethylene or water was found in the mass spectra. Thus, on n-type germanium the total measurable decomposition occurs via

$$C_2H_5OH \longrightarrow H_2 + C_2H_4O \qquad (29)$$

This result is in agreement with Volkenshtein's proposed mechanism (See II. Theoretical Background, equations (4) to (6)). Frolov and Krylov (32), who studied ethanol decomposition on germanium crushed in air and subsequently reduced in hydrogen, found only reaction (29) on both n-type and p-type germanium. In addition, they found that p-type germanium was more active than n-type for reaction (29). Both of these results are in contradiction to Volkenshtein's mechanism.

The decomposition data are listed in Table I and presented graphically in Figures 7 and 8. The maximum conversion based on

TABLE I

DECOMPOSITION OF ETHYL ALCOHOL ON N-TYPE GERMANIUM

Run No.	Pressure Mass Spec. (Arbitrary Units)	Temp. °C	$1/T_{°K} \times 10^3$	P_{EOH} (Arbitrary Units)	P_{EOH} Pressure Corrected	$\ln \frac{P^o_{EOH}}{P_{EOH}}$	P_A (Arbitrary Units)	P_A Pressure Corrected	$\ln \frac{P^o_{EOH}}{P^o_{EOH} - P_A}$	Percent Conversion Ethanol	Percent Conversion Acetaldehyde
					CLEAN SURFACE						
1	3.20	200.50	2.111	70.50	72.70	0.0618	4.00	4.12	0.0536	6.02	5.32
2	2.60	260.00	1.875	30.70	38.98	0.6845	29.82	37.85	0.6710	49.60	50.10
3	3.35	234.75	1.970	70.85	69.81	0.10075	11.80	11.01	0.1526	9.76	14.60
4	3.35	224.00	2.011	76.65	75.55	0.02273	9.05	8.92	0.1222	2.33	11.80
5	3.30	215.50	2.047	72.75	72.75	0.0611	6.55	6.55	0.08715	5.96	8.68
6	2.80	249.50	1.899	42.50	50.10	0.4339	20.80	24.50	0.3830	35.30	33.30
7	3.00	235.60	1.966	57.50	63.20	0.1918	12.69	13.96	0.1989	18.30	18.50
8	3.30	267.50	1.849	37.30	37.30	0.7280	48.75	48.75	0.9935	51.80	64.10
9	2.90	29.00		62.90	77.35						
					HYDROGEN TREATED SURFACE						
10	2.90	210.00	2.070	65.90	63.60	0.1070	0.65	0.628	0.0089	10.26	0.88
11	2.80	221.50	2.022	63.40	63.40	0.1095	1.30	1.300	0.01785	10.44	1.87
12	2.80	240.60	1.949	59.80	59.80	0.1680	2.20	2.200	0.305	16.40	3.12
13	2.80	264.25	1.862	55.00	55.00	0.2515	11.60	11.60	0.1781	22.30	16.70
14	2.80	256.50	1.889	57.70	57.70	0.2038	8.80	8.80	0.139	18.50	12.20
15	2.80	218.40	2.035	64.00	64.00	0.1000	2.16	2.16	0.03005	10.20	3.07
16	2.70	207.00	2.083	63.25	65.60	0.0706	1.70	1.75	0.0247	7.35	2.48
17	2.60	29.00		65.75	70.80						

P_{EOH} = Ethanol Partial Pressure

P_A = Acetaldehyde Partial Pressure

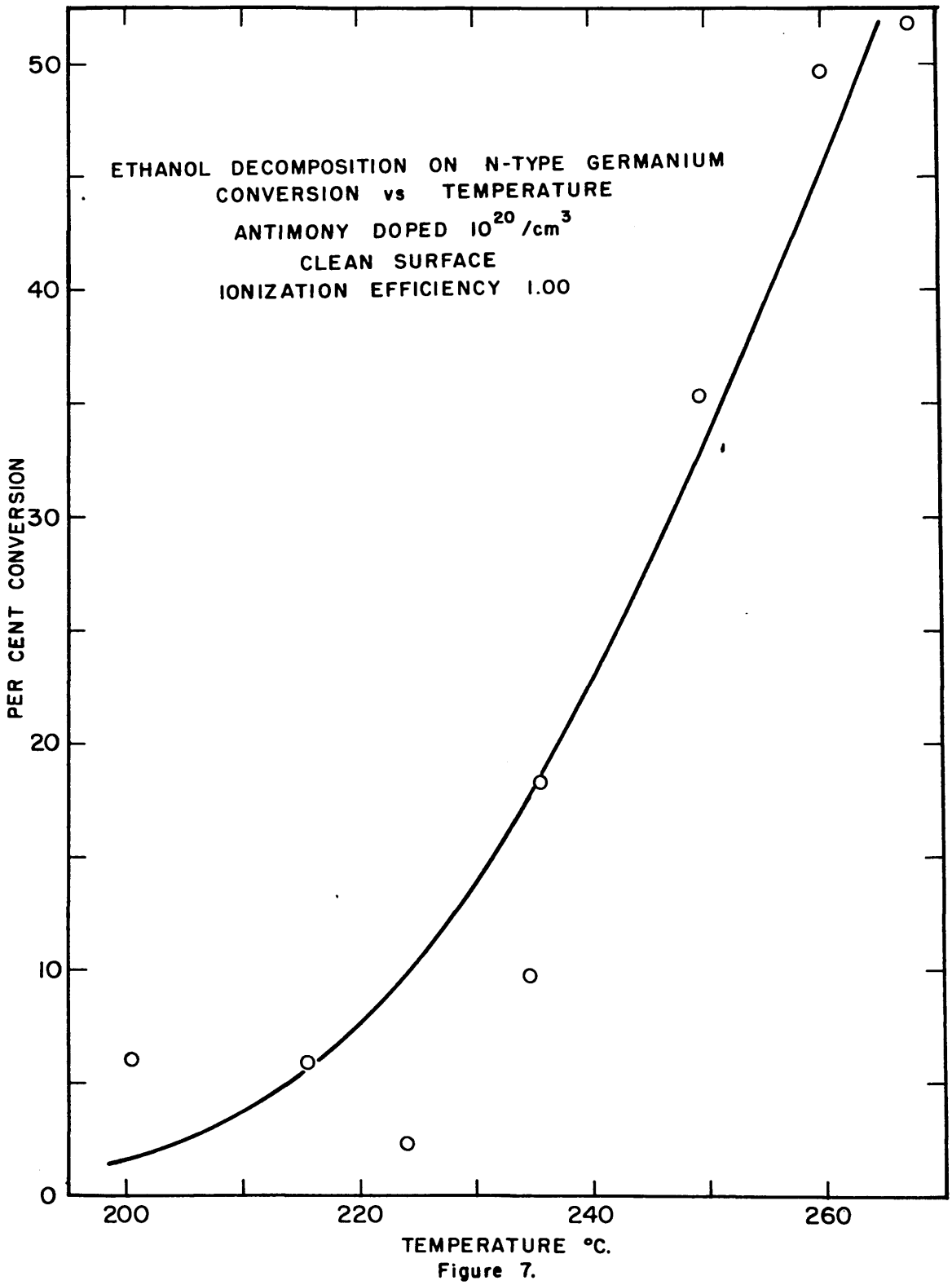
ETHANOL DECOMPOSITION ON N-TYPE GERMANIUM
CONVERSION vs TEMPERATURE
ANTIMONY DOPED 10^{20} /cm^3
CLEAN SURFACE
IONIZATION EFFICIENCY 1.00
PER CENT CONVERSION
0
10
20
30
40
50
200
220
240
260
TEMPERATURE °C.

Figure 7.

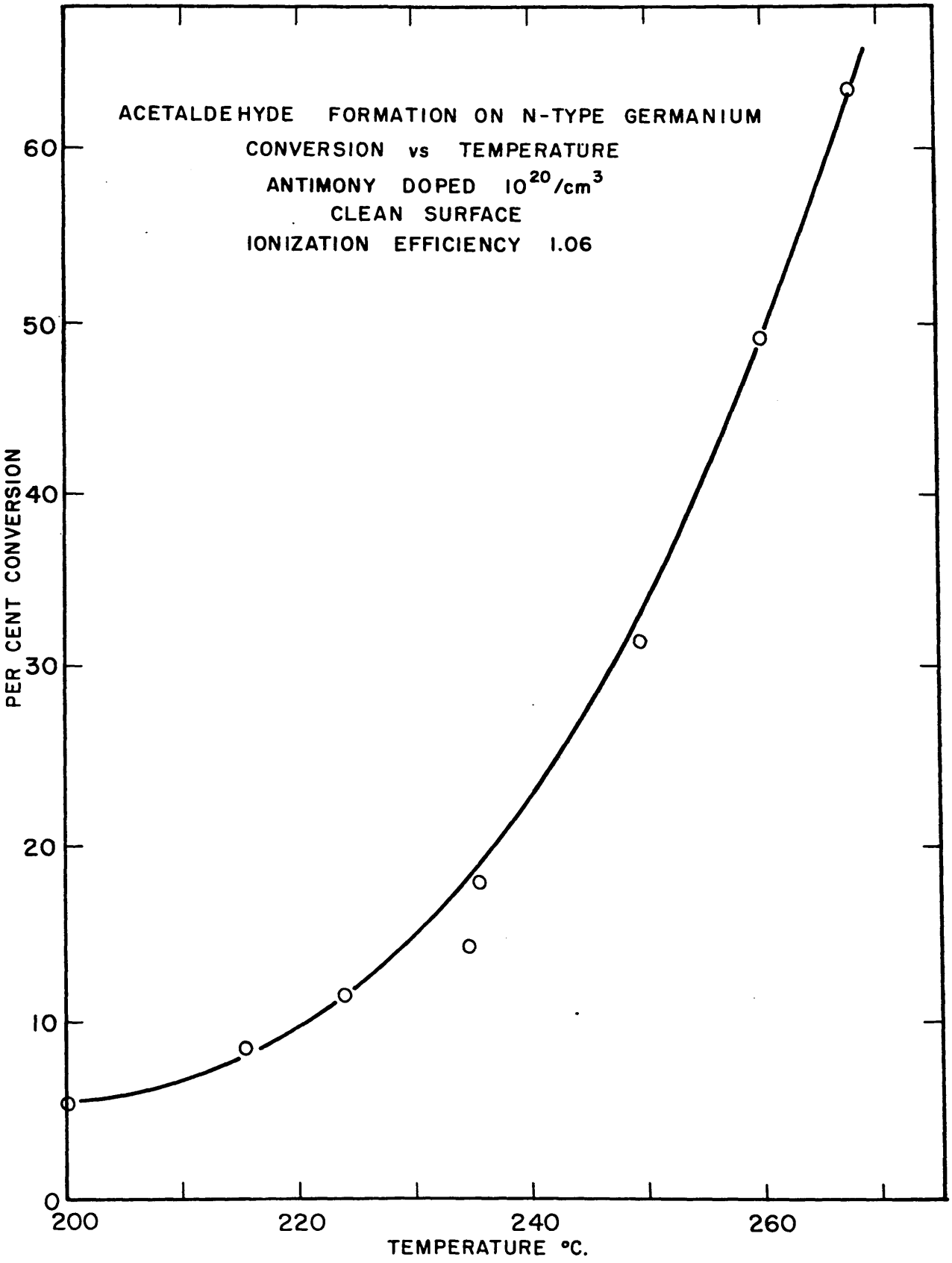
ACETALDEHYDE FORMATION ON N-TYPE GERMANIUM
CONVERSION vs TEMPERATURE
ANTIMONY DOPED $10^{20}/cm^3$
CLEAN SURFACE
IONIZATION EFFICIENCY 1.06
PER CENT CONVERSION
0
10
20
30
40
50
60
200
220
240
260
TEMPERATURE °C.

Figure 8.

ethanol decomposition (Figure 7) is 50 percent while that for acetaldehyde formation is 60 percent. In analyzing the mass spectra it was assumed that the relative ionization efficiency of acetaldehyde compared to ethanol is approximately unity. A value of 0.96 for this efficiency is reported by Humble Oil (55), and the U. S. Army Quartermaster Corps (56) found 0.79. An ionization efficiency of 0.85 would result in correspondence at the high conversions. It will be important in future work to make definitive measurements of these efficiencies with the r.f. mass spectrometer.

Another possible reason for the higher apparent conversions based on acetaldehyde may be that the 60 percent conversion point in Figure 8 is for some reason too high. This possibility will be discussed later.

Frolov and Krylov (32) found ethanol decomposition on germanium to be first order with respect to ethanol. Thus the data in Figures 3 and 4 were fitted to the first order rate equation:

$$\frac{dP_{EOH}}{d\Theta} = k_D W_c A P_{EOH} \qquad (30)$$

where:

P_{EOH} = ethanol partial pressure (mm Hg)
Θ = time (seconds)
a = specific surface area of catalyst (m^2/g)
W_c = catalyst weight (g)
k_D = specific rate constant $(M^2 sec)^{-1}$

Suitable substitution and integration results in:

$$\ln[\ln\frac{P^o_{EOH}}{P_{EOH}}] = -\frac{E_a}{RT} + \ln C_D + \ln\frac{aW_c^2 P_m}{(1-\epsilon)P_c F} \qquad (31)$$

where:

P^{o}_{EOH} = inlet partial pressure of ethanol (mm Hg)
P_{EOH} = outlet partial pressure of ethanol (mm Hg)
ϵ = porosity of catalyst bed
P_m = molar density [moles/m^3]
P_c = catalyst density [g/m^3]
C_D = decomposition pre-exponential
E_a = apparent activation energy

and:

$$k_D = C_D \exp(\frac{E_a}{RT})$$

Details of this integration are in Appendix E Mathematical Treatment of the Kinetic Data.

A plot of the left side of equation (31) versus reciprocal temperature should be a straight line (Arrhenius plot). The data are presented in this manner in Figure 9. An apparent activation energy of 27 Kcal per mole was calculated from the slope and the intercept gives 19.5 for the value of $\ln C_D$. There is considerable scatter in the low temperature data. This is not surprising as very small variations in the measured rate at low conversions can give large variations in the abscissa of Figure 9 since the logarithm of the pressure ratio is taken twice (see equation 31). The 27 Kcal activation energy was based on a fit of the high temperature points.

If the calculations are based on the formation of acetaldehyde, then the integrated rate equation becomes:

$$\ln[\ln\frac{P^{o}_{EOH}}{P^{o}_{EOH} - P_A}] = -\frac{E_a}{RT} + \ln C_A + \ln\frac{aW_c^2 P_m}{(1-\epsilon)P_c F} \qquad (32)$$

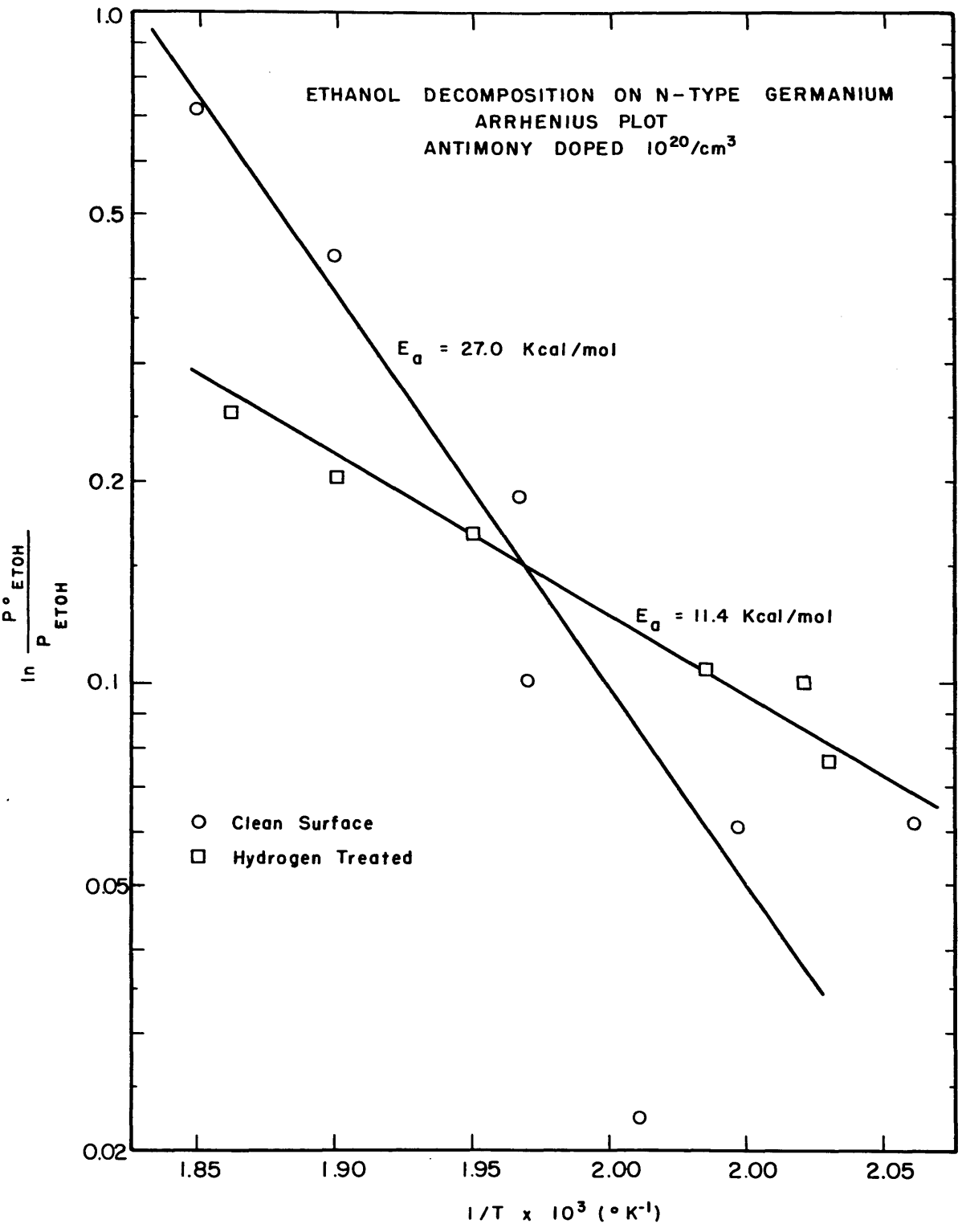
ETHANOL DECOMPOSITION ON N-TYPE GERMANIUM
ARRHENIUS PLOT
ANTIMONY DOPED $10^{20}/cm^3$
E_a = 27.0 Kcal/mol
E_a = 11.4 Kcal/mol
Clean Surface
Hydrogen Treated
$\ln \frac{P^\circ_{ETOH}}{P_{ETOH}}$
1.0
0.5
0.2
0.1
0.05
0.02
1.85
1.90
1.95
2.00
2.00
2.05
$1/T \times 10^3$ ($^\circ K^{-1}$)

Figure 9.

where:

P_A = partial pressure of acetaldehyde (mm Hg)

C_A = pre-exponential based on acetaldehyde $(M^2 \text{ sec})^{-1}$

An Arrhenius plot based on equation (32) is seen in Figure 10. If the low temperature data are neglected here also, then the 27 Kcal line is a good fit for the data. The dotted line shows a fit giving the low temperature points more weight. The activation energy based on this fit is only 21.6 Kcal/mole. The pre-exponential for the 27 Kcal line is given by $\ln C_A = 19.8$ compared with a value of 19.5 based on ethanol conversion.

In the Arrhenius plots (Figures 9 and 10) the high conversion point based on acetaldehyde (60 percent) is considerably higher than the line, while that based on the ethanol conversion (54 percent) is only slightly below the line. Because of the close correspondence between the intercepts, it is very likely that the 60 percent conversion is in fact anomalously high as suggested earlier.

2. Studies on a Hydrogen Treated Catalyst

After completion of the studies on vacuum crushed germanium, the catalyst was aged for 12 hours in 10^{-3} mm of hydrogen at 500°C. The decomposition reaction was then measured over the same temperature range (200°C to 270°C). The pressure was maintained at 10^{-3} mm Hg and the flow rate was 6.49×10^{-10} moles/sec. As before, only acetaldehyde and hydrogen were found in the reaction products. The

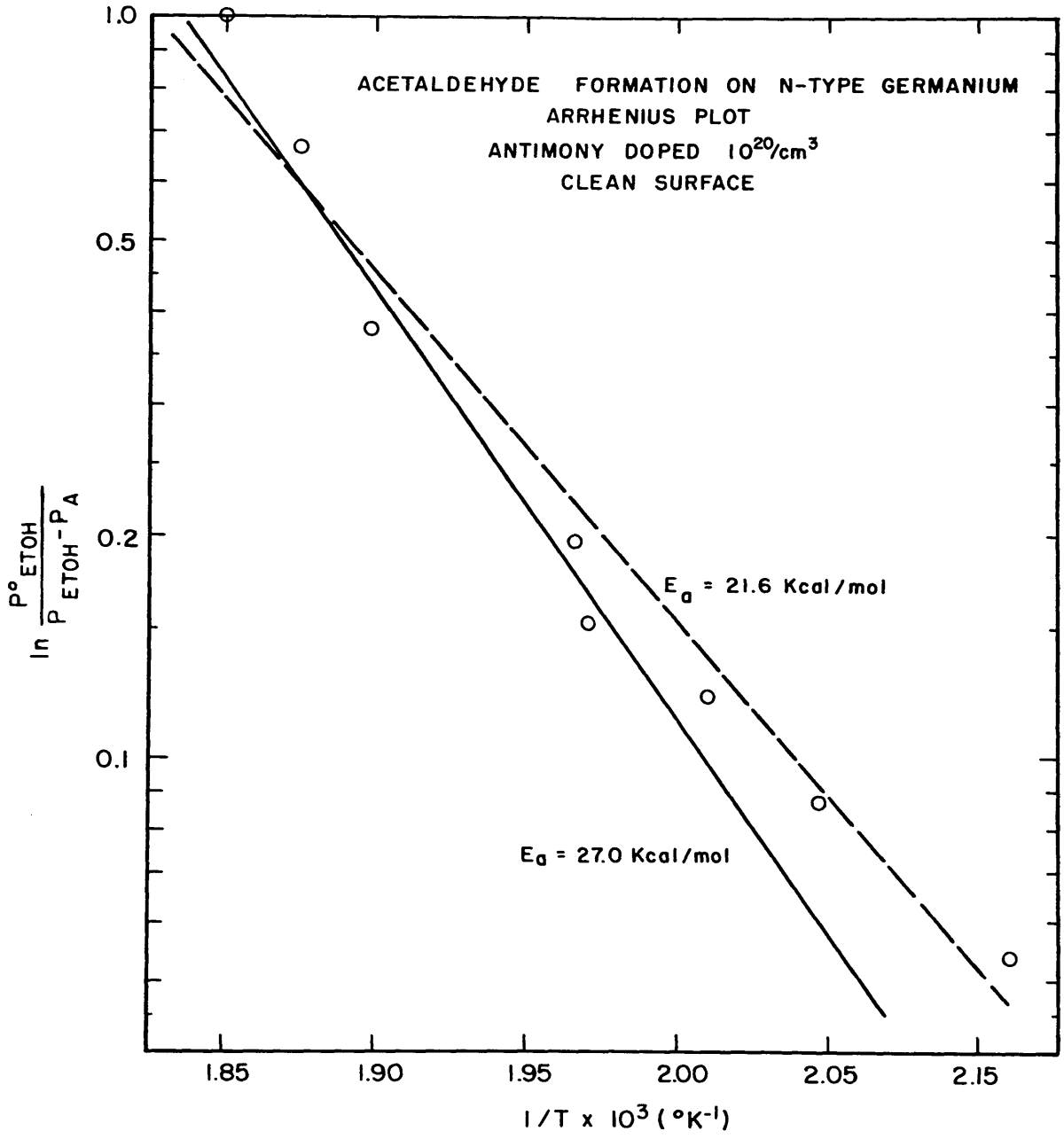
ACETALDEHYDE FORMATION ON N-TYPE GERMANIUM
ARRHENIUS PLOT
ANTIMONY DOPED $10^{20}/cm^3$
CLEAN SURFACE
E_a = 21.6 Kcal/mol
E_a = 27.0 Kcal/mol
$\ln \frac{P^o_{ETOH}}{P_{ETOH}-P_A}$
1.0
0.5
0.2
0.1
1.85
1.90
1.95
2.00
2.05
2.15
$1/T \times 10^3$ ($^oK^{-1}$)

Figure 10.

surface, however, was considerably less active. The decomposition data are seen in Table I and are presented in Figures 11 and 12. The maximum conversions were 17-18 percent. Conversions at the higher temperatures based on acetaldehyde were in fair agreement with those based on ethanol.

The data in Figure 9 show an activation energy of only 11.4 Kcal/mole for the hydrogen treated catalyst. The scatter is considerably less for this catalyst than for the untreated catalyst, and this is attributed to a greater familiarity with the operation of the equipment and hence better control of variables. The value of ln C_D calculated from the intercept of Figure 9 is 5.7. The Arrhenius plot for acetaldehyde formation (Figure 13) is much less satisfactory. The data show considerable scatter, especially at the lowest conversions, and the best fit line exhibits an activation energy (dotted line) twice that derived from the disappearance of ethanol. The 11.4 Kcal line is drawn through the two highest conversion points and this line gives ln $C_A = 5.6$, which is in reasonable agreement with the ethanol decomposition line. The value of 11.4 Kcal/mole is probably the more likely value for the activation energy.

It is possible that the low conversion points in Figure (9) which fall considerably below the 11.4 Kcal line are a result of bias in the calculation of acetaldehyde concentration in the product gas. The 29 peak in the mass spectra was used to calculate acetaldehyde conversions. Ethanol also exhibits a minor peak at 29. At

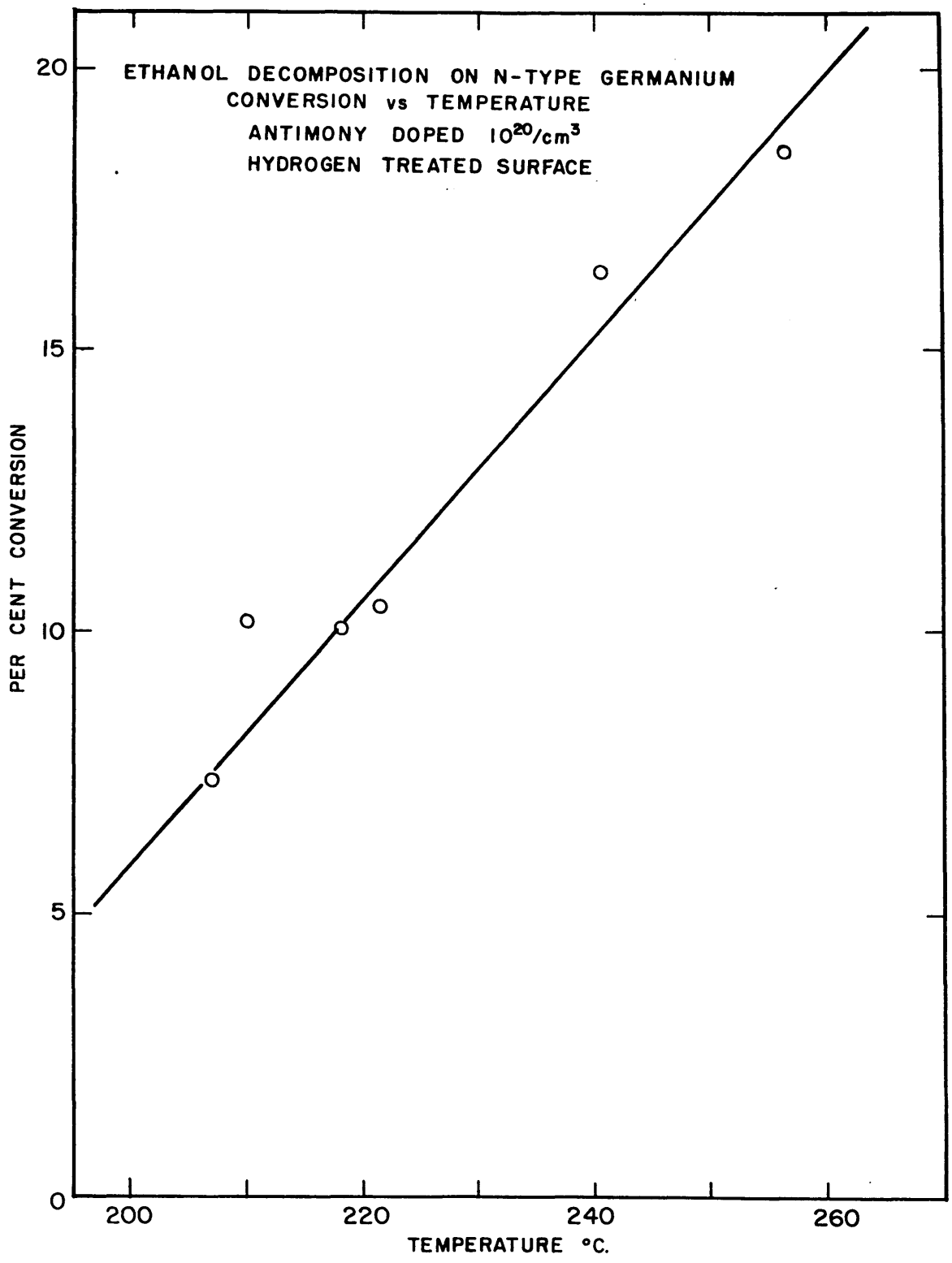
ETHANOL DECOMPOSITION ON N-TYPE GERMANIUM
CONVERSION vs TEMPERATURE
ANTIMONY DOPED $10^{20}/cm^3$
HYDROGEN TREATED SURFACE
PER CENT CONVERSION
0
5
10
15
20
200
220
240
260
TEMPERATURE °C.

Figure 11.

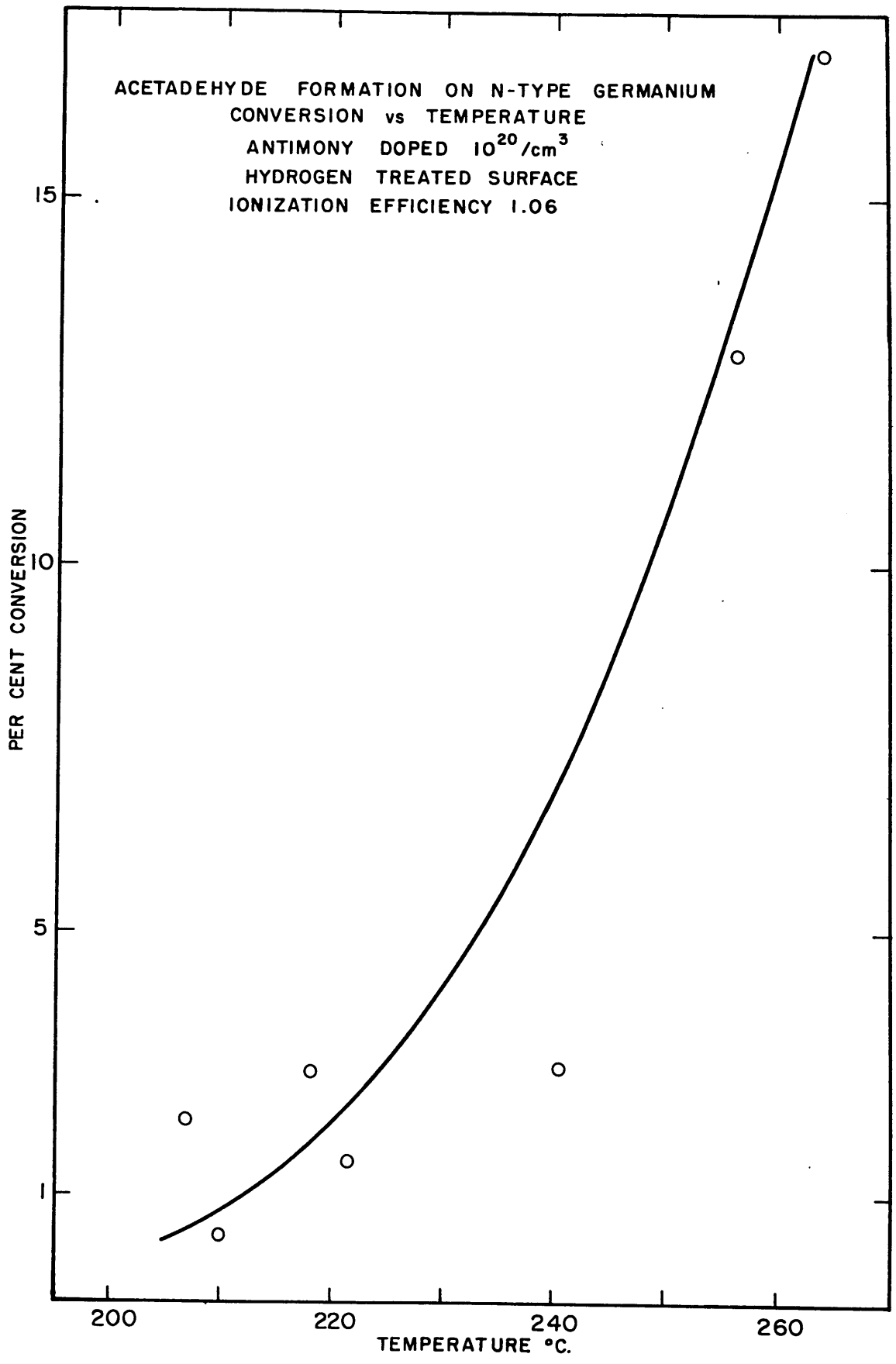
ACETADEHYDE FORMATION ON N-TYPE GERMANIUM
CONVERSION vs TEMPERATURE
ANTIMONY DOPED $10^{20}/cm^3$
HYDROGEN TREATED SURFACE
IONIZATION EFFICIENCY 1.06
PER CENT CONVERSION
15
10
5
1
200
220
240
260
TEMPERATURE °C.

Figure 12.

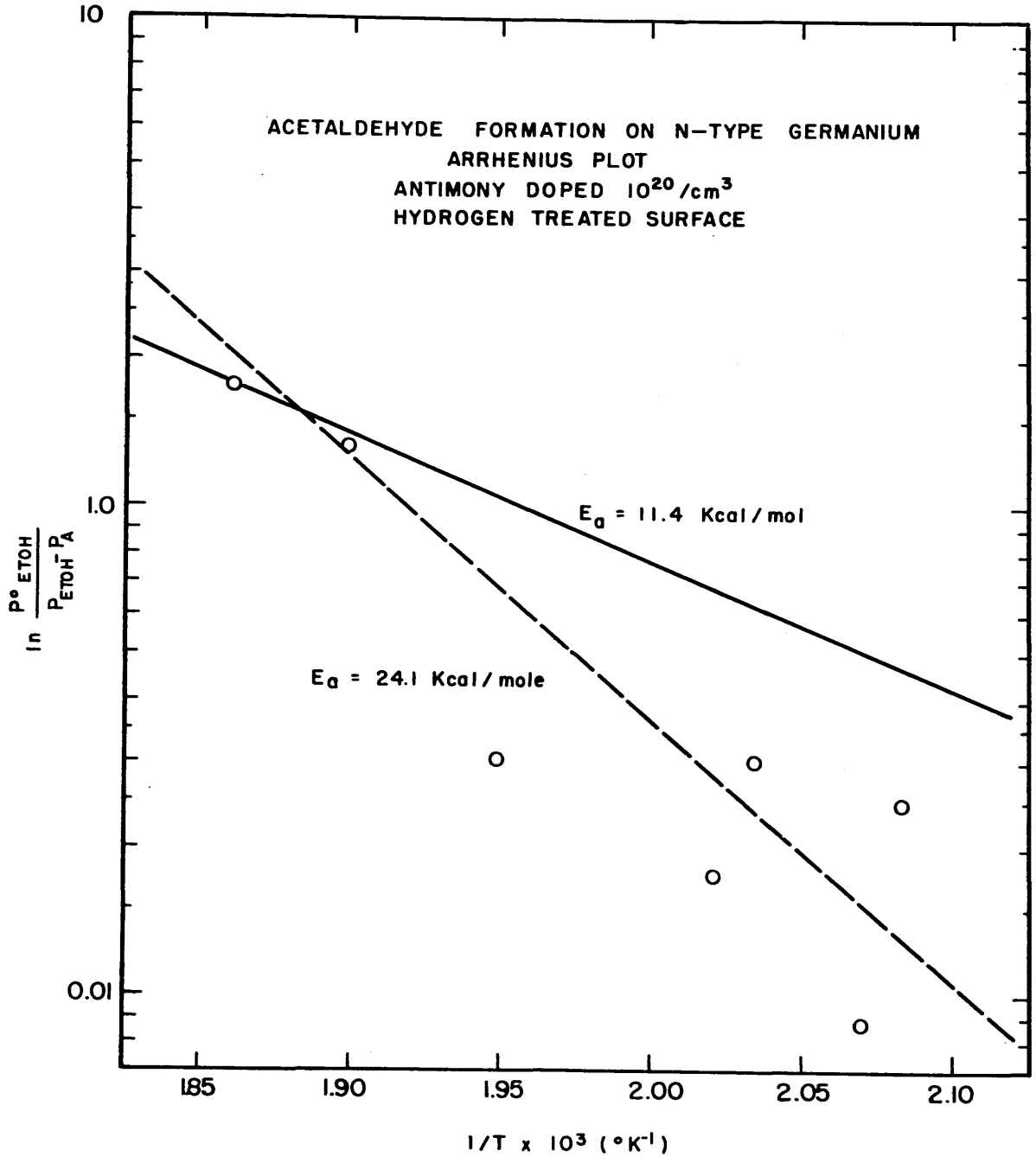
ACETALDEHYDE FORMATION ON N-TYPE GERMANIUM
ARRHENIUS PLOT
ANTIMONY DOPED $10^{20}/cm^3$
HYDROGEN TREATED SURFACE
E_a = 11.4 Kcal/mol
E_a = 24.1 Kcal/mole
10
1.0
0.01
$\ln \frac{P^o_{ETOH}}{P_{ETOH} - P_A}$
1.85
1.90
1.95
2.00
2.05
2.10
$1/T \times 10^3$ ($^oK^{-1}$)

Figure 13.

low conversions the 29 peak of the product spectrum is nearly equal to that for a pure ethanol spectrum. Thus, very small errors in the 29 peak result in large scatter of the acetaldehyde concentrations. Furthermore, if the ratio of the 29 peak to the 31 peak for ethanol (this ratio was re-established for each new run) is slightly too large, then the acetaldehyde concentrations at low conversions would all be much too low, while at high concentrations they could be quite accurate.

Assume, for example, that the 29/31 peak ratio for ethanol is in error just enough to raise the 11.4 Kcal line of Figure 10 so that ln C_A is 5.7 (the value of ln C_D obtained from Figure 9). Then the scatter of the low conversion points is reduced by about 1/8 and the points lie along the 11.4 Kcal line as drawn in Figure 10. Thus a small error in the ethanol spectrum could account for the observed discrepancy between the Arrhenius plot for ethanol decomposition and that for acetaldehyde formation.

3. Comparison with Previous Studies

The 27 Kcal activation energy found on vacuum crushed germanium is very close to activation energies measured by Frolov and Krylov (32) for decidedly n-type germanium, and ln C_D is greater than their value by a factor of 2. In other words, their work gave rates lower than this work by a factor of 10 .

Treatment of the catalyst with hydrogen reduces the activation energy and ln C_D, but there is over-compensation (i.e., the rate on the low activation energy surface is less than it is on the high activation energy surface). None of the systems investigated previously has shown such a result with changes in bulk doping ~~(see Figure 11)~~. Apparently the change produced by the presence of hydrogen is more drastic than could be expected if the hydrogen were merely a doping agent. It is known, for instance, that germanium forms several hydrides. Germanium mono-hydride is a solid at ordinary conditions (67), but no information is presently available (65) on the detailed thermodynamics of the system. It is possible, nevertheless, that the kinetics on the hydrogen treated surfaces are really characteristic of some sort of germanium hydride surface.

Maxwell and Green (66) have shown that when a clean surface is hydrogenated and then exposed to oxygen, the surface adsorbs at least a mono-layer of oxygen. During the uptake of oxygen no evolution of hydrogen or water occurs. Apparently an oxy-hydrogen surface complex is formed with the germanium. It is likely that a similar complex would form on oxygenated surfaces that are treated with hydrogen. Thus, the work of Krylov and Frolov (32) which was conducted on germanium crushed in air and then reduced with hydrogen may have been done on germanium catalysts unlike either the vacuum crushed catalyst or the hydrogen treated catalyst. It is not surprising, therefore, to find differences such as those which have been noted. In future work it would be interesting to examine the

kinetics on a sample from the same single crystal whose surfaces were (1) cleaned in vacuum, (2) cleaned in vacuum and treated with hydrogen, (3) cleaned in vacuum and treated with oxygen, then hydrogen, and (4) cleaned in air and treated with hydrogen.

B. Electrical Measurements

1. High Temperature Welded Contacts

It is necessary to anneal the surface of the conductivity samples after ion bombardment. To accomplish this the sample, including the electrical leads, must be held between 500°C and 600°C for several hours (33). Thus, the contacts used to make the electrical measurements must be stable at these temperatures. Handler (69) used welded molybdenum leads at high temperatures in a similar study, but it was found that the molybdenum-germanium weld is extremely brittle, so much so that it was not possible to make the necessary auxiliary connections to the molybdenum leads.

Welded contacts with a number of other metals were tried, and platinum was found to give the best results, although even the platinum-germanium weld is quite brittle. Nevertheless, it is possible to handle the samples and make the required connections to integrate the test samples into the measuring circuit without breaking the contacts.

2. Conductivity Measurements with an Ordinary Single Input Amplifier

Figure 14 gives the schematic diagram for making the electrical measurements. While any DC bias too great for the oscilloscope

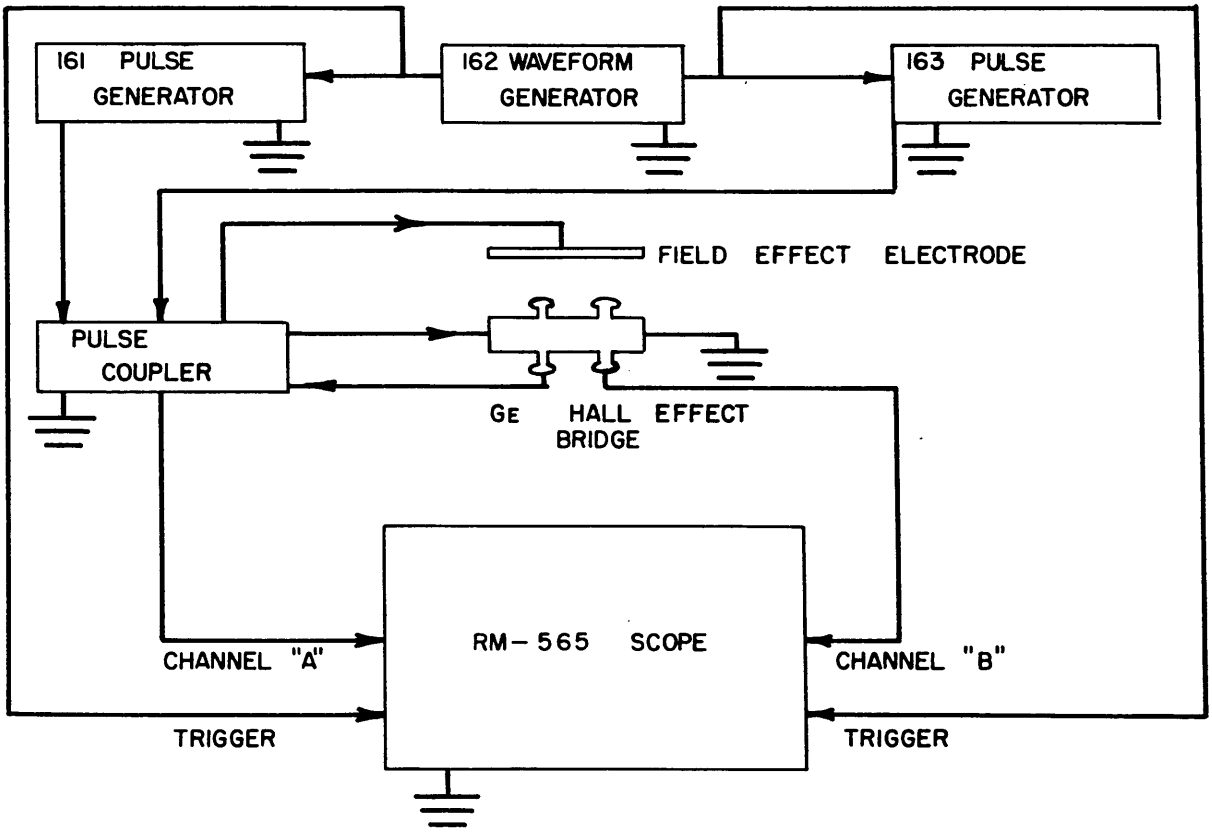

BLOCK DIAGRAM OF SYSTEM FOR MAKING SURFACE ELECTRICAL MEASUREMENTS

Figure 14.

displacement controls can be subtracted at the pulse coupler, it is not possible to subtract pulsed voltages that develop at the current contacts. Thus, if one uses an ordinary amplifier on the input to the vertical axis of the voltage beam on the dual beam oscilloscope, only the voltage from one of the side arms to ground can be detected. If the pulse voltage developed at the current contact is an appreciable portion of the total voltage across the sample, then the ultimate precision of the drop between the two arms will be low.

Figure 15 shows the result of such measurements on a 0.005 inch thick slice of nominally 1 ohm-centimeter n-type germanium doped with antimony. The curve shows marked rectifying characteristics. In the negative sector the slope of the curve is constant. This corresponds to the "easy" direction. For positive voltages the curve rises very sharply at first and then levels out to an ohmic region which has a slope five times the slope in the negative sector. The nearly vertical portion represents the voltage required to overcome the contact potential and surmount the barrier into the semiconductor. The ohmic portion at the higher voltages represents the resistance in the "hard" direction.

The "easy" direction corresponds to the flow of electrons from n-type germanium into the platinum, and the "hard" direction corresponds to the reverse. The maximum possible value at the barrier, however, would be the sum of the band gap width of the semiconductor and the difference between the work functions of the two materials.

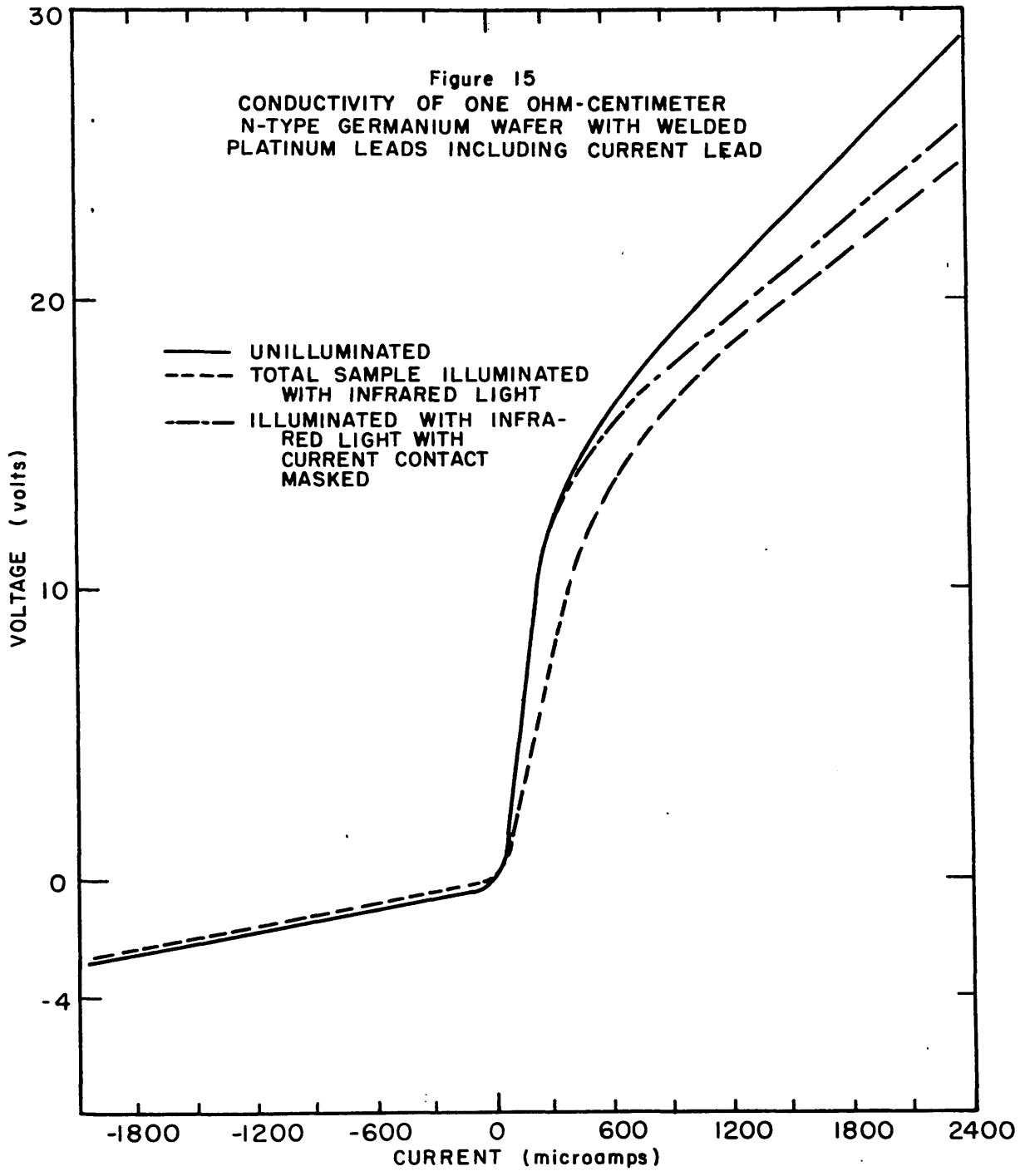
Figure 15
CONDUCTIVITY OF ONE OHM-CENTIMETER
N-TYPE GERMANIUM WAFER WITH WELDED
PLATINUM LEADS INCLUDING CURRENT LEAD
UNILLUMINATED
TOTAL SAMPLE ILLUMINATED WITH INFRARED LIGHT
ILLUMINATED WITH INFRA-RED LIGHT WITH CURRENT CONTACT MASKED
VOLTAGE (volts)
30
20
10
0
-4
-1800
-1200
-600
0
600
1200
1800
2400
CURRENT (microamps)

The band gap for germanium is approximately 0.8 ev (70); the work function for germanium is 4.8 ev (63); and the work function for platinum is 5.4 ev (71). These data give a maximum possible barrier height of only 1.3 ev, while the steep portion of Figure 15 is 10 volts or more. It must be that the platinum weld is not a simple metal to semiconductor contact. Perhaps the oxide layer on the germanium is incorporated in some way into the contact. A barrier height of 10 volts is certainly not unreasonable for a metal to oxide contact.

3. Conductivity Measurements with a Differential Amplifier

Because of the difficulty with the non-ohmic characteristics of the platinum-germanium welds, a differential vertical amplifier for one beam of the oscilloscope was obtained. The amplifier permits either the simultaneous display of the voltage at both side arms on the sample or the display of the difference between them. When displayed simultaneously, the voltages are imperceptibly different within the precision of the sensitivity required to display the full waveform. When the difference of the two voltages was displayed, it was possible to increase the sensitivity on both channels of the amplifier so that the voltage between the two side arms could be measured to a precision of 10 percent. In figure 16 these voltage differences are plotted as a function of current through the sample. Up to about 200 μamps the curve is linear for negative currents. Above this it reaches a minimum and starts up again.

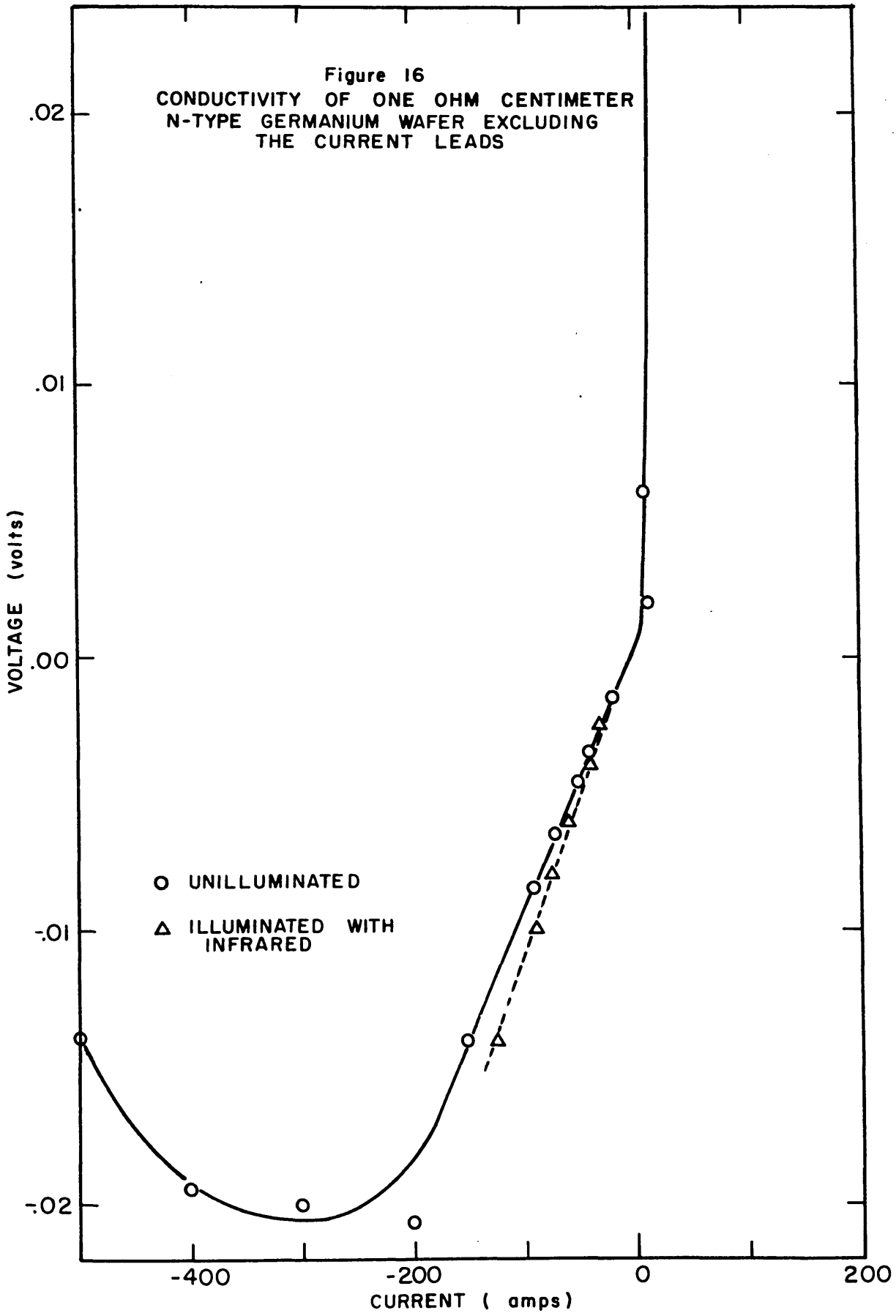
Figure 16
CONDUCTIVITY OF ONE OHM CENTIMETER
N-TYPE GERMANIUM WAFER EXCLUDING
THE CURRENT LEADS
.02
.01
.00
-.01
-.02
VOLTAGE (volts)
O UNILLUMINATED
Δ ILLUMINATED WITH
INFRARED
-400
-200
0
200
CURRENT (amps)

It is believed that the anomalous minimum in Figure 16 is a result of loading by the differential amplifier. At the point deviation from ohmic behavior, the effective resistance of the sample was about 5 percent of the input impedance of the vertical amplifier (1 megohm). Thus, about 5 percent of the current input to the sample would be required to operate the amplifier. The total voltage across the sample was 15 volts so that about 3/4 volt could be expected across both voltage contacts. If these contacts had identical resistances, then no difficulties would accrue ~~from this~~ since it is the difference of the two voltages which is measured. If, however, the contact closest to ground has a resistance only 1 percent to 5 percent greater than the other contact, then deviations such as those seen in Figure 16 would result. Such deviations are certainly to be expected, and this is probably the cause of the non-ohmic behavior above 200 μamps.

The resistance for positive currents is from 5 to 25 times greater than it is for negative currents. Thus, the positive sector of Figure 16 shows no ohmic behavior (even at voltages much higher than those shown in the figure). The non-ohmic behavior is apparently dominated by the contact resistances.

It is possible, however, to measure the resistance of the thin slice over a very narrow range of negative currents (0 to 200 μamps) without the complication of the non-ohmic contacts. This represents only a 1.5 centimeter deflection on the oscilloscope screen even at the highest sensitivity so that the precision is at

best only 10 percent. A high-impedance low-gain pre-amplifier could be used to improve the measurement considerably. The present input impedance is 1 megohm, and the highest sensitivity is 0.01 volts per centimeter. An input impedance of 10 megohms with a gain of 10 would be useful, but 100 megohms with a gain of 100 would be desirable.

4. Field Effect Measurements and the Effect of Light

Attempts were made to measure the effect of a transverse electric field on the conductivity of the sample. Observance of such a field effect would (1) demonstrate that the electrical properties measured were in fact affected by changes in the surface conductivity and (2) show the utility of this approach to the measurement of surface recombination velocity. It was found to be extremely difficult, however, to position the field effect electrode accurately on the quartz shims without shorting out the sensing contacts. Such difficulty in air where it was possible to manipulate the electrode freely with tweezers made it seem very unlikely that success would be achieved within the vacuum system by remote means. Accordingly, this approach was abandoned.

An alternate method for changing the surface charge carrier density is to illuminate with infrared light. Gallium arsenide diodes are presently available (58) which emit an appropriate frequency. Furthermore, these diodes can be switched very rapidly (less than 1 μsecond), and it would be possible to illuminate the

surface with a square wave pulse of a μ second risetime. Details of this approach are given in Appendix D. Measurement and Interpretation of Surface Electrical Properties.

In order to test the feasibility of this method, the surface of the 1 ohm-centimeter germanium was illuminated with infrared light from an ordinary laboratory heating lamp. At the same time, conductivity measurements similar to those previously discussed were made. The results are shown in Figures 15 and 16.

In Figure 15 the effect of light appears to be very large, particularly for positive currents, and it was suspected that absorption of light at the contacts was significantly altering the contact resistances. This suspicion proved correct when the measurements were repeated with one of the contacts partially masked. The mask covered only about 1 percent of the sample area, but as can be seen in Figure 15, it had a major effect on the positive current characteristics.

In Figure 16 the effect of this illumination is seen in the negative current region when the differential amplifier was used. Thus, it may be concluded that (1) the conductivity of the thin slice as measured by the negative portion of Figure 16 is appreciably affected by changes in the surface conductivity and (2) illumination with infrared light can be used to inject electrons into the surface layer. It is expected that the effects will be considerably greater with a radiation diode since their effective temperatures can be in

excess of 10,000°K. The effects shown in the figures were definitely not due to heating of the sample as evidenced by their immediate disappearance when the light was turned off. If the light was left on for long periods of time, then even greater changes occurred, and these persisted for up to 20 seconds after turning off the light. It is these latter effects which are due to heating of the sample by general absorption of infrared radiation by the germanium.

Thus, though the physical manipulations required for recombination velocity measurements by field effect techniques are prohibitively difficult, it appears to be possible to make these measurements photometrically.

VIII. CONCLUSIONS

A. Theory

The statistical description of chemisorption on semiconductors has shown that when charge transfer achieves equilibrium, the fraction of the adsorbed species which are ionized and the desorption activation energy are related to the work function, ϕ, and hence the bulk doping of the semiconductor. If an un-ionized, n-type absorbed specie is involved in a rate limiting step, then compensation will occur in the Ahrrenius equation as the bulk doping is changed. If an ionized specie is involved, then no compensation is expected. For the simplified model used, the rate of change in the vibrational partition function is largely responsible for the difference between the bond energy and the chemical potential of bonding electrons. Systems whose sorption bond is strongly perturbed by charge transfer then will saturate at low values of surface ionization and vice versa. The model is adequate to describe the general features of presently available data on hydrogenation-dehydrogenation reactions on germanium.

B. Experiment

Clean surfaces of n-type germanium are shown to be slightly more active than oxygenated surfaces treated with hydrogen. When a clean surface is hydrogen treated, a lower activity results apparently because of some germanium hydride formation at the surface. Only dehydrogenation occurs on clean surfaces whether or not they are treated with hydrogen.

Surface conductivity can be measured with adequate precision using the equipment which has been designed. Recombination measurements by pulsed field effect are very difficult, but photo excitation shows considerable promise.

IX. RECOMMENDATIONS

The system is well-suited for the simultaneous measurements of kinetics and surface electrical properties which have been proposed in this thesis. The techniques for all of the required measurements have been demonstrated, and it is recommended that the program outlined be continued.

Relative ionization efficiencies for the mass spectrometer should be made. This will clear up the problem of obtaining a tight mass balance should the selectivity of p-type germanium be different from that of n-type as proposed by Volkenshtein.

The temperature range of the investigation should be extended up to perhaps 300°C so that the Arrhenius plot can be unambiguously established without the use of the low conversion points. A series of runs on the same catalyst crushed in air and reduced in hydrogen, a clean surface, and a hydrogen treated clean surface should be made to provide a better reference between this work and that which has previously been reported on air crushed samples.

It is recommended that photo-excitation with a square wave of light from a gallium-arsenide diode be used for the recombination rate measurements because of the mechanical difficulties of positioning the field effect electrode after ion bombardment.

X. APPENDIX

A. Experimental Apparatus

1. High Vacuum Reactor System

The high vacuum reactor system consists of a gas-handling manifold, the reactor, a cell for making surface conductivity measurements, the mass spectrometer tube, the pumping system, and associated valves and gages for control and pressure measurement. Figure 5 shows a block diagram of the reactor system. The reactor, conductivity cell and mass spectrometer are circled and dotted arrows indicate the main flow of gas through the system.

Ethanol enters the manifold from the ethanol receiver which is controlled at $0^{\circ}C$. It passes through the handling manifold, the first Type C Granville-Phillips valve and into the holding volume outside the variable leak. It is metered into the system through the leak, passes into a vycor trap with a square meter or so of virgin germanium surface and through a freshly flashed aluminum getter. An ionization gage between the aluminum getter and the reactor permits measurement of inlet pressure. A bypass line before the disc providing support for the catalyst permits rapid pump-down through a Type C valve. The reaction mixture passes from the reactor, into the cell where electrical measurements are made and then into the high vacuum manifold. When necessary the conductivity cell can be isolated from the rest of the system by closing the two Type C valves. A parallel stream permits sampling of the reaction mixture into the mass spectrometer.

The reactor and the germanium getter are supplied with fitted heating mantles by Glas-Col Apparatus Company. The mantles are fabricated of quartz fiber and are capable of achieving 600°C. The entire system between and including the variable leaks and the 2-inch valve, but excluding the roughing line Type C valve is bakeable to 450°C by lowering a counter-weighted oven over the vacuum system. The actual arrangement of the glassware and oven are seen in the photographs in Figures 6, 17, and 18.

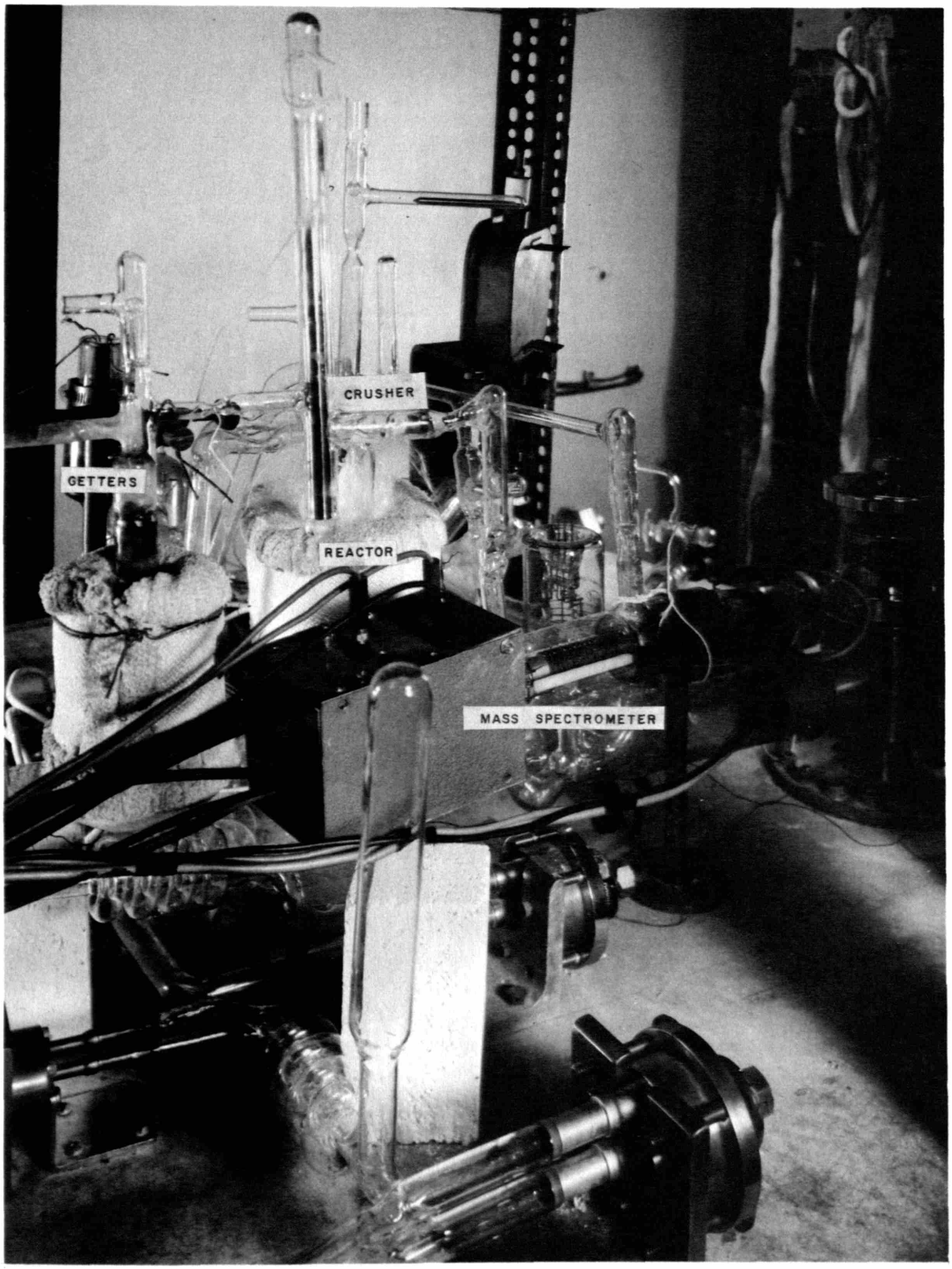

FRONT VIEW OF VACUUM REACTOR SYSTEM

Figure 17.

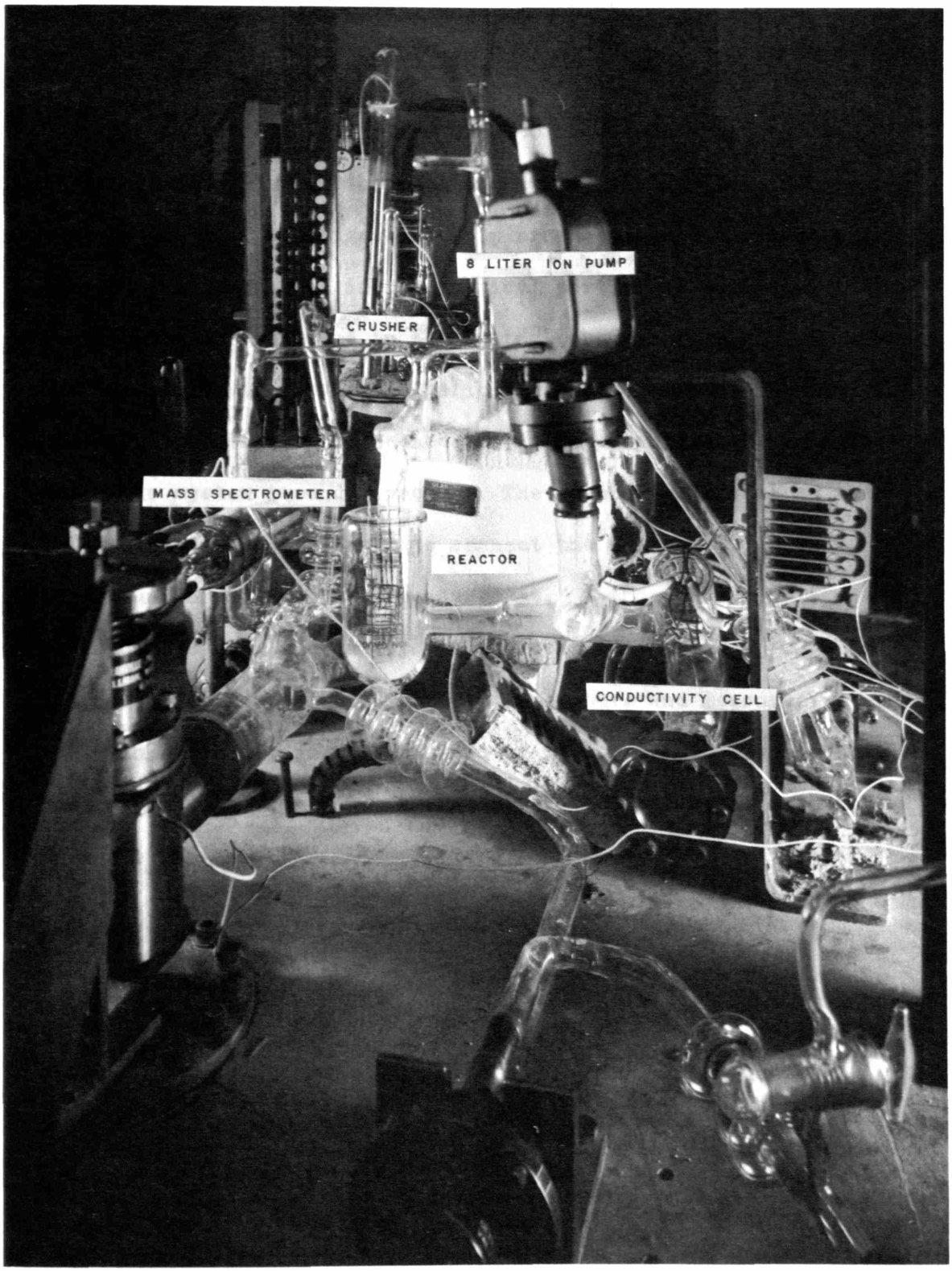

END VIEW OF VACUUM REACTOR SYSTEM

Figure 18.

X. APPENDIX (Cont.)

A. Experimental Apparatus

2. Catalytic Reactor

The catalyst is supported on a 30 mm diameter fitted disc. Gas flows down through the disc and a by-pass line permits pumping of both sides of the disc. Freshly crushed catalyst can be added through the break seal in the vertical portion of the inlet tube. The reactor is connected to the system through pinch-off zones where the tubulation is constricted slightly and thickened. At the close of a run the reactor is pinched-off at these points and removed while the system is under vacuum. The second break seal on the inlet tube can then be used to connect the reactor to a B.E.T. apparatus for surface area measurement. A thermowell positions a thermocouple over the catalyst support disc. During a run this thermocouple is referenced at ice temperature and measured with a potentiometric bridge. A new reactor is constructed for each set of runs on any one catalyst. A drawing of the reactor is seen in Figure 19.

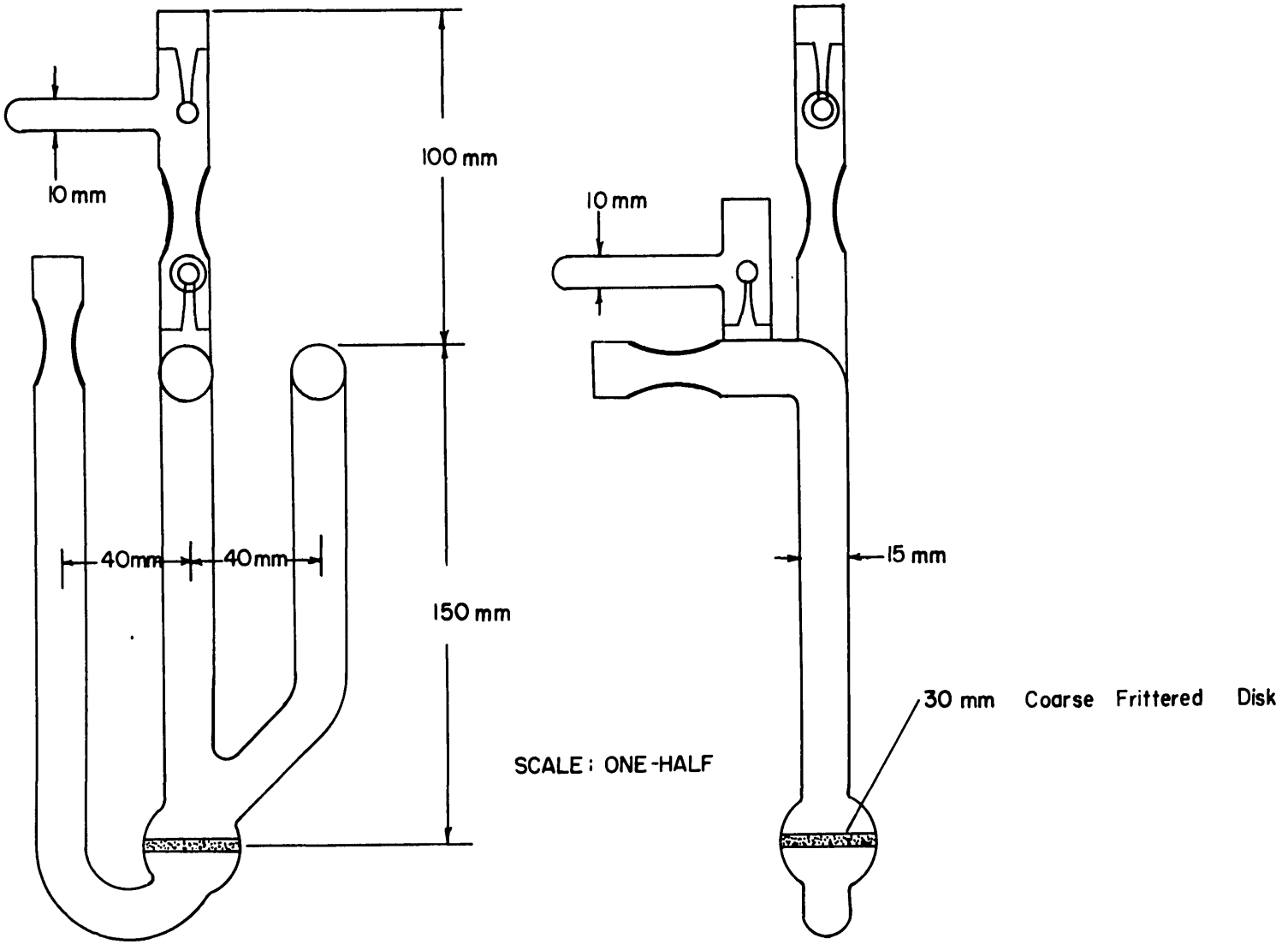

DETAIL OF CATALYTIC REACTOR
Figure 19.

X. APPENDIX (Cont.)

3. Surface Conductivity Cell

The cell for the measurement of the surface electrical properties provides means for cleaning the sample by argon ion bombardment and making the desired electrical measurements. A detailed drawing of the conductivity cell assembly is seen in Figure 20. The sample holder is supported by two of the eight leads in the press which is fused on to the 1-1/2-inch Varian conflat flange. After inserting the sample this flange is attached, positioning the sample in the center of the measuring cavity. When so located the sample is 4 inches from the ion source which is stationed to give the ion beam a 45° angle of incidence. A second conflat flange with the same axis as the first permits inclusion of a bellows assembly for positioning a field effect electrode when desired (see Figure 21). Alternately the second flange can be blanked off when only surface conductivities are measured.

A detail of the sample holder is seen in Figure 4. The holder is constructed of quartz to permit high temperature annealing of the ion bombarded sample. A shallow quartz dish with four holes to admit electrical leads holds an 1/16-inch thick optical flat. Molybdenum clips on the dish permit attachment to the press leads. The sample is placed on the quartz flat and the leads carefully fed through the holes provided. Connection to the press leads is made outside the sample holder.

A heater positioned underneath the sample holder is used to control the temperature of the sample. The bottom of the quartz flat is etched slightly to give good radiation dispersion. A thermocouple is spring loaded to rest on the optical flat near the sample, and measures the temperature of the sample. Quartz shims can be placed as shown to give a 0.001-inch spacing between the sample and the field effect electrode.

Gas is admitted through a 10 mm port immediately adjacent to the sample holder so that it impinges on the surface of the sample (this port not shown in Figure 20 for simplicity). The reaction mixture is pumped out through a 10 mm port (not shown in Figure 20) in the flanged section holding the 8 lead press. A 25 mm port (not shown in Figure 20) adjacent to the ion source connects the cell to the 8 liter ion pump and ionization gage.

A detailed drawing of the ion source is seen in Figure 21. Five inches of 0.006-inch tungsten wire wound in 1/8-inch diameter coil and attached across two of the four leads. Each of the other two leads supports an anode grid. Electrons from the tungsten filament are collected at the anode and produce positive ions. These are accelerated to the sample by a negative voltage. A third plate held at filament potential shields the sample from sputtered tungsten.

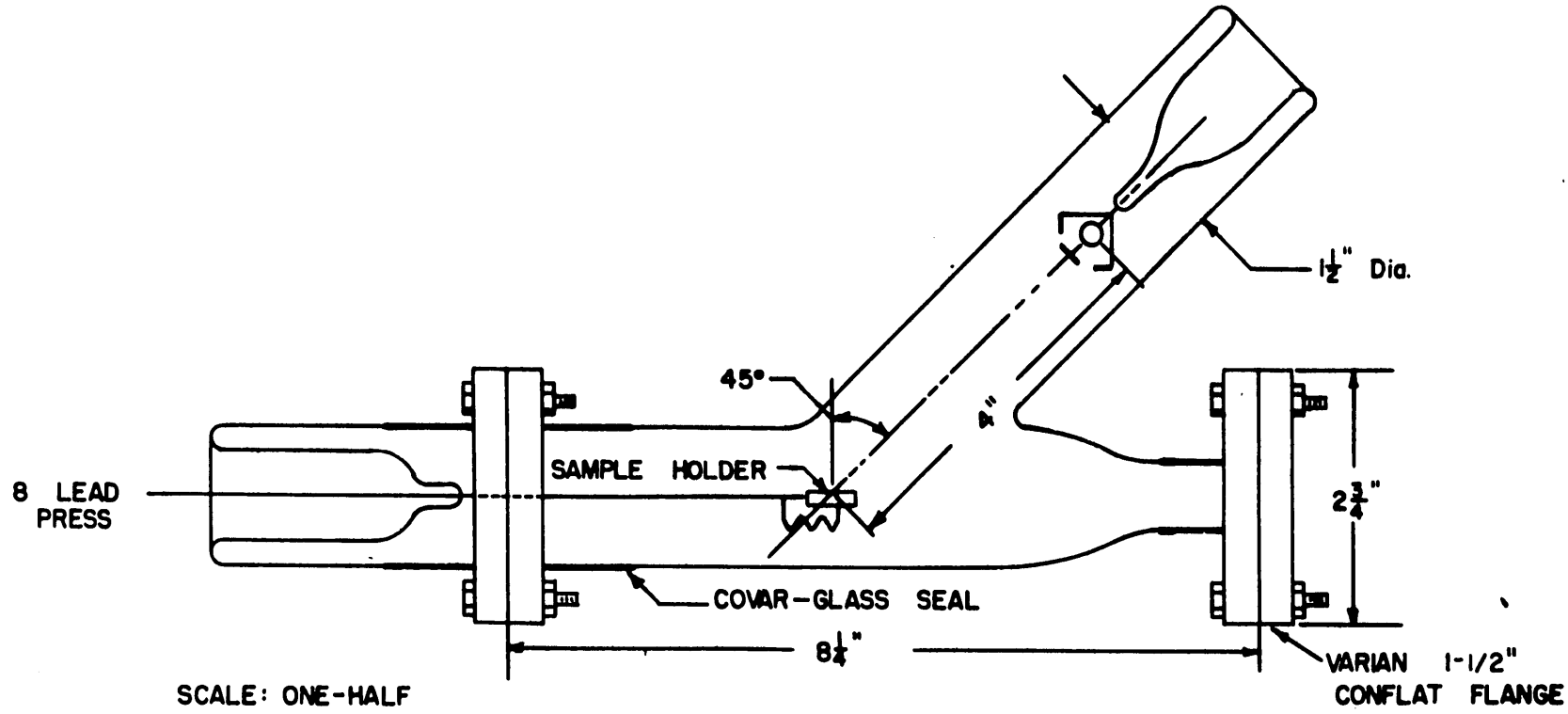

SURFACE CONDUCTIVITY CELL
Figure 20.

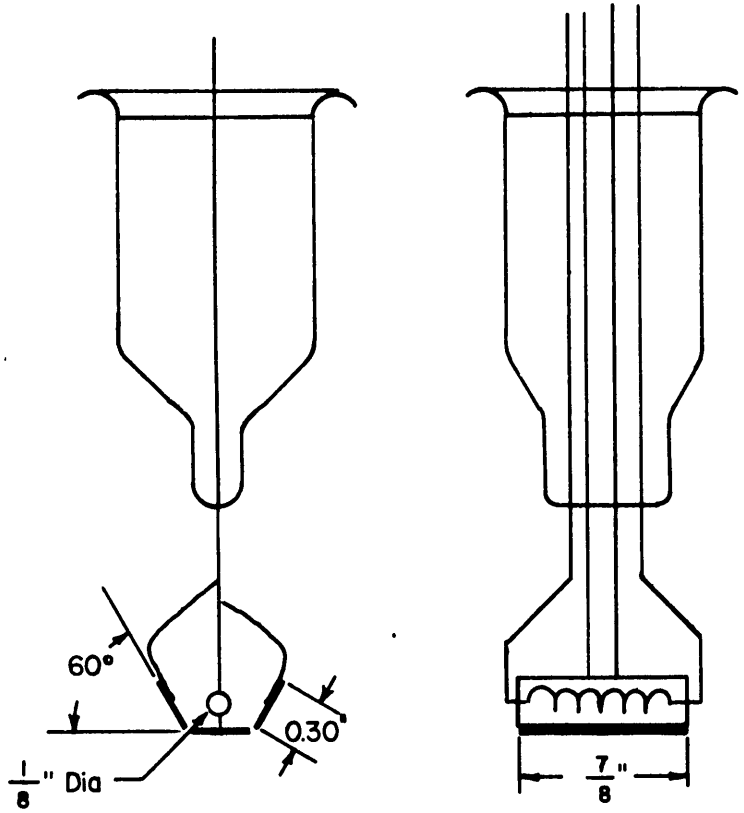

ION SOURCE DETAIL

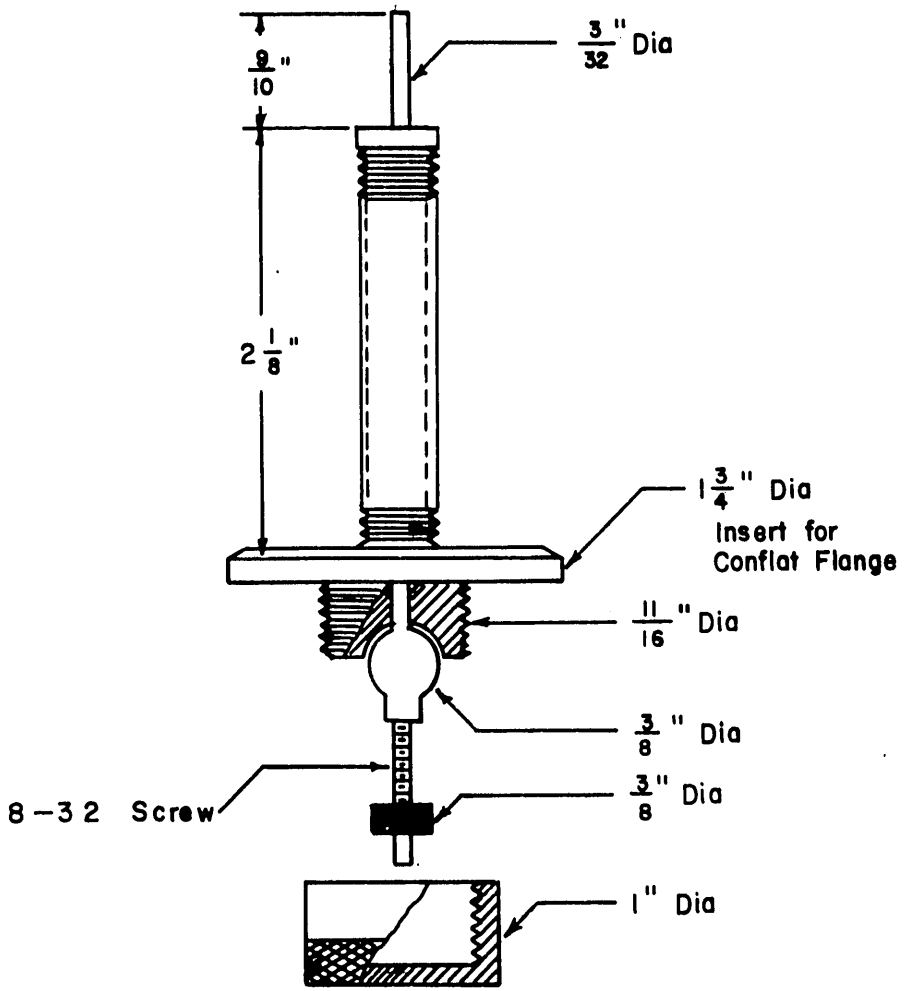

BELLOWS ASSEMBLY FOR FIELD EFFECT ELECTRODE

Figure 21.

X. APPENDIX (Cont.)

4. Ethanol Feed System

Ethanol is metered into the system through the Granville-Phillips variable leak. The setting on the leak is maintained constant throughout each run. A constant flow rate is maintained by controlling the ethanol pressure on one side of the leak. This is done by precisely controlling the temperature of liquid ethanol exposed to the leak.

A schematic diagram of the constant temperature bath is shown in Figure 22. A wide mouthed dewar is placed below a hole in the transite table-top outside the bake-out oven. Mixing is achieved by means of an air lift pump composed of two concentric glass tubes. Air passed through the outer tube sluggs water up the annular space between. A syphon permits drainage for addition of ice. Temperature is indicated by a Beckmann differential thermometer. Such an ice bath can be made to maintain temperatures constant within $0.001^{\circ}C$. In the experiments performed temperature was maintained within $0.005^{\circ}C$.

The vapor pressure of ethanol as a function of temperature is plotted in Figure 23. Variation of $0.005^{\circ}C$ can give rise to pressure changes of 0.03 percent of the vapor pressure in the region of $0^{\circ}C$.

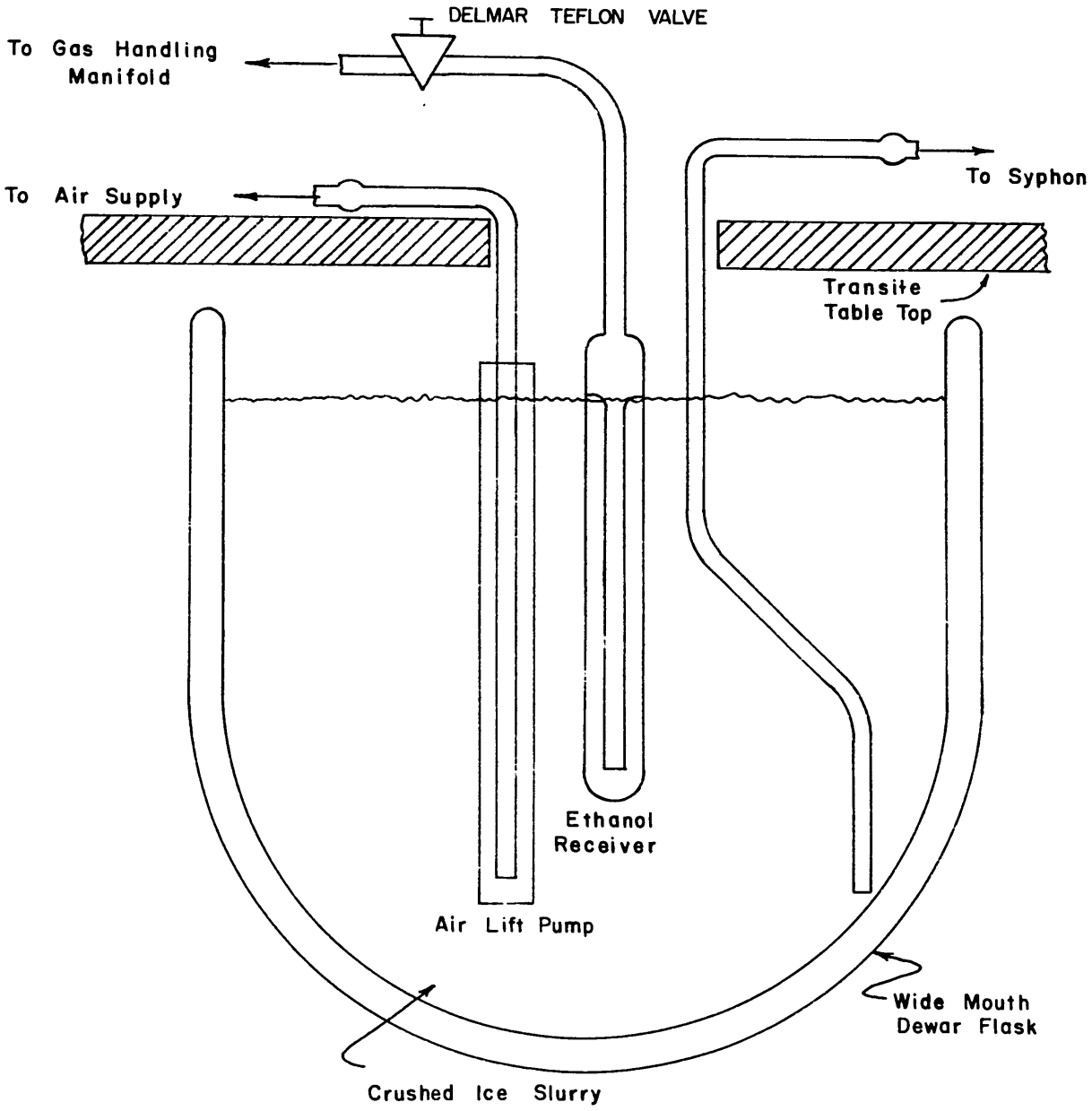

CONSTANT TEMPERATURE BATH FOR ETHANOL
Figure 22.

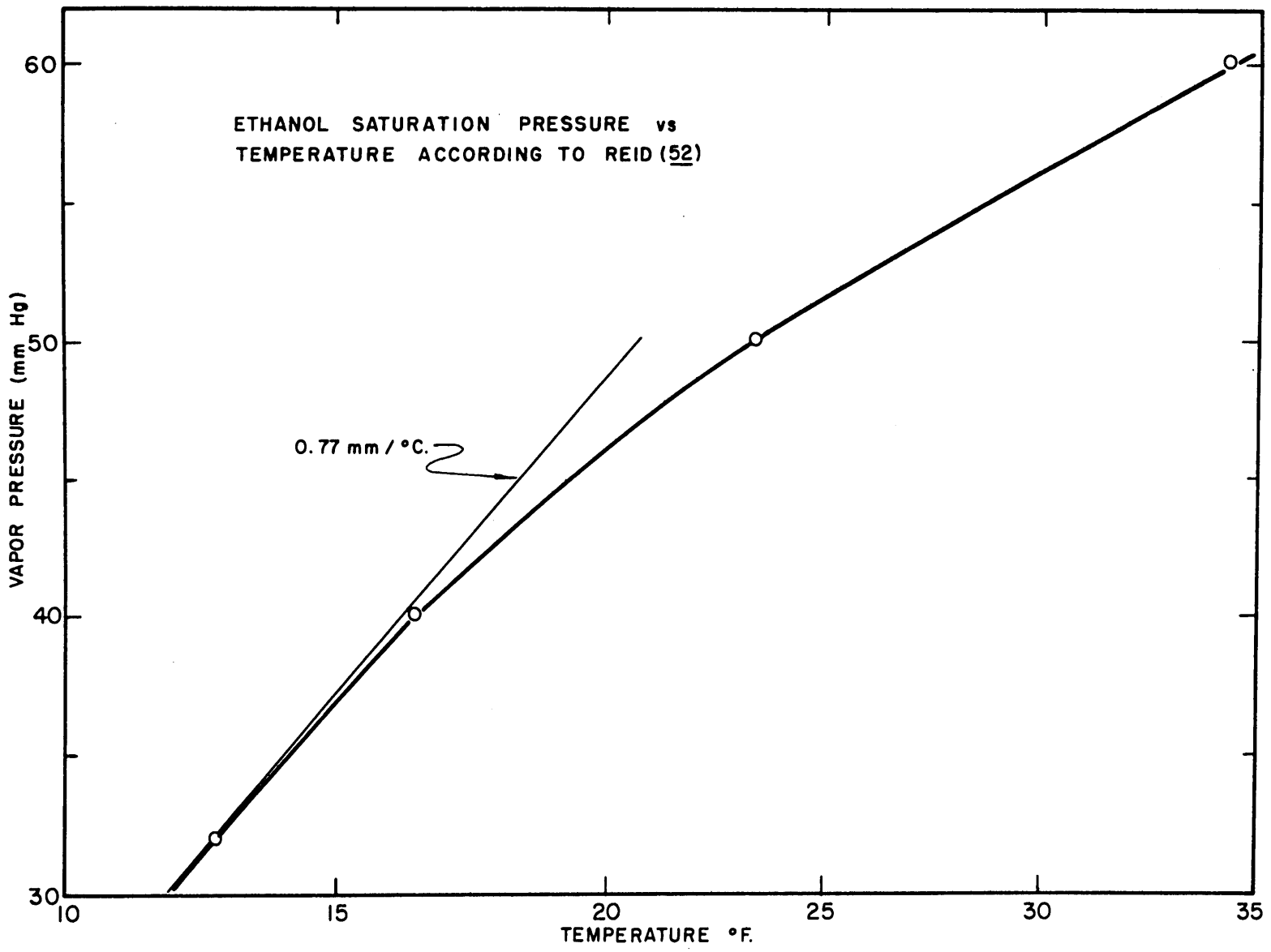
ETHANOL SATURATION PRESSURE vs
TEMPERATURE ACCORDING TO REID (52)
0.77 mm / °C.
VAPOR PRESSURE (mm Hg)
60
50
40
30
10
15
20
25
30
35
TEMPERATURE °F.

Figure 23.

X. APPENDIX (Cont.)

5. Radiofrequency Mass Spectrometer

a. General

In order to maintain clean uncontaminated catalyst surfaces at realizable ethanol pirities and in order to lower the oxygen background of the reactor system it is desirable to conduct the whole study at reduced pressures (10^{-3}torr and below). The problem of analyzing for the reaction products at such low pressures is a difficult one. Mass spectrometers which characteristically operate at pressures lower than 10^{-3}torr are the most promising.

Most mass spectrometers, however, focus by means of crossed magnetic and electric fields. Thus such a spectrometer could not be baked out to the high temperatures required to produce the low pressures which are needed without removing the focusing magnets. Re-positioning the magnets after the bakeout is a slow and tedious procedure. Furthermore most mass spectrometers have a very high residual water background and many require that water be removed from the sample before admission to the spectrometer tube. Thus conventional mass spectrometers are not suited to the product analysis in this study.

A relatively recent development in the field is the radio frequency mass spectrometer. The instrument combines a conventional ion gun in-line with a small linear accelerator and a retarding grid. Ions whose entrance velocity is such that they are in phase with the

alternating potential on the linear accelerator receive additional energy as they pass through the accelerator. The potential of the retarding grid is adjusted to repel all the ions not so accelerated. A grid prior to the accelerator permits concurrent measurement of the total ion current.

A tube of this kind, the ML494A by Machlett Laboratories, is bakeable to 450°C and has resolution and sensitivity adequate for analysis of the ethanol reaction mixture. This tube has been integrated into the vacuum reactor system. A schematic diagram of the ML494A and its associated electronics is seen in Figure 24.

b. Design of Mass Spectrometer System

Since no commercial system for the control and operation of this tube is marketed it was necessary to develop the electronic system. It has been constructed along lines suggested by Machlett. Several important innovations, notably a push-pull radiofrequency source, feed back control circuit and auxiliary degassing circuit were required to complete the analysis of ethanol decomposition products.

In general commercial components were purchased and modified as necessary to complete the system. The ion source is operated and controlled with a Veeco ionization gage control unit. This unit was modified by the manufacturer to permit alternate operation of the two ionization gages. In the present system one of these is coupled to the spectrometer ion source and total pressure grid.

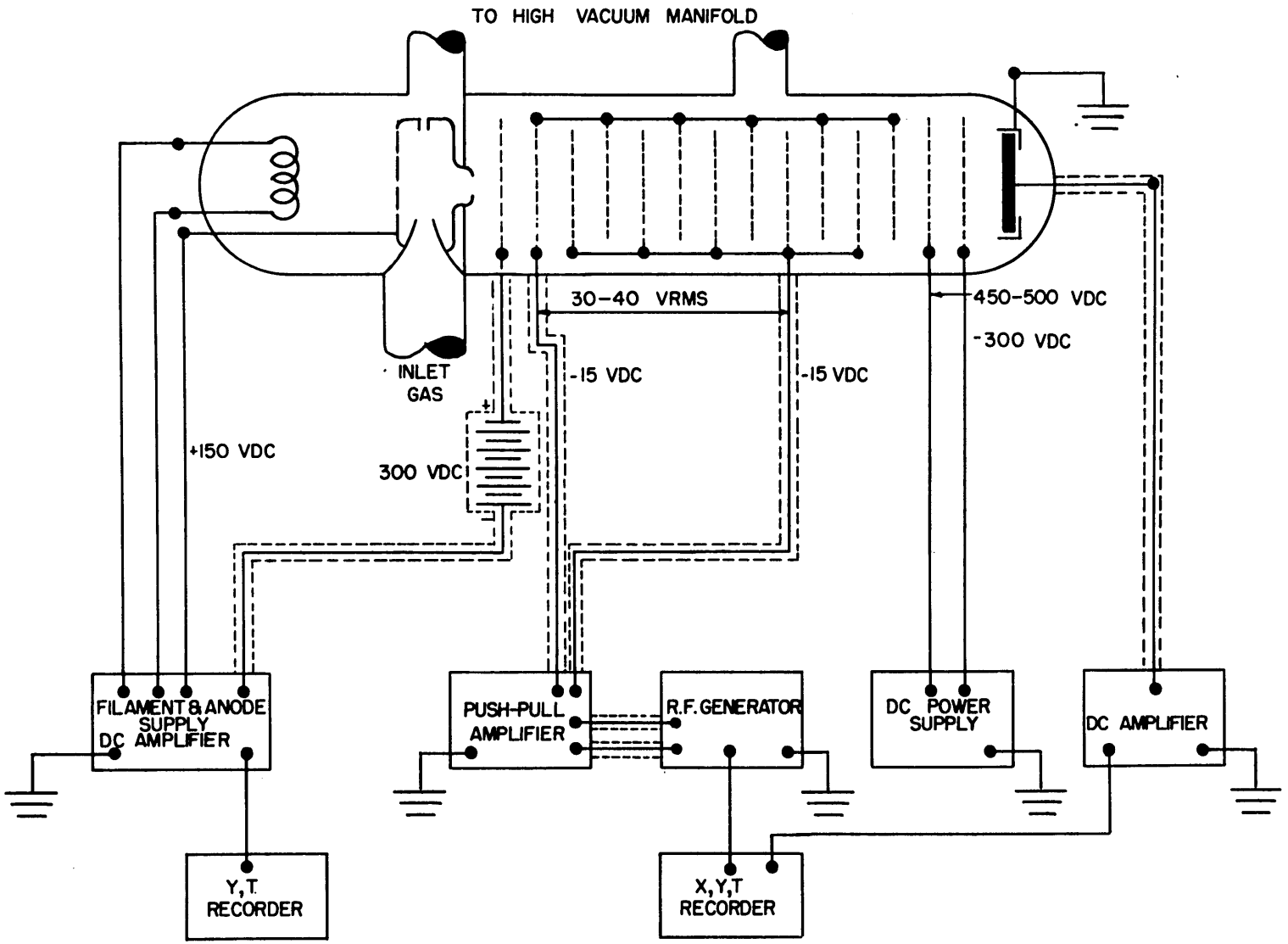

BLOCK DIAGRAM OF RADIO FREQUENCY MASS SPECTROMETER

Figure 24.

A shielded battery in the total pressure measuring circuit achieves the necessary bias on the total pressure grid. Current in this circuit is never greater than 0.1 ua or so and hence the battery is adequately stable. A D.C. power supply by Hewlett Packard (Model 712B) provides the remaining biasing voltages:

0 to 150	volts variable for linear accelerator
0 to +500	volts variable for retarding grid
-300	volts fixed for focusing grid

The Hewlett Packard power supply has been modified to permit vernier control of the 0 - 500 volt retarding potential. A 10,000 ohm variable resistor has been added as shown in Figure 25.

The radio frequency voltage is produced by a Tektronix 190B signal generator. This generator produces a controlled output from a few kilocycles to 50 megacycles. The region of interest for the ethanol analysis is 4 - 35 megacycles which corresponds to 1 - 60 AMU. The maximum output of the oscillator, however, is only 10 volts peak to peak or 3.5 volts RMS, while the tube requires at least 30 volts RMS. Thus the output of the Tektronix is passed through a wideband amplifier by Instruments for Industry Model 500. While this amplifier has a gain of 10 in the frequency range of interest and a very flat response, major distortions (largely the second harmonic) occur at output voltages above 22.5 volts RMS. A single undistorted signal at high enough voltages is not possible, then, with such a system. By operating the tube push-pull, i.e., feeding two signals of equal voltage but 180° out of phase to opposite sets

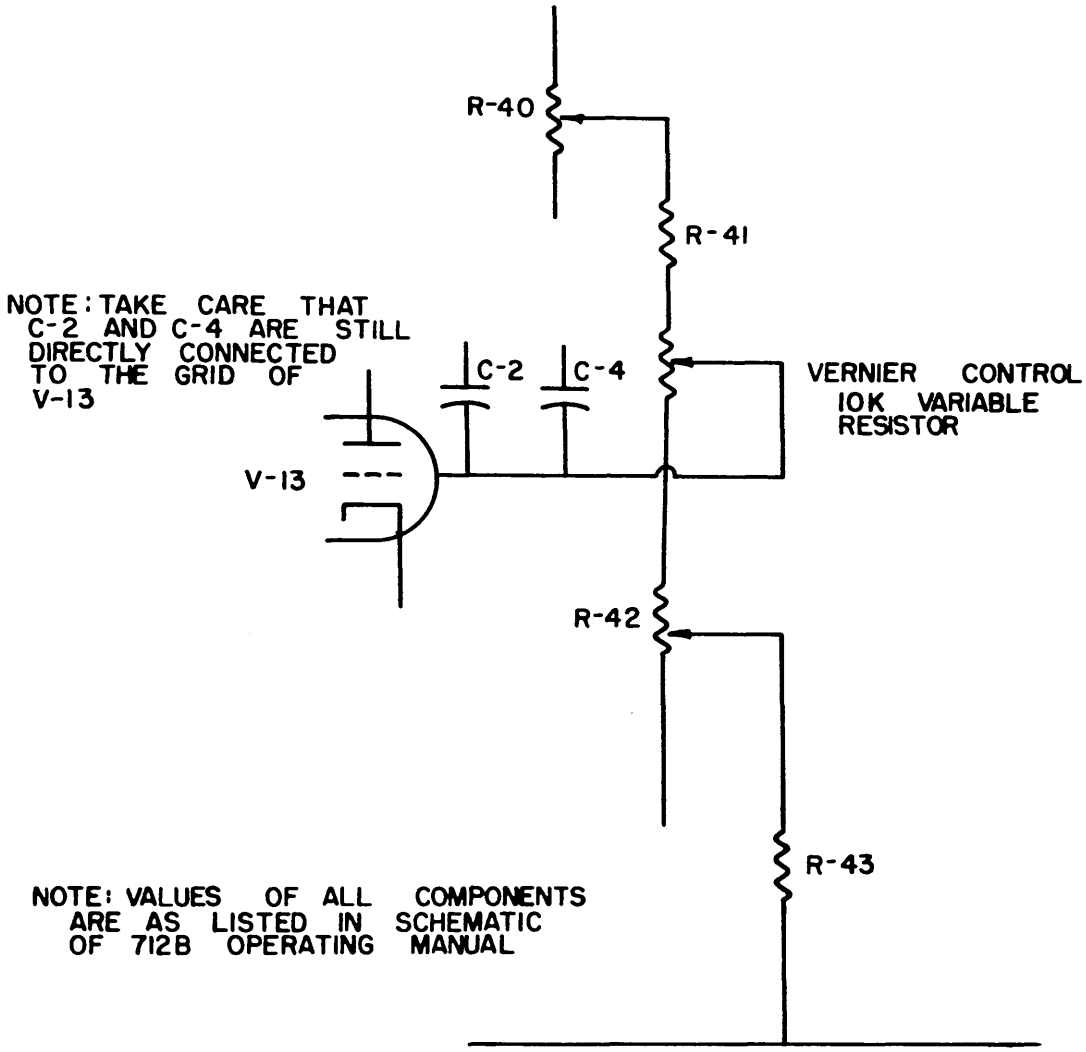

MODIFICATION OF HEWLETT-PACKARD MODEL 712B

Figure 25.

of grids in the accelerator, the effective voltage can be doubled. This mode of operation has been adopted.

In order to achieve a push-pull output from the Tektronix oscillator an additional secondary winding was added to the output inductors, L-33, L-34 and L35 (see Tektronix operator's manual for a detailed schematic of 190B). The center tap of the resulting secondary was grounded and the relative positions of the two coils adjusted to give two outputs of equal voltage 180° out of phase. An additional wafer was added to the band selector switch to permit synchronous switching of the two outputs. Each of the two outputs were then input to separate wide-band amplifiers and the outputs of the parallel amplifiers were fed push-pull to the linear accelerator on the mass spectrometer tube.

A feed-back sampling circuit has been designed to operate from the spectrometer tube input in conjunction with the feed-back control loop of the Tektronix oscillator. This consists essentially of a set of sampling diodes operating across a voltage doubling circuit to give a D.C. sampling voltage equal to the peak to peak voltage of the radio frequency signal. The voltage is passed through a 20 to 1 divider, filtered for residual r.f., and fed into the conventional Tektronix control loop. A schematic of this feed-back circuit is seen in Figure 26. Voltages of 150 volts peak to peak with less than 1 percent variation from 4 - 35 megacycles have been achieved with this system. Time drift after two hours of warm-up is less than 0.1 percent. A particular advantage of this mode of operation is that it eliminates distortion due to the second harmonic.

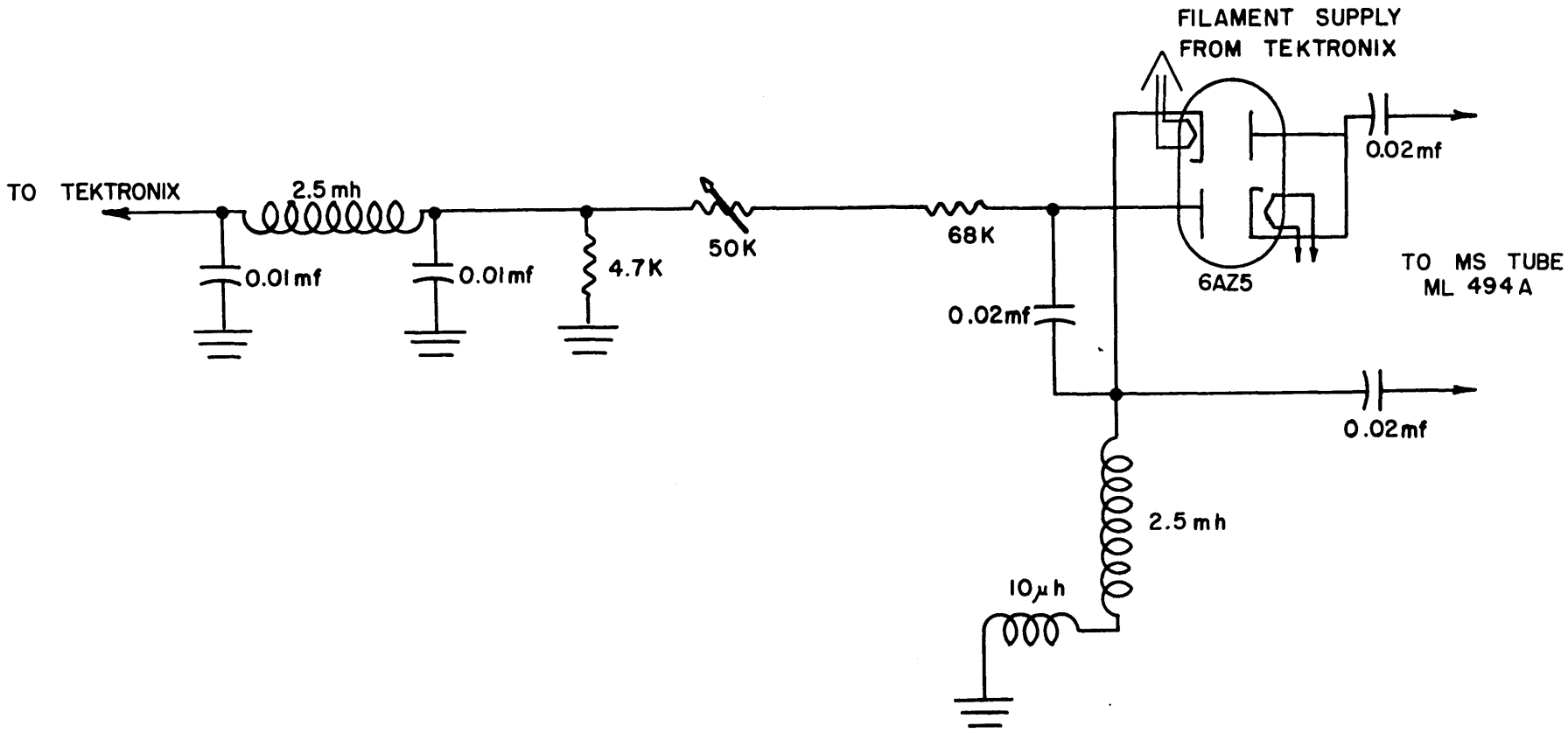

PUSH - PULL FEED - BACK CIRCUIT

Figure 26.

Some additional considerations in the radiofrequency supply were necessary in order to achieve these results. The oscillator was located as close as possible to the two amplifiers and the amplifiers in turn were located as close as possible to the tube. Low loss r.f. cable RG 62 A/U was used for the connections. The front panel connections were all shunted out and the only coaxial connectors used in the r.f. circuit were the input and output leads of the two r.f. heads on the amplifiers. These precautions were taken to minimize cable losses and reflections. There is a large impedence mismatch between the wide band amplifier and the mass spectrometer tube. This gives rise to substantial circulation currents in the amplifiers. As a result it was necessary to double the power rating of the input and output load resistors. In order to permit adding of the D.C. bias to the linear accelerator the output load resistor was disconnected from ground and grounded through a 120 pf capacitor. An external tap was added above the capacitor and the bias voltage from the Hewlett Packard supply was added at the amplifier output.

The oscillator is belt driven by a self-reversing synchronous motor. Coupled with the motor is a potentiometer which can output a D.C. voltage proportional to the frequency. In one mode of operation this voltage is fed to one axis of an x-y recorder.

Ions which are focused into the shielded collector are proportional to the abundance of the specie from which they were

derived, and the current in this circuit, plotted as a function of frequency, constitutes the mass spectrum of the gas being analyzed. This partial ion current is amplified by a Keithly 417 pico-ammeter. The Keithly output can be plotted directly as a function of frequency on the x-y recorder or as a function of time during the synchronous sweep of frequency. In either case nearly Gausian peaks are obtained. The total pressure is monitored on a 6-inch strip chart recorder.

Degassing of the tube is accomplished by operating the filament at a temperature high enough to emit 100 - 150 ma of electron current. Simultaneously the voltage on the anode box is increased from 150 v to 500 v. The resulting high energy electron bombardment is capable of heating the anode box (the most massive piece of metal in the tube) to incandescent red in a minute or so. To degass the tube, the filament and anode voltages from the Veeco unit are decoupled: the retarding potential is switched from the retarding grid to the anode box: and a 6.3 volt filament supply from the Hewlett Packard supply is coupled to the tube through a variable resistor to permit manual control of the emission current.

In incorporating the tube into the vacuum system it was found necessary to ensure a pump out speed for the tube envelope of at least 100 times the sample inlet speed. This has been accomplished by using a very short line between the tube and the high vacuum manifold. If this rapid pump-out is not maintained residual backgrounds due to pyrolysis and desorption from the wall become excessive.

The tube is protected against unexpected increases in the tube pressure. A relay in the Veeco unit shuts off the filament voltage when the pressure exceeds 1.5 times the full scale deflection on the total pressure meter. A 115 volt output from the control unit is switched with this relay and is used to control a second relay which decouples the retarding potential. In normal operation voltages of 800 volts can be developed between the retarding grid and the focusing grid. Thus a rise in pressure to a few microns would result in a glow discharge between these two grids. The large currents developed under these conditions would burn out the tube connections to these grids. Decoupling the retarding potential as indicated eliminates this problem. Thus the tube is protected against all but catastrophic increases in pressure. In this case because of the finite heat capacity of the thoriated tungsten filament, the filament temperature may be high enough at atmospheric pressure to cause serious damage.

c. Calibration

Early work with the mass spectrometer system, even before all the refinements noted above were made, established that the tube had a linear response from 10^{-8} to 10^{-4} mm Hg. A typical example of such work is seen in Figure 27 where the total ion current, which is proportional to total pressure, is plotted against partial ion current for nitrogen. Both the 28 and 14 peaks are nearly parallel and show slopes of approximately one over the four-fold pressure range. Deviations from linearity at the lowest pressures are to be

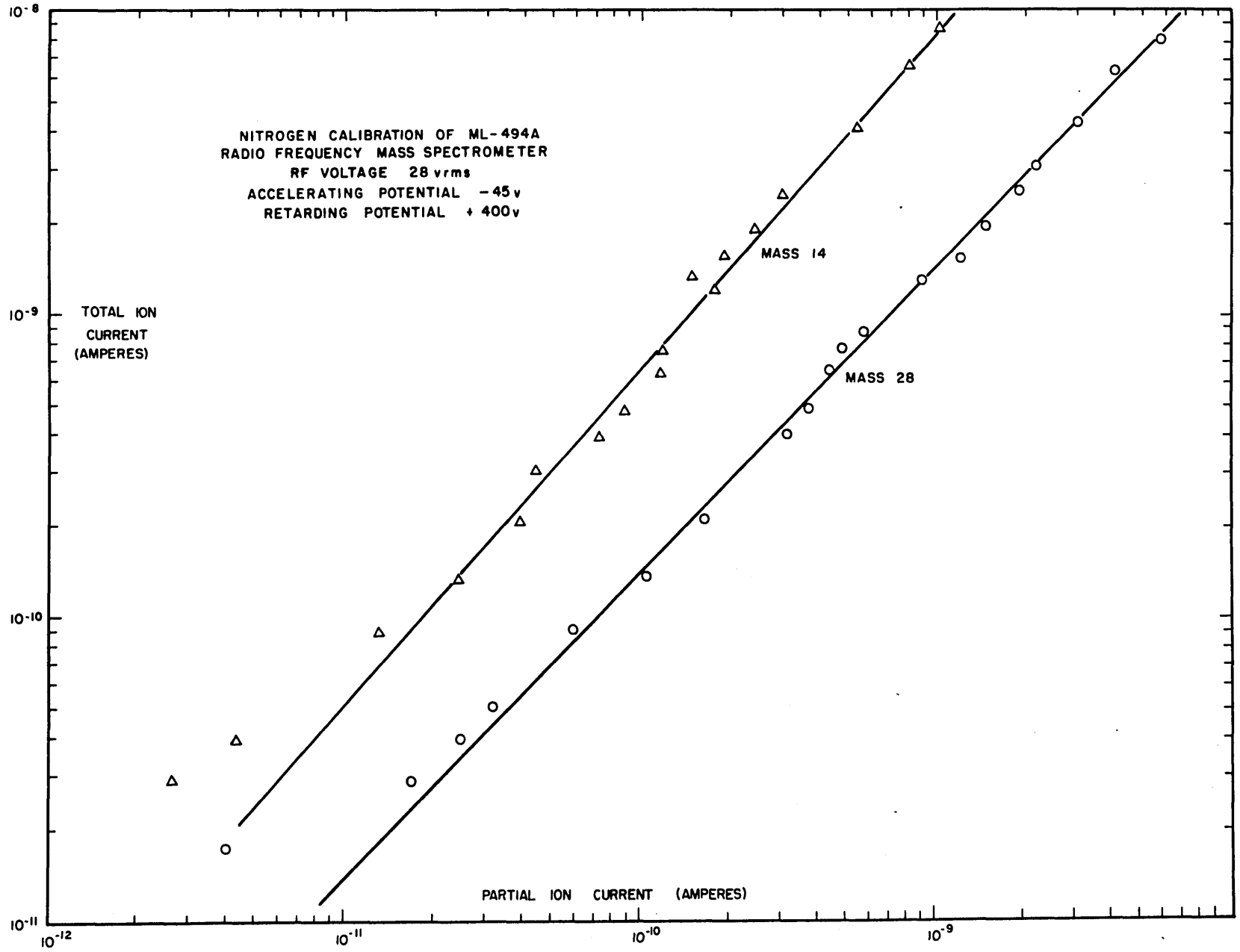
NITROGEN CALIBRATION OF ML-494A
RADIO FREQUENCY MASS SPECTROMETER
RF VOLTAGE 28 vrms
ACCELERATING POTENTIAL −45 v
RETARDING POTENTIAL + 400v
MASS 14
MASS 28
TOTAL ION CURRENT (AMPERES)
PARTIAL ION CURRENT (AMPERES)
10-8
10-9
10-10
10-11
10-12
10-11
10-10
10-9

expected since the residual background of the tube is an appreciable portion of the total ion current at the low pressures. The tube is better than the scatter in Figure 27 since these data were taken with only a few minutes between points. Later work has indicated that in a flow system of this kind a considerably longer period is needed to establish steady state.

Cracking patterns for acetaldehyde, ethanol and hydrogen were taken at about 10^{-5} mm Hg. The results of these tests are tabulated in Table II and compared with the cracking patterns on commercial mass spectrometers which are available from the literature. Figure 28 shows typical reproductions of these spectra along with a spectrum taken during a run at 35 percent conversion.

It is seen that in general the salient features of the literature spectra are the same as with the ML494A. The one exception is the appearance of a large 28 peak for ethanol. It is believed that this may be due to CO desorption from pyrolysis products deposited in the tube. If so the 16 and 12 peaks may not be accurate either. In the analyses none of these peaks is used. The cracking patterns are generally reproducible from day to day with 1 - 2 percent precision.

The voltages used for these calibrations are as follows:

Filament	+ 30 volts
Anode Box	+180 volts
Total Pressure Grid	-300 volts
Linear Accelerator	- 15 volts
Retarding Grid	+500 volts
Focusing Grid	-300 volts
RF Accelerator voltage	96 volts peak to peak

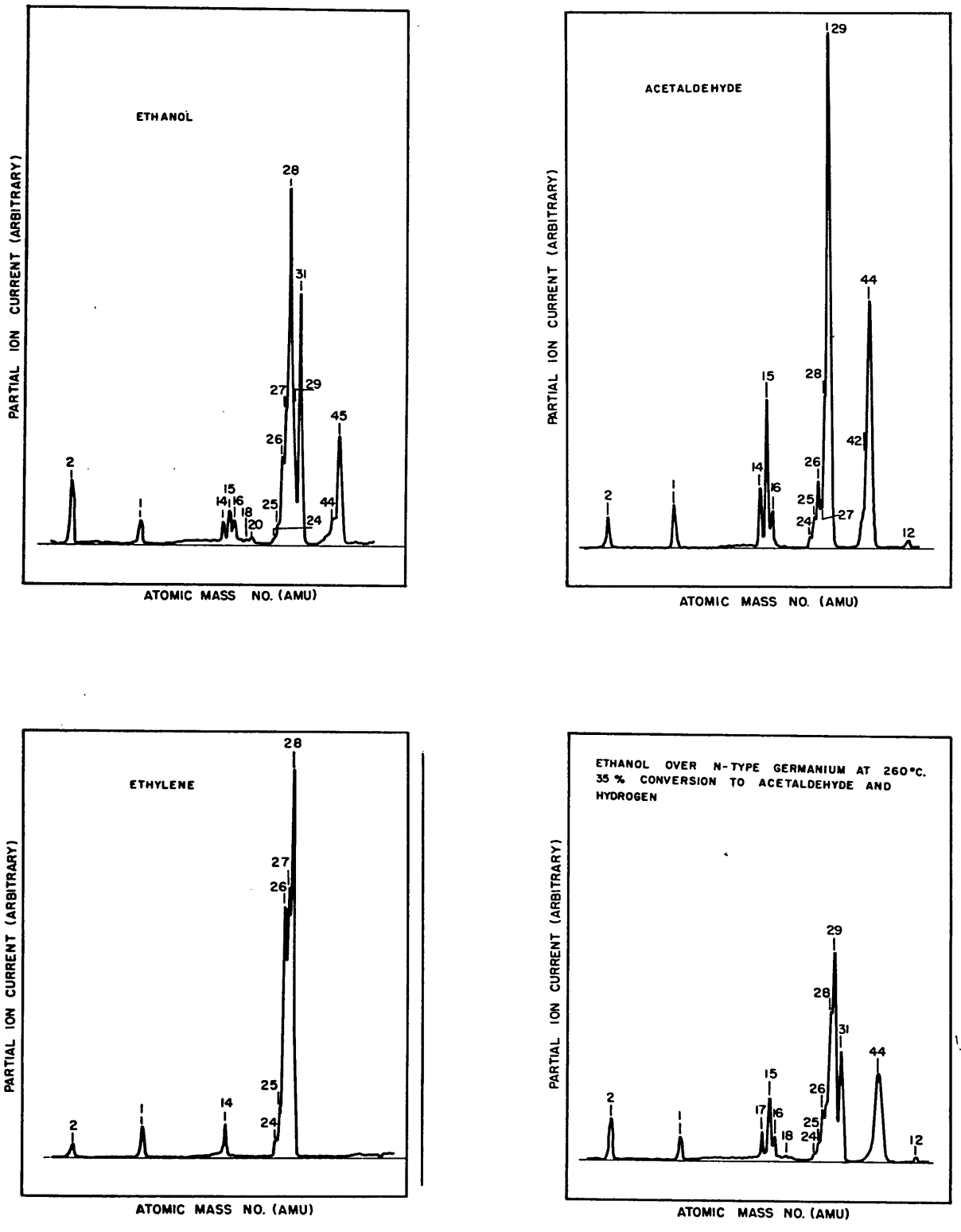

TYPICAL SPECTRA FROM ML-494A

Figure 28.

TABLE II

CRACKING PATTERNS OF ETHANOL AND DECOMPOSITION PRODUCTS

Compound Source	C_2H_4		C_2H_4O			C_2H_5OH				H_2		
	API*	ML-494A	API*	API*	ML-494A	API*	API*	API*	ML494A	API*	API*	ML-494A
1	3.85	8.29			8.196			1.00	1.08			2.00
2	0.56	3.41			5.35				2.06	100.00	100.00	100.00
12	1.77				1.60				0.23			
13	3.22											
14	0.58	8.85			11.81				9.05			
15					28.84				13.70			
16					7.199				9.02			
17			.33		.482				3.11			
18					.482		5.48		1.72			
19							3.02					
20			.12						2.00			
21							0.03					
22												
23												
24	3.20	3.92	1.56		2.43		0.38	0.44	2.46			
25	11.50	12.28	4.76		6.30	1.31	1.94	2.18	6.85			
26	61.20	64.40	9.10	5.56	13.195	5.93	8.34	9.38	32.30			
27	62.30	69.55	4.54	3.54	7.60	17.89	22.20	23.70	51.20			
28	100.00	100.00	2.66	9.02		8.87	5.49	4.73	111.60			
29	2.26		100.00	100.00	100.00	23.91	22.48	25.10	52.90			
30			1.14	0.92		5.36	5.68	6.06				
31			0.25	0.42		100.00	100.00	100.00	100.00			
32						1.47	1.14					
33							0.20					
39						0.07	0.06					
40			0.93	0.86		0.27	0.24					
41			3.86	0.44		1.42	0.95	1.09				
42			9.16	14.87	8.62	4.35	3.02	3.36				
43			26.70	50.00		13.93	7.71	8.46				
44			45.70	88.31	47.75	8.47	1.66	1.79	10.80			
45			1.24	2.31		52.18	35.21	35.50	46.70			
46			0.10			7.30	15.45	16.30				
47						0.65	0.43					

*American Petroleum Institute - Research Project No. 44 Mass Spectral Data

These voltages result in a relationship between mass number and frequency as follows:

$$M = \frac{1080}{f^2} \qquad \text{(A-1)}$$

M = mass number
f = frequency in megacycles

X. APPENDIX (Cont.)

6. Aluminum and Germanium Getters

The aluminum getter consists of two conically wound tungsten wire baskets. These are mounted concentrically in a 5 cm x 5 cm cavity. The outer basket is used as a heater to outgass the inner basket. A detailed drawing of the getter is seen in Figure 29. The wire baskets are mounted on a four-lead press which is then sealed onto the cavity. A blind side arm permits admission of the aluminum to the inner basket. In operation the aluminum is flashed from the inner basket after degassing. A rectangular flow pattern through the getter ensures that all molecules passing through will strike a gettering surface during passage.

The design of the germanium getter permits intimate contacting of the flowing gas with the crushed germanium without restricting the conductance of the system. A detail of the getter is seen in Figure 30. The getter is essentially a small cold trap constructed out of vycor glass to permit heating to 600°C for regenerating the gettering surface. Gatos and co-workers (51) have shown that heating to excess of 550°C volitizes germanium monoxide from germanium surfaces.

In this work when the germanium getter was heated to 600°C for several hours, brown deposits (presumably GeO) appeared on the cooler portions of the inlet and outlet tubulation.

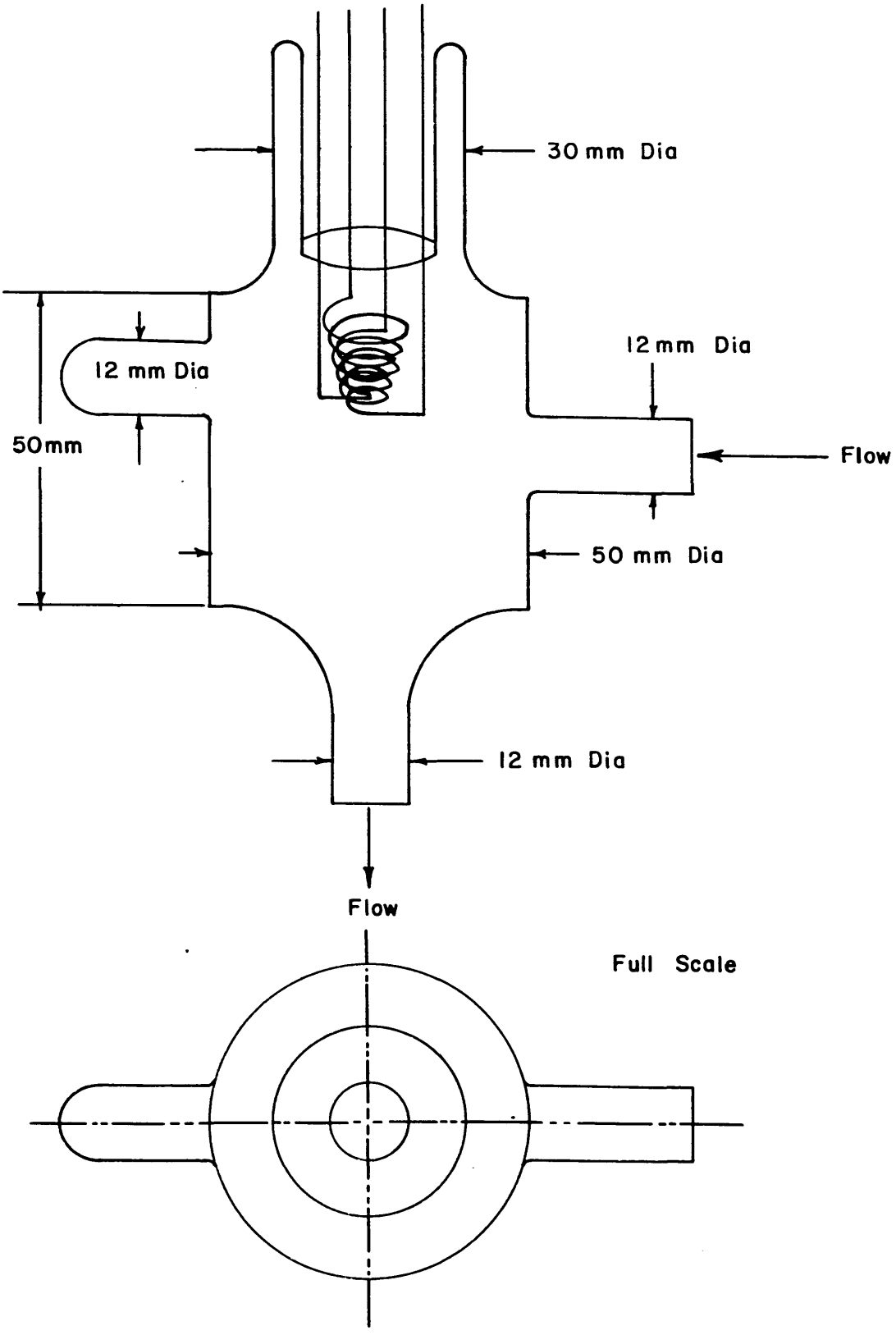

DETAIL OF ALUMINIUM GETTER

Figure 29.

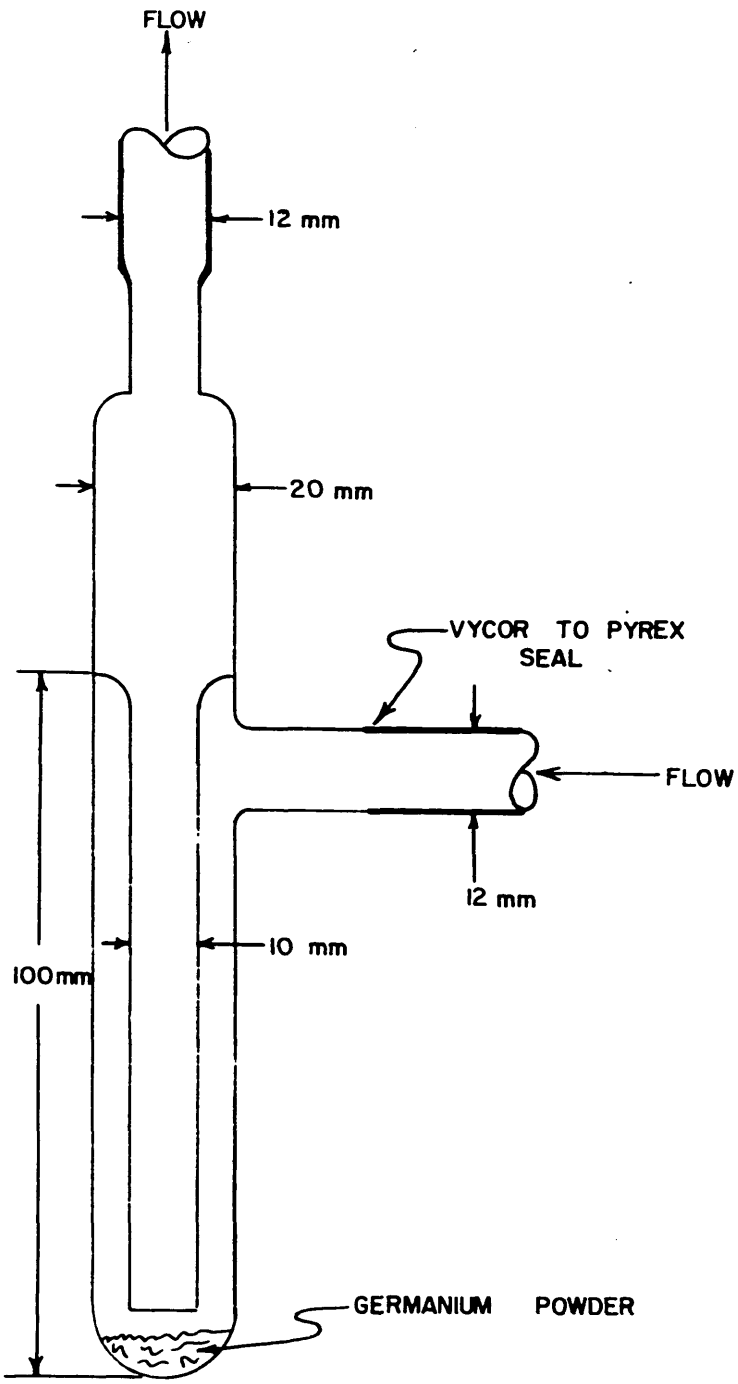

DETAIL OF GERMANIUM GETTER

Figure 30.

X. APPENDIX (Cont.)

7. Germanium Vacuum Crushing Apparatus

The clean surface for the kinetic measurements is produced by crushing massive chips to a fine powder under ultra high vacuum. A drawing of the crushing apparatus is seen in Figure 31.

The bottom of a piece of heavy-walled pyrex tubing is thickened and then flattened to produce the crushing anvile. The magnetic hammer is sealed in the crushing tube. The top portion of the hammer is 416 stainless, which is ferro-magnetic, and the lower portion is 316 which is non-magnetic. Thus when the top portion of the hammer seeks the center of a solenoid coil dropped over the crushing tube, it is possible to position the hammer arbitrarily close to the bottom of the crushing tube. Crushing is accomplished by pulsing the solenoid with 7 amps D.C. through a cam operated switch circuit. The frequency of the pulse can be continuously adjusted by the variable speed motor which drives the cam.

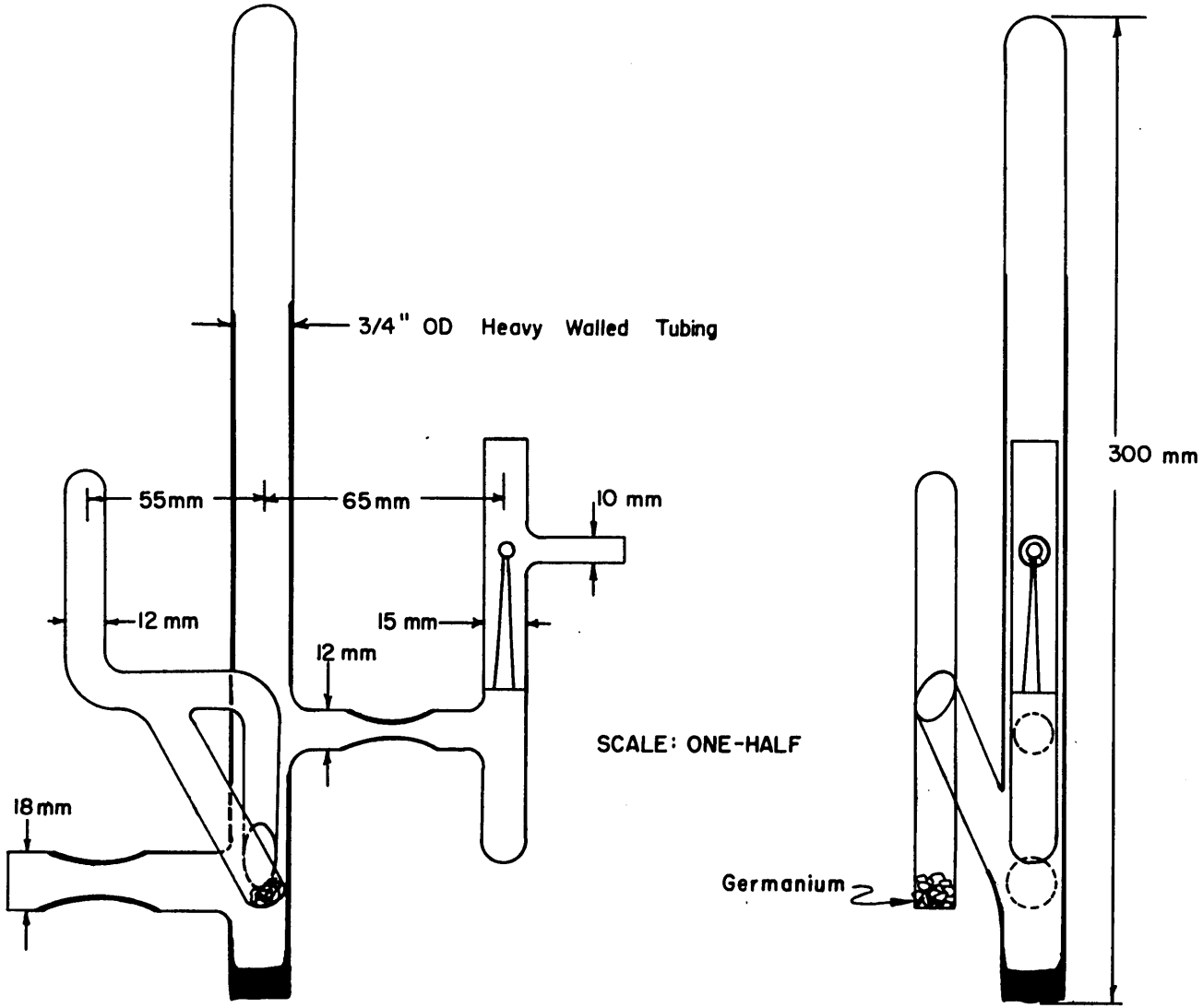

GERMANIUM VACUUM CRUSHING APPARATUS

Figure 31.

X. APPENDIX (Cont.)

8. Electrical Measurements

The surface electrical measurements of interest are surface conductivity and surface recombination velocity (see Appendix D. Measurement and Interpretation of Surface Electrical Properties for details). In this section the power supplies for producing the necessary square wave pulses are described and their integration into a measuring system is detailed.

To avoid resistance heating of the sample, the conductivity is measured by means of a low density-cycle pulse. This pulse is produced by a Tektronex 161 pulse generator. It has a variable amplitude up to 50 volts and the wave form duration of the pulse can be continuously varied between 100 μ seconds and 1 second. The pulse width can be independently varied between 10 μ seconds and 10 m seconds. The pulse has both positive and negative polarity and can be delayed up to 99 percent of the wave-form duration. In operation the output of the 161 generator is fed to the current leads of the hall effect bridge through a variable limiting resistor and viewing resistor contained in the pulse coupler (see Figure 32 for schematic). The voltage across the viewing resistor is monitored on one channel of a Tektronix RM-565 dual beam oscilloscope. The oscilloscope is triggered externally by the sawtooth used to trigger the 161 generator (Tektronix Type 162 Waveform Generator.).

The pulse coupler contains a 0 - 15 mv bias which can be used to eliminate contact potentials from the voltage measurements which

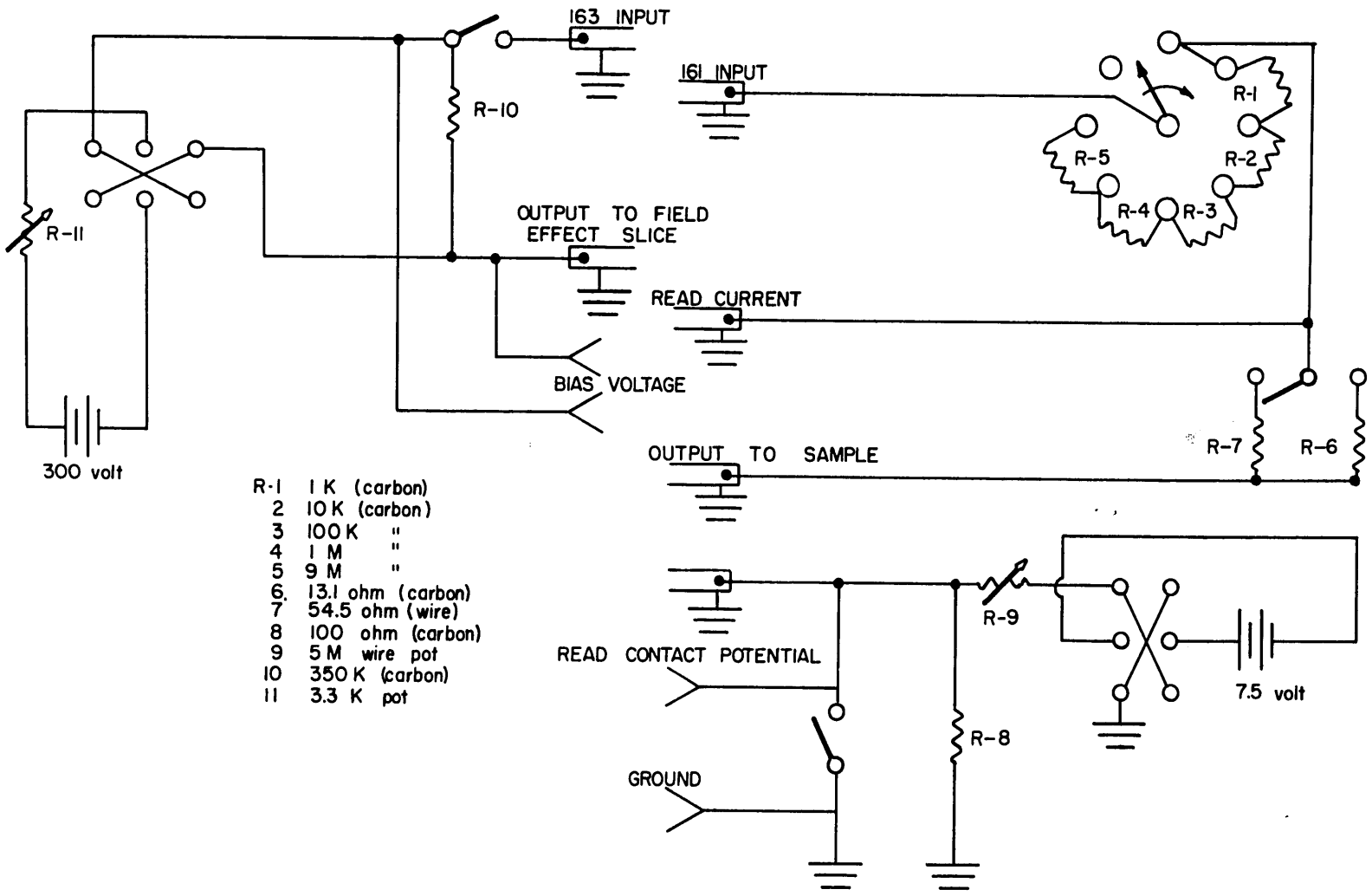

SCHEMATIC OF PULSE COUPLER

Figure 32

are measured by the other beam of the oscilloscope from leads on two adjacent side tabs of the Hall effect bridges.

When the auxiliary germanium electrode is positioned for the field effect measurements, a transverse pulse can be placed across a 0.001-inch space. This pulse is produced by a Tektronix 163 pulse generator. The 163 generator is similar to the 161 except that pulse widths of 1 μ second are achieveable with - 0.2 second rise times, the pulse has only a positive function, and pulse amplitudes are available only up to 25 volts. The 163 can be biased through the pulse coupler up to 300 volts. This results in field strengths up to 5×10^5 volts/cm. Measurements reported in the literature are typically made with 10^6 volts/cm (60). A block diagram of the integrated measuring set-up is seen in Figure 14.

As pointed out in Appendix D. Measurement and Interpretation of Surface Electrical Properties there may be some advantages in using light emitted from gallium-arsenide diodes to study the surface recombination velocities. In this case the output of the 163 pulse generator would be amplified by a current amplifier to drive the diodes. Gains of 10 to 100 would be required. Such amplifiers are presently available (61) with rise-times of a few nano-seconds. The diodes could be operated either at room temperature or $77^{\circ}K$.

X. APPENDIX (Cont.)

B. Experimental Procedure

1. Catalyst Preparation

Germanium was cleaved by impact with a carbon steel chisel on a glass plate into pieces approximately 1/8 inch x 1/8 inch. The pieces were quire angular as might be expected since the (111) plane is a plane of easy cleavage. These chips were cleaned in acetone and inserted into the side arm of the crusher with surgical tweezers. The hammer was then placed in the crushing tube and the tubulation closed. The crusher was sealed into the high vacuum manifold of the reactor system.

When electrical measurements were made a thin wafer (.005-inch thick) cut from the (111) plane of the same crystal as the cleaved material was placed on the optical flat which rests in the sample holder inside the conductivity cell. Electrical connections to the leads on this wafer were made by sandwiching the platinum lead from the sample and a platinum lead connected to the feeders in the press between a 0.004-inch thick platinum fold. The connection was then made secure by spot welding the sandwich.

The crystals were oriented and sliced to 0.003-inch thick by Lincoln Laboratories through Ed Warefort. The Hall effect bridges were made by Donald Sandstrom of the Raytheon Manufacturing Company. The bridges were then optically ground to 0.005-inch and one side was polished by A. D. Jones Optical Company. The 0.002-inch

diameter platinum leads were electronically welded to the bridges by Victor Myette of Raytheon. The original crystals have been obtained from Bell Telephone Laboratories and Lincoln Laboratory.

After the bakeout and subsequent pump-down the crusher was sealed off from the vacuum system and each chip singly crushed by hitting it approximately 600 times. The powder is then passed to the capsule under the break-seal and a new chip was admitted to the crushing tube. Time required to crush a two to four gram sample is four to six hours.

After crushing, the capsule containing the catalyst powder was pinched off from the crusher and the break-seal section was sealed on to the top of the reactor. The space between the two seals was pumped out for several hours with a roughing pump and then sealed off. The lower break-seal was then broken and the inter-seal space evacuated through the system for three to four hours. The maximum increase in system pressure was about one-half order of magnitude. The upper break-seal was then broken and approximately two-thirds of the sample was admitted to the reactor. The break-seal portion was then pinched off and the residual catalyst saved for surface area measurement.

X. APPENDIX (Cont.)

2. Bakeout Procedure

Bakeouts were accomplished by heating the whole system to temperatures from 350°C to 400°C for a period of 36 hours. Before lowering the oven two auxiliary heaters were placed next to the conductivity cell, the heating mantles were placed on the reactor and germanium getter, and the drivers were removed from all valves within the bakeout oven. Glass tubulation protruding from the oven to the roughing line and the gas handling manifold were wrapped with heating tapes up to and including the Type C valves. Temperatures here were maintained at about 200°C.

All temperatures were controlled with variacs to the various heating circuits and measured with Chromel-alumel thermocouples. Temperatures must be increased slowly at first or the rapid evolution of gas will swamp the ion pump. At bakeout completion, the heating circuits were turned off and the system allowed to cool slowly in the oven for several hours.

Pressures of 10^{-9} Torr were then routinely obtained after a twenty-four hour pump-down.

X. APPENDIX (Cont.)

3. Kinetic Measurements

Ethanol was admitted to the system immediately after the removal of the two break seals used to introduce the catalyst. The reactor was then brought to reaction temperatures. Usually it required approximately two to three hours to achieve steady state temperatures. During this time mass spectra of the reaction mixture were continuously taken and the total pressure was monitored. After at least one half hour of no perceptible change in either the temperature or the mass spectra a set of four complete spectra were taken. At the close of each run a room temperature spectrum was taken and used as a basis for the calculations.

The ethanol in the manifold was then pumped out and the high vacuum system evacuated until a pressure below 10^{-8} was obtained. The two-inch valve was then closed; ethanol was re-admitted to the gas handling manifold; and the thirty-one peak was monitored as a function of time. The linear portion of this rise in pressure was taken as a measure of the flow rate. Pressure drops through the mass spectrometer leak and the catalyst bed were then measured.

The volume of the system was measured by connecting a calibrated volume of air to the gas handling manifold. With the manifold and the high vacuum system evacuated the calibrated volume was leaked successively into the manifold and the vacuum system. At each stage the pressure was measured with a manometer so that the volumes could be easily calculated.

Surface area measurements were conducted by Stanley Mitchell of the Metallurgy Department, M.I.T.

X. APPENDIX (Cont.)

C. Purification of Ethanol

A purification scheme was devised to reduce the level of water and oxygen in ethanol before it was admitted to the vacuum system. Absolute ethyl alcohol, reagent quality by U. S. Industrial Chemicals Company was used as a starting material.

A schematic diagram of the apparatus is seen in Figure 33. After the apparatus was assembled it was evacuated to pressure of one micron for 24 hours with the Cu trap held at 250°C. During this time the Drierite trap was heated several times to 150°C. The system was brought to air and 200 ml of absolute ethanol were charged to the flask. Stopcocks two and four were then closed and one was opened so that the ethanol receiver and phosphorous pentoxide trap could be evacuated while hydrogen was passed through the copper and Drierite traps. The copper trap was maintained at 250°C until no evidence of water evolution was present. Hydrogen was vented through stopcock one and the Drierite trap heated until all water was removed. Stopcock one was closed and three opened. Simultaneously nitrogen was admitted through valve one instead of hydrogen. Valve one was adjusted to give a nitrogen flow of a few milliliters per minute and the ethanol brought to boiling temperature. The ethanol was refluxed and deoxigenated for 36 hours.

It has been estimated (50) that the oxygen content of nitrogen treated in the way described above is of the order of 10^{-19}

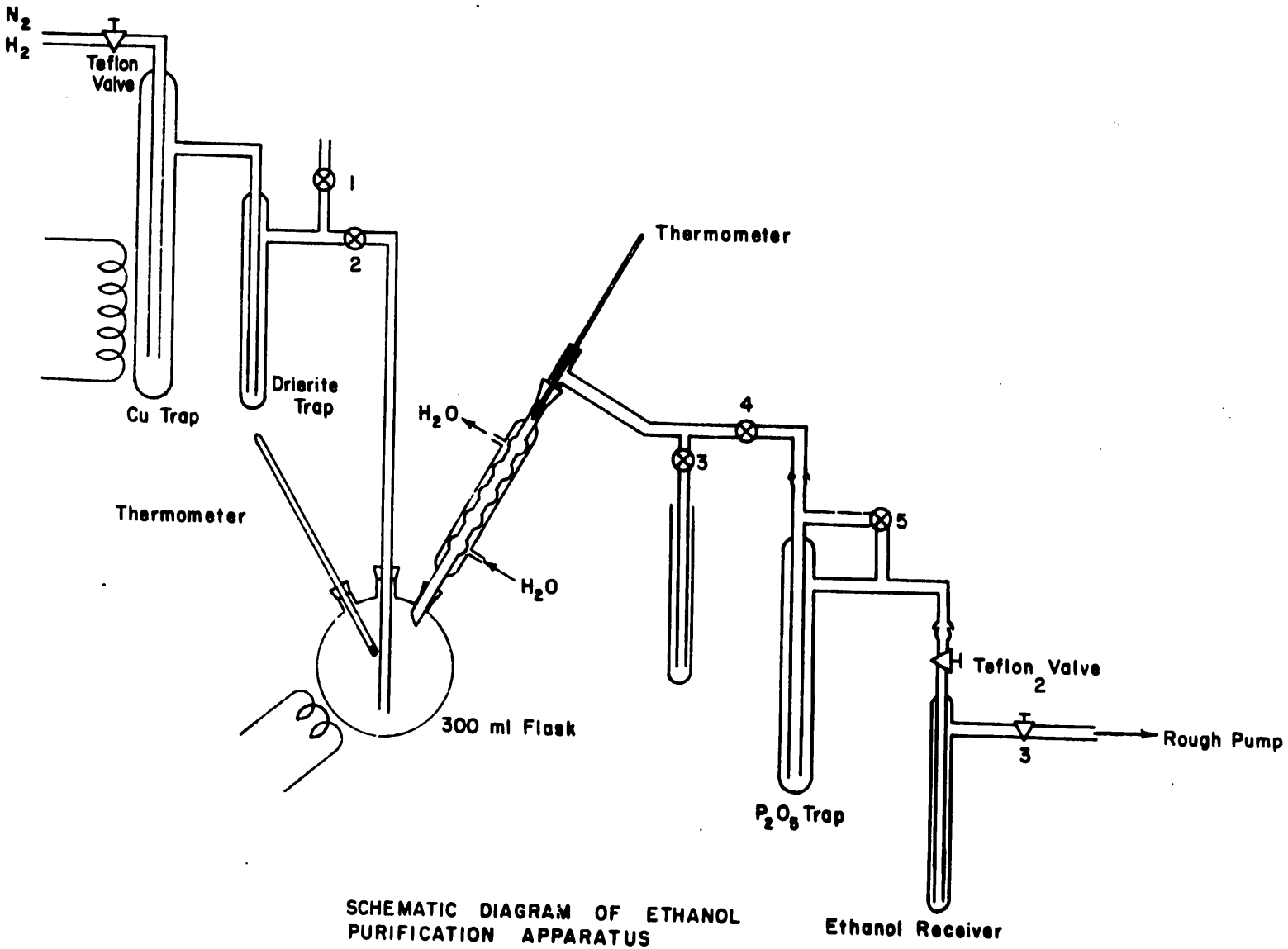

SCHEMATIC DIAGRAM OF ETHANOL PURIFICATION APPARATUS

Figure 33.

atmospheres. Assuming reasonable values for oxygen solubilities this results in less than one oxygen molecule per cubic centimeter of ethanol. From charging curves taken in electrolyte treated for several hours with nitrogen deoxygenated in this way, Selvidge (50) found less than a monolayer of oxygen on a square centimeter of germanium surface.

After refluxing the nitrogen was shut off at valve one and stopcock two was closed. The ethanol was cooled to room temperature and valve two was closed. With stopcock five open, stopcock four was opened to admit nitrogen to phosphorous pentoxide trap. Then valve two was opened slightly to permit bleeding-off of the nitrogen. Ethanol was then distilled over at a few degrees below room temperature. The first few milliliters were evacuated through the roughing pump with stopcock five open. The phosphorous pentoxide trap was then cooled to liquid nitrogen temperature and stopcock five closed. About 40 - 60 ml. of ethanol were distilled over and stopcock four closed. The ethanol in the phosphorous pentoxide trap was then evacuated for one hour at one micron. The trap was then allowed to warm up with the vacuum pump valved off. After warming the trap was evacuated for a few seconds and then refrozen. Several cycles of this procedure permitted intimate mixing of ethanol and phosphorous pentoxide and degassing of the mixture.

Next about four ml. were distilled out of the phosphorous pentoxide trap through the roughing pump. The ethanol receiver was

cooled to liquid nitrogen temperature and 8 - 12 milliliters of ethanol collected. The receiver was then closed off from the rest of the system and degassed as above. Valve three was then removed by vacuum pinch-off and the ethanol receiver connected to the gas handling manifold through valve two. In making this connection the ball and socket joint was removed and the receiver was attached permanently to the manifold.

D. Measurement and Interpretation of Surface Electrical Properties

The basic postulate of the charge-transfer theory of catalysis is that the electronic configuration of the surface has a major effect on the tendency of the absorbed species to exchange charge with the surface. Electronic parameters which may prove to be of fundamental importance to catalysis, are the surface excess of charge carriers, Γ, the electrical potential of the surface compared to the bulk $(\psi_s - \psi_o)$ and the recombination velocity s at the surface. It is expected that Γ and s will be important fundamental quantities in kinetic steps which involve charge transfer while the quantity, $(\psi_s - \psi_o)$, for the case when charge transfer reaches equilibrium, can be shown to be directly related to the driving force for charge transfer at zero surface charge. At equilibrium, and $(\psi_s - \psi_o)$ can be related. Garrett and Brattain (43) have shown Γ to be described by:

$$\Gamma_p = n_i \mathcal{L} \exp \frac{e}{2kT} (\varphi_p - \psi_s) \qquad (33)$$

$$\Gamma_n = n_i \mathcal{L} \exp \frac{e}{2kT} (\psi_s - \varphi_n) \qquad (34)$$

where $\Gamma_{p\ n}$ = surface excess of holes and electrons, respectively.

n_i = bulk concentration of electrons in the intrinsic semiconductor

$\mathcal{L}$ = $[\epsilon\epsilon_o kT/2\pi e^2 n_i]^{1/2}$, the Debye length for the intrinsic material

$\epsilon\epsilon_o$ = permitivity of the semiconductor and free space, respectively.

e = unit charge.

k = Boltzman's constant

T = absolute temperature

$\mathcal{P}_p, \mathcal{P}_n$ = quasi-Fermi level for electrons and holes, respectively.

ψ_s = electrostatic potential at the surface.

The quasi-Fermi levels, $\mathcal{P}_p$ and $\mathcal{P}_n$, are employed by Garrett and Brattain to describe a quasi equilibrium situation where the electrochemical potential of the electrons and holes, while constant through the space-charge region, is not equal to the Fermi energy of the semiconductor. Equations (33) and (34) represent the limiting cases of decidedly n-type and decidedly p-type materials. The relations for the general case involve integrals which cannot be expressed in terms of simple functions, but these limiting cases can be used without loss of fundamental generality, since the general case could also be evaluated numerically for any given set of conditions. More recently Lee and Mason (17) have derived analytical equations for several other cases of interest.

Applying (33) and (34) at the equilibrium conditions yields for Γ_p,

$$\Gamma_p = n_i \alpha \exp \frac{e}{2kT} (\mathcal{P}_o - \psi_s) \tag{35}$$

but in addition

$$\frac{n_i}{p_o} = \exp \frac{e}{2kT} (\psi_o - \mathcal{P}_o) \tag{36}$$

and combining (27) and (28),

$$\Gamma_p = (p_o n_i)^{1/2} \mathcal{L} \exp \frac{e}{2kT} (\psi_o - \psi_s) \tag{37}$$

A similar argument gives,

$$\Gamma_n = (n_o n_i)^{1/2} \mathcal{L} \exp \frac{e}{2kT} (\psi_s - \psi_o) \tag{38}$$

for n-type materials where:

P_o = bulk concentration of holes

n_o = bulk concentration of electrons.

Equations (37) and (38) relate and $(\psi_s - \psi_o)$ for the case of charge transfer equilibrium. A quantity $(\psi_s - \psi_o)$ can be calculated from (37) and (38) for the non-equilibrium case and is a measure of the perturbation of the system from equilibrium.

If the conductivity of a thin slice of material (.005 inch or so) is measured, the surface conductivity, ΔG, can be calculated by subtracting the conductivity of a piece of material the dimensions of the slice with bulk electrical properties. Equation (18) gives ΔG as a function of Γ

$$\Delta G = \mu_{eff} \Gamma \tag{39}$$

where μ_{eff} is the effective mobility of majority carriers. The equation is only valid for negligibly small numbers of minority carriers, but Garrett and Brattain (44) have dealt with the general case where the quantity, $(\psi_s - \psi_o)$, can be calculated, though not so simply, from ΔG. For the simple case, Γ is available from (39) and $(\psi_s - \psi_o)$ from (37) and (38), if μ_{eff} is known.

Schrieffer (45) has calculated the ratio of the effective mobility of the surface to that in the bulk from a consideration of the isotropic scattering of majority carriers in the space charge "potential well". His arguments have been carried further by Zamel and Petritz (46) who found the theory in fair quantitative agreement with surface Hall-effect measurements on germanium in oxygen ambients.

Thus, it is possible to obtain Γ and $(\psi_s - \psi_o)$ from conductivity measurements of a thin slice of catalyst.

If a transverse electric field is applied to the catalyst surface, then additional carriers are injected into the space charge layer, causing an additional contribution to ΔG and $(\psi_s - \psi_o)$. If the transverse electric field is removed and the change in conductivities monitored, the recombination velocity of majority carriers can be determined (41).

Ruprect (57) has used such a pulsed field effect technique to measure the concentration and energy of surface states on germanium and silicon. In addition he measured recombination rates and varied the oxidation state of the surface.

Another approach to the measurement of recombination rates is to illuminate the surface with light. Absorption of the light results in exitation of electrons into the conduction band at the surface. Recombination characteristics can then be calculated from the conductivity decay when the light is turned off.

Two problems are present with ordinary light sources (1) sources are not abailable with high intensity in a narrow band of wave lengths and (2) it is very difficult to produce a mathematically describable light pulse with rise-times of the order of 1μ second with a mechanical shutter

A light source which overcomes both of these problems is the gallium arsenide recombination radiation diode. It was first announced by Keys and Quist (58). A p-n junction of gallium arsenide is reversed biased and recombination of holes and electrons injected into the junction results in the emission of photons with nearly 100 percent efficiency. A number of laboratories (see for example (59)) have announced work with these diodes and some (59) have succeeded in producing laser action by optically grinding the p-n junction and operating at high current densities.

In order not to disturb substantially the population of surface states whose energies lie within forbidden gap, the energy of the incident photons must be greater than 0.7 ev. To avoid the complication of electron emission the incident photons should not have energies greater than 4.5 ev. This is not a stringent requirement but if the details of the recombination rate are to be evident one should have nearly mono-energetic photons since a broad spectrum would seriously complicate the mathematical treatment of the data. Thus any narrow band source between 0.7 and 4.5 ev which could be switched with rise times of a 1μ second would be acceptable. The

energy of the photons emitted from gallium-arsenide diodes is about 1.4 ev and the band width is less than 1 percent of the value. Intensities can be carefully controlled by controlling the diode current up to levels greater than gas lasers but somewhat less than ruby lasers. Rise times of a few nonoseconds are achieveable. The use of this source presents the possibility of injecting a square wave of almost arbitrarily large numbers of electrons into the conduction band near the surface without substantially disturbing the population of the surface states within the forbidden gap.

The experimental system for the measurement of surface electrical properties including recombination rates by electrostatic field effect is detailed in Appendix A. Experimental Apparatus. Also included is a description of the modifications necessary to use gallium-arsenide diodes to make photo-effect recombination studies.

X. APPENDIX (Cont.)

E. Mathematical Treatment of Kinetic Data

Decomposition of ethanol on germanium has been found to be first order with respect to ethanol (32). The rate equation can be formulated as follows:

$$-\frac{dP_{EOH}}{d\theta} = k_D W_c a P_{EOH} \qquad (40)$$

where:

P_{EOH} = ethanol partial pressure (mm Hg)
θ = time (seconds)
a = specific surface area of catalyst (m^2/g)
W_c = catalyst weight (g)
k_D = specific decomposition rate constant $(m^2 sec)^{-1}$

Consider a section of the catalyst bed of area, A, and thickness, dl, perpendicular to flow. Gas passes through the bed at velocity, v, then

$$d\theta = \left(\frac{dl}{v}\right) = \left(\frac{A\,dl}{Q}\right) \qquad (41)$$

where:

v = velocity (m/sec)
l = distance (m)
Q = volumetric flow (m^2/sec)
A = cross-sectional area (m^2)

but A dl is just the differential volume of the catalyst bed and Q is the molar feed rate divided by the molecular density. Thus (40) becomes:

$$-\frac{dP_{EOH}}{dV} = \frac{k_D a W_c \rho_m}{F} P_{EOH} \qquad (42)$$

where:

F = molar feed rate of ethanol (moles ethanol/second)

ρ_m = molar density of ethanol

Integrating (42) and noting that the volume of the catalyst bed is the weight of the catalyst divided by its bulk density one obtains:

$$\ln\frac{P^o_{EOH}}{P_{EOH}} = \frac{k_D a W_c^2 \rho_m}{(1-\epsilon)\rho_c F}$$

where:

P^o_{EOH} = inlet partial pressure of ethanol (mm Hg)

P_{EOH} = outlet partial pressure of ethanol (mm Hg)

ϵ = porosity of the catalyst bed (dimensionless)

ρ_c = density of germanium (g/m^3)

It is assumed that k_D follows the Arrhenius law, so that the natural log of (43) gives:

$$\ln\left(\ln\frac{P^o_{EOH}}{P_{EOH}}\right) = -\frac{E_a}{RT} + \ln\frac{C_D a W_c^2 \rho_m}{(1-\epsilon)\rho_c F} \qquad (44)$$

where:

C_D = pre-exponential of the decomposition rate constant

E_a = apparent activation energy (calories/mole)

T = absolute temperature (degrees Kelvin)

R = Boltzman's constant (calories/mole ^oK)

Thus a plot of the left-hand side of (44) versus 1/T gives a straight line whose slope is E_a/R. The value of C_D can be calculated

from the zero intercept. A similar treatment for the rate of appearance of one of the decomposition products yields:

$$\ln\left(\ln\frac{P^{o}_{EOH}}{P^{o}_{EOH} - P_i}\right) = -\frac{E_a}{RT} + \ln\frac{C_i a W_c^{2} \rho_m}{(1 - \epsilon)\,\rho_c F} \qquad (45)$$

where:

P_i = partial pressure of any decomposition product

C_i = pre-exponential of decomposition rate constant

From these equations the overall decomposition rate and the rates of dehydrogenation and dehydration can be calculated.

Equations (44) and (45) are particularly convenient to use with the mass spectrometer, since only pressure ratios occur in the intergrated rate equation. Thus the mass spectra can be used directly without quantitative interpretation of the pressure. The feed rate, F, is measured at the end of each run.

X. APPENDIX (Cont.)

F. Sample Calculations

1. Quantitative Treatment of Mass Spectrometer Analyses

The interpretation of the mass spectrometer data obtained in this investigation consisted essentially of reading the spectra obtained and successively removing the contributions of ethanol, acetaldehyde, ethylene and hydrogen from a product spectrum to obtain the complete analysis of the product gas mixture. The details of the analysis are given in the following stepwise procedures.

a. Reading Spectra

1. General Procedure

When a spectrum was taken the RF frequency corresponding to a particular peak was recorded, and this frequency was converted to mass number by equation (A-1).

Peak heights were read as graphical diversions between the top of a peak and the top of the base line in a spectrum. In most spectra the base line was straight. For some spectra the base line was not perfectly straight but by consistently measuring peak height from the same location on the base line, the different spectra could be compared.

X. APPENDIX (Cont.)

b. Product Spectra for n-type Germanium Catalyst

The peak heights for mass number 31 could easily be read within less than a division or at least 1 - 2 percent. At high conversions the 29 and 44 mass number peaks could be read with 2 - 5 percent accuracy. The smaller peaks could be read much less accurately but it was clearly shown that negligible dehydration occurred so only the 31 and 29 peaks were important in the analyses for studies on n-type germanium.

At low conversions there was no distinct 29 peak; so the 29 peak height was measured as the distance from the base line to the point of inflection on the low frequency side of the 28 peak. The 29 peak value thus obtained gave the most satisfactory results in reaction rate temperature plots.

X. APPENDIX (Cont.)

2. Ethanol, Acetaldehyde, Ethylene, and Hydrogen Spectra

The peak heights of the different mass numbers in an ethanol spectrum were recorded and the ratio of each peak height to the 31 peak height were obtained. This was done for a number of ethanol spectra and the average ratios were calculated. Similarly ratios of the peak heights to the 29 peak height for pure acetaldehyde spectra and the ratios of the peaks to the peak height for pure ethylene spectra were obtained. Table I contains the resulting ratios.

These ratios were used to determine the contribution of ethanol, acetaldehyde, ethylene and hydrogen to the product spectra. This procedure is illustrated by Table III. The first column tabulates average values for the peak heights obtained in a series of spectra for the run and conditions indicated. To determine the ethanol contribution to a product spectrum, the value for the 31 peak in the product spectrum is multiplied by the 31 peak ratios found for the pure ethanol spectrum. Subtracting the ethanol spectrum from the product spectrum gives the spectrum in column 3. The value for the 29 peak in column 3 is multiplied by the 29 peak ratios found for the pure acetaldehyde spectrum to give the acetaldehyde in the spectrum. Subtracting the acetaldehyde spectrum gives the contribution of hydrogen to the product spectrum. The presence of residual values for mass numbers other than 2 represents the limitations of the accuracy of this procedure for the smaller peaks

TABLE III

SAMPLE CALCULATION FOR 35 PERCENT CONVERSION ON VACUUM-CRUSHED GERMANIUM

Mass No.	Raw Spectrum	Ethanol	Spectrum Less Ethanol	Acetaldehyde	Spectrum Less Acetaldehyde
1	6.20	4.58	1.62	1.705	-0.085
2	13.80	8.76	5.04	1.235	3.805
12	2.08	0.99	1.09	0.33	0.763
14	5.90	3.85	2.05	2.450	-0.400
15	11.70	5.85	5.85	5.999	-0.149
16	6.10	3.83	2.27	1.498	0.872
17	1.18	1.32	-0.14	0.100	-0.240
18	1.19	0.73	0.46	0.100	0.360
20	1.12	0.85	0.27		
24	1.47	1.00	0.47	0.506	-0.036
25	4.60	2.92	1.68	1.311	0.369
26	16.70	13.75	2.95	2.743	0.207
27	22.90	21.80	1.10	1.580	-0.480
28	64.20	49.50	14.70		
29	43.30	22.50	20.80	20.800	0.00
31	42.50	42.50	0.00		0.00
44	14.20	4.75	9.45	9.920	-0.47
45	20.10	17.50	2.60		2.60

When ethylene and water are present in the product gas, their contributions are obtained from the value of the 26 peak in column 5 and the 26 peak ratios for pure ethylene and the 18 peak for water.

X. APPENDIX (Cont.)

3. Pressure Correction

The spectra were not all taken with the same pressure in the mass spectrometer tube. However, the variation was not great and it was found that the peak heights responded linearly to pressure variations for the conditions encountered. Therefore, before calculation of rate constants the peaks were all reduced to a base pressure by the correction:

$$\text{CORRECTED PEAK HEIGHT} = \frac{(\text{Actual Peak Height})(\text{Base Pressure})}{(\text{Actual Pressure})}$$

The peak height values obtained from the spectra have physical significance in being proportional to the partial pressure of the molecular species in the product gas. Hence the peak heights were substituted for the partial pressures in the rate equations derived in Appendix E. Mathematical Treatment of Kinetic Data. The 31 peak was used to measure the partial pressure of ethanol; the 29 peak, after subtraction of ethanol, measured acetaldehyde partial pressure; the peak, after removal of ethanol and acetaldehyde, measured ethylene; the remaining 2 peak measured hydrogen; and 18 measured water.

The proportionality constant relating peak height to partial pressure was not needed when Eg were used to determine rates and percent conversions. The proportionality constant was needed for equations involving both ethanol and acetaldehyde partial pressures.

The procedure is illustrated below by calculating the entries in Table I for Run D 31-32.

$$P_{ETOH} = \frac{\alpha_{ETOH}\,(\text{Actual Peak Height ETOH})\,(\text{Base Pressure})}{\text{Actual Pressure}}$$

$$P_{ACO} = \frac{\alpha_{ACO}\,(\text{Actual Peak Height ACO})\,(\text{Base Pressure})}{\text{Actual Pressure}}$$

α_{ETOH} = proportionality factor relating peak height to partial pressure of ethanol

α_{ACO} = proportionality factor relating peak height to partial pressure of acetaldehyde

Substituting:

Actual Peak Height ETOH	= 42.50
Actual Peak Height ACO	= 20.80
Base Pressure	= 3.3
Actual Pressure	= 2.8

$$P_{ETOH} = \alpha_{ETOH}\,\frac{(42.50)(3.3)}{2.8} = 50.10\,\alpha_{ETOH}$$

$$P_{ACO} = \frac{\alpha_{ACO}(20.80)(3.3)}{2.8} = 24.50\,\alpha_{ACO}$$

$$P^{o}_{ETOH} = 77.35_{\ ETOH}$$

$$\ln\frac{P^{o}_{ETOH}}{P_{ETOH}} = \ln\frac{77.35\ ETOH}{50.10\ ETOH} = 0.4339$$

$$\ln\frac{P^{o}_{ETOH}}{P^{o}_{ETOH} - P_{ACO}} = \ln\frac{\alpha_{ETOH}\ 77.35}{\alpha_{ETOH}\ 77.35 - \alpha_{ACO}\ 24.50}$$

Assuming $\alpha_{ACO} = \alpha_{ETOH}$ gives

$$\ln \frac{P^o_{ETOH}}{P^o_{ETOH} - P_{ACO}} = 0.3830$$

$$\text{Fraction Ethanol Conversion} = \frac{P^o_{ETOH} - P_{ETOH}}{P^o_{ETOH}}$$

$$= \frac{\alpha_{ETOH}\, 77.35 - 30.10\alpha_{ETOH}}{\alpha_{ETOH}\, 77.35}$$

$$= 0.3525$$

X. APPENDIX (Cont.)

G. Nomenclature

Symbol	Meaning	Units
A	Helmholtz Free Energy Cross Sectional Area	Calories/molecule $(\text{meter})^2$
E	Energy	Electron volts
F	Molar Feed Rate	Moles/second
G	Conductivity	Ohm-centimeter
K	Vibrational Force Constant	Dyne/centimeter
M	Number of Adsorption Sites	$(\text{Centimeter})^{-2}$
N	Number of Adsorbed Molecules Normalizing factor for composite wave function	$(\text{Centimeter})^{-2}$ Dimensionless
P	Pressure	Torr
Q	Multi-particle Partition Function Volumetric Flow Rate	Dimensionless $(\text{meter})^3/\text{second}$
R	Boltzman's Constant - Gas Constant Separation Distance	Calories/mole $^{\circ}C$ Centimeters
R'	Separation Distance when U(R) = 0	Centimeters
U	Dissociation energy for chemisorbed species	Electron Volts
a	Specific Surface Area	$(\text{meter})^2/\text{gram}$
e	Value of Unit Charge	Coulomb
h	Planck's Constant	ERG-seconds
k	Specific Rate Constant Boltzman's Constant	$(\text{moles})(\text{meter})^2$ Ergs/molecule $^{\circ}C$
l	Axial Distance through Catalyst Bed	Meters
m	Vibrational Mass	Grams

Symbol	Meaning	Units
n	Vibrational Quantum number Bulk Concentration of Charge Carriers	Dimensionless $(\text{meters})^{-3}$
q	One particle partition function	Dimensionless
s	Surface Recombination velocity	$(\text{centimeter})^{-2}$ $(\text{second})^{-1}$
U(R)	Electronic energy as a function of R	Electron Volts
v	Superficial Gas Velocity	(meter)(second)
Γ	Surface Excess Concentration of Charge Carriers	$(\text{meter})^{-2}$
ϕ	Work Function	Electron Volts
Ψ	Electrostatic Potential in Bulk of Semiconductor Quantum Mechanical Wave Function	(ESU)(centimeter) Dimensionless
ϵ	Permativity Porosity	Farad/centimeter Dimensionless
ρ	Density	Gram/meters^3
φ	Quasi-Fermi Energy	Electron Volts
θ	Time Fraction Ionized	Seconds Dimensionless
μ	Chemical Potential Charge Carrier Mobility	Electron Volts $\text{Ohm-(centimeter)}^3$

Subscripts

o	Unionized and unperturbed or bulk quantities
+	Positively ionized quantities
1	one particle quantities
D	quantities related to decomposition reaction
e	electronic quantities

Symbol	Meaning
	Subscripts cont.
F	Denotes Fermi Energy
i	Internal or Intrinsic quantities
n	Electrons
p	Holes
s	Surface Properties
x,y,z	Coordinate directions
EOH	Ethanol

X. APPENDIX (Cont.)

H. Location of Original Data and Detailed Calculations

The original data and detailed calculations are in the custody of the author. Permanent copies of all this material are held by Professor Raymond F. Baddour at M.I.T., Room 12-184.

X. APPENDIX (Cont.)

I. Literature Cited

(1) Heinemann, H., "Proceedings of the Second International Congress on Catalysis", Editions Technip, Paris, 1961, p. 129.

(2) Balandin, A. A., Z. Physik. Chem. B2:289 (1929).

(3) Balandin, A. A., Advances in Catalysis, 10, 96 (1958).

(4) Balandin, A. A., and Teterni, P., Doklady Akad. Nauk SSSR 132, 577-80 (1960).

(5) Balandin, A. A., Doklady Akad. Nauk SSSR 133, 1073-6 (1960).

(6) Wagner and Hauffe, Z., Elektrochem. 44, 172 (1938).

(7) Hauffe, Glange, Engell, Z. Physik. Chem. 201, 221 (1952).

(8) Hauffe, Semiconductor Surface Physics, R. H. Kingston Ed., p. 283 (1957).

(9) Hauffe, Advances in Catalysis 7, 213 (1955).

(10) Dowden, D. A., J. Chem. Soc., p. 285 (1950).

(11) Volkenshtein, Th. Zhur. Fiz. Khim. SSSR 22, 311 (1948).

(12) Volkenshtein, Th. and Roginsky, S. Z., Zhur. Fiz. Khim. SSSR 29, 485 (1955).

(13) Volkenshtein, Th. and Sandomirski, V. B., Compt. Rend. Acad. Sci. SSSR 118, 980 (1958).

(14) Volkenshtein, Th. and Kogan, Zhur. Fiz. Khim. 211, 282-93 (1959).

(15) Volkenshtein, Th., Advances in Catalysis 12 189 (1960).

(16) Balandin, A. A., Second International Congress on Catalysis, Paris, France (1960).

(17) Lee, V. J., and Mason, D. R., J. Appl. Phys. 34 2660 (1963).

(18) Garrett, C. G. B., J. Chem. Phys., 33 966 (1960).

(19) Wagner, C., and Hauffe, K., Z. Elektrochem. 44, 172 (1938).

(20) Beck, O., Rev. Mod. Phys. 17, 61 (1945).

(21) Beek, O., Disc. Farad. Soc. 8, 124 (1950).

(22) Dowden, D. A., and Reynolds, P. W., J. Chem. Soc. (London) 265, 1950.

(23) Lo, M. N., Sc.D. Thesis, M.I.T., Dept. of Chem. Eng., Cambridge, Mass, (1962).

(24) Schwab, G. M., and Block, J., Z. Elektrochem. 58 756 (1954).

(25) Parravano, G., J. Am. Chem. Soc. 75, 1448, 1452 (1955).

(26) Law, J. T., Semiconductors, A. C. S. Monograph, 140 Ed. Hannay, Reinhold Pub. Co., (1959) p.676.

(27) Schwab, G. M., Semiconductor Surface Physics, Ed. R. H. Kingston, U. of Pennsylvania Press (1957) p. 283.

(28) Ibid.

(29) Penzkofer, Dissertation, Munich (1956).

(30) Bielanski, A., J. Deren and J. Haber, Nature, 179, 668 (1957).

(31) Bielanski, A., Deren, J., Haber, J., and Slocqynski, J., Proceedings of the Second International Congress on Catalysis, Paris, France, 1960; Editions Technip, Paris (1961) V. 2, p. 1653.

(32) Frolov, V. M., and Krylov, O. V., Doklady Akad. Nauk SSR 126, 107 (1959).

(33) Farnsworth, H. E., Semiconductor Surface Physics Loc. Cit. p. 3.

(34) Palmer, D. R., and Dauerbaugh, C. E., Bull. Am. Phys. Soc. Series II, 3 138 (1958).

(36) Shooter, D., and Farnsworth, A. E., J. Phys. Chem. 66, 222 (1962).

(37) Sandler, V. L., and Gazith, M., J. Phys. Chem. 63, 1095 (1959).

(38) Loebl, E. M., Address to the Chemical Section, New York Academy of Science, March 7, 1961.

(39) Loebl, E. M., Personal Communication, April 5, 1962.

(40) New York Academy of Sciences, "Conference on Clean Surfaces", April 4, 5, and 6, 1962. New York, N. Y.

(41) Banbury, Law and Nixon, Semiconductor Surface Physics, Loc. Cit. p. 70.

(42) Gatos, H. C., Personal Communication.

(43) Temkin, M. I., Kipperman, S. L., and Luk'yamona, L. I., Doklady Akad. Nauk SSSR 74, No. 4 (1950).

(44) Garrett, C. G. B., and Brattain, W. H., Phys. Rev. 99, 376 (1955).

(45) Schrieffer, J. R., Phys. Rev. 97, 641 (1955).

(46) Zemel, J. W., and Petritz, R. L., Bull. Am. Phys. Soc., 2, 131 (1957); Phys. Rev. 110, 1263 (1958).
Petritz, R. L., Phys. Rev. 110, 1254 (1958).
Zemel, J. W., Phys. Rev. 112, 762 (1958).

(47) Weisz, P. B., and Kearn, W. P., J. Phys. Chem. 65, 417 (1961).

(48) Selvidge, Waldman, Cooper and Kurtz, 10.91 Project M.I.T. Department of Chemical Engineering (February 1962)
Robles, J., Personal Communication, August 1961.

(49) Gobeli, G. W., and Allen, J. G., Phys. Rev. 150, 141 (1963).

(50) Selvidge, C. W., S.B. Thesis, M.I.T., May 17, 1963.

(51) Robinson, P. H., Rosenberg, A. J., and Gatos, H. C., J. Appl. Phys. 27, 962 (1956).

(52) Reid, R. C., M.S. Thesis, Purdue Univeristy, February 1951.

(53) Moore, G. E., Smith, H. A., and Taylor, E. H., J. Phys. Chem. 66, 1241 (1962).

(54) Litovchenko, V. G., Lyashenko, V. I., and Frulov, O. S., Poverkhn. Sovistva Poluprov., Akad. Nauk SSSR, Inst. Elektrokhim. 1962 147-64.

Srinivasan, G., Chessick, J. J., and Zettlemoyer, A. C., J. Phys. Chem. 66, 1819 (1962).

Burshtein, R. Kh., Larin, L. A., and Sergeeu, S. I., Poverkhn. Sovistva Poluprov., Akad. Nauk SSSR, Inst. Elektrokhim 1962 34-55.

Suhrmann, R., Kruel, M., and Wedler, G., Naturforsch. 18a, 633-8 (1963).

(55) Humble Oil and Refining Co., American Petroleum Institute Tables of Mass Spectra, No. 293 and 283.

(56) U. S. Army Quartermaster Corps, Personal Communication, February 10, 1964.

(57) Ruprect, G., Ann. N. Y. Akad. Sci. 101, 857-68 (1963).

(58) Keys, R. J., and Quist, T. M., IRE-AIEE Solid State Devices Conference, July 9-11, Durham, N. H., 1962, Proc. IRE 50, 1822 (1962).

(59) Nathan, M. I., and Burns, G., Phys. Rev. 129, 125 (1963).

(60) Margoninski, Y., Ann. N. Y. Acad. Sci. 101, Art. 3, 915 (1963).

(61) Personal Communication, Andre Kruchekof, Spencer Laboratory, Raytheon Manufacturing Co., Burlington, Mass., February 10, 1964.

(62) Mayer, J. E., and Mayer, M. G., Statistical Mechanics, John Wiley and Sons, New York, 1940, p. 158.

(63) Dillon, J. A., and Farnswirth, H. E., J. Appl. Phys. 28, 174 (1957).

(64) Heiland, G., and Handler, P. J., Appl. Phys. 30, 446 (1959).

Handler, P., and Portnoy, W. H., Phys. Rev. 116, 516 (1959).

(65) Personal Communication, E. G. Rochow, Harvard University, and A. W. Loubengayer, Cornell University, February 1964.

(66) Maxwell, K. H., and Green, M., Phys. and Chem. Solids 14, 94-103 (1960).

(67) Personal Communications with H. Gatos and G. Erlich.

(68) Handbook of Chemistry and Physics, p. 496 (1950).

(69) Handler, P., Semiconductor Surface Physics Loc. Cit., p. 23.

(70) Deker, A. J., Solid State Physics, Prentice Hall, Inc., Englewood Cliffs, N. J., p. 321 (1957).

(71) Deker, A. J., Ibid. p. 223.